1989

# A PRECONCENTRATION TECHNIQUE FOR THE DETERMINATION OF TRACE ELEMENTS

ANDREA JANE AMBROSE

PHD

# A PRECONCENTRATION TECHNIQUE FOR THE DETERMINATION OF TRACE ELEMENTS

AMBROSE, ANDREA JANE

**Award date:**
1989

*Awarding institution:*
University of Plymouth

A thesis entitled

# A PRECONCENTRATION TECHNIQUE FOR THE DETERMINATION OF TRACE ELEMENTS

presented by

**ANDREA JANE AMBROSE, B.Sc.**

in part fulfilment of the
requirements for the degree of

**DOCTOR OF PHILOSOPHY**

**of the**

**COUNCIL FOR NATIONAL ACADEMIC AWARDS**

Department of Environmental Sciences
Analytical Chemistry Research Unit
Polytechnic South West
Drake Circus
PLYMOUTH
Devon

Collaborating establishment:
BDH Ltd.
Broom Road
POOLE
Dorset

November 1989

# A PRECONCENTRATION TECHNIQUE FOR THE DETERMINATION OF TRACE ELEMENTS

ANDREA JANE AMBROSE

## ABSTRACT

A novel preconcentration technique for the determination of trace metal impurities in fine chemicals has been developed. The technique involved forming metal chelates in solution with Chrome Azurol S, and adsorbing them onto powdered activated carbon. After separation by filtration, the enriched carbon was made into a slurry and analysed by ICP-AES. Ca, Cu, Fe(III), Mg, Mn and Ni, were all successfully adsorbed onto the carbon from water with recoveries of 100, 96, 100, 98, 97 and 100% respectively. Cu was adsorbed from aqueous solutions of glucose (30%), sucrose (20%) and potassium nitrate (10%), with recoveries of 100, 96 and 100% respectively. Adsorption equilibrium took less than five minutes. Mg was not adsorbed to any great extent in these media.

Purity of the sorbent phase was a problem. Making activated carbon from cellulose by air activation produced an activated carbon low in metals, but which was unable to adsorb Fe (III) from water. Surface areas of the cellulosic carbon and commercial activated carbon using the BET equation were $420 m^{2} g^{-1}$ and $838 m^{2} g^{-1}$ respectively. Clean up of commercial activated carbon by HF/HCl was investigated. A reduction of metal content was seen but high levels of Al, Ca, Mg and Fe ($89.4 \mu g g^{-1}$, $170 \mu g g^{-1}$, $230 \mu g g^{-1}$ and $54.8 \mu g g^{-1}$ respectively) still remained. Although not satisfactory, this was used in subsequent experiments.

Enriched carbon slurries were introduced to the plasma by flow injection as well as by continuous nebulisation. In an attempt to reduce dispersion of the flow injected sample in the carrier stream, four spray chamber designs were investigated - a Scott double pass spray chamber (SDPSC), a single pass spray chamber (SPSC), a bulbous-ended spray chamber (BESC) and a reduced volume spray chamber (RVSC). Transport efficiencies on a 1% activated carbon slurry were calculated as 0.91% for the RVSC, 0.66% for the BESC, 0.43% for the SPSC and 0.42% for the SDPSC. Simplex optimisation was used to optimise each spray chamber with regards to plasma operating conditions, for Cu and Mn. For each element, operating conditions were similar for each spray chamber. Using the optimised conditions, flow injection characteristics were investigated. There were only small differences in dispersion between each spray chamber. At higher carrier stream flow rates ($4.5 ml min^{-1}$) the BESC had the best precision (3.1%,RSD), however, further work was carried out on the RVSC which yielded FI peaks of a Gaussian shape. The validity of the slurry atomisation FI-ICP-AES approach was confirmed by the analysis of two CRM soils, SO1 and SO2.

For continuous nebulisation of the carbon slurries an internal standard, Sc, was used successfully to correct for variations in sample delivery and viscosity effects.

Trace metal impurities (Cd, Cu, Fe, Pb and Ni) in urea, sucrose and potassium chloride were determined by the preconcentration technique both with continuous nebulisation and FI of the slurry into the ICP. The results showed quite good agreement with a liquid-liquid extraction procedure but RSDs were poor for the FI, but good with internal standardisation.

## ACKNOWLEDGEMENTS

I would like to express my greatest thanks to Professor L. Ebdon for his excellent guidance, support and belief in me, throughout this work. Also to Dr. P. Jones for his invaluable expertise, knowledge and wit.

I am grateful for the extremely useful industrial supervision of Dr. E. Newman and Mr. R. Farrow, and to Mrs. J. Collins for her tremendous help with the ICP.

Thanks must be extended to my colleagues for their many interesting discussions and comments - not all of which were taken!

Finally, I would like to thank my parents, especially Mum, who painstakingly typed this thesis, despite all the odds (!) and to Huw, for his help, patience and support throughout the writing of this thesis. Diolch o galon.

## CONTENTS

## LIST OF FIGURES

## LIST OF TABLES

# CHAPTER 1

# INTRODUCTION

## 1.1 INTRODUCTION

### 1.1.1 The need for analysis of high purity substances

One of the main tasks of analytical chemistry is the determination of trace metal impurities in a variety of matrices. Of great importance is the accurate determination of trace metal impurities in high purity materials. The chemical purity of a material often dictates its applicability in new fields of science and engineering (1). Trace impurities in materials, such as semi-conductors and glasses, have a profound effect upon their electrical, magnetic, mechanical, nuclear and optical properties (2). In response to the need for trace impurity determinations, multi-element methods of analysis have been developed. However, the analysis of pure substances not only demands sensitive analytical instrumentation but also imposes stringent controls upon methodology including the cleanliness of all chemical operations and reagent purity. Thus, a need has been generated to determine levels of trace metal impurities in standards and reagents below routine detection limits to ensure analytical grade chemicals do not introduce errors into analytical procedures. Often, these impurities are in themselves, present at very low levels and are below the relative detection limits of the determination technique. These levels can only be measured if a preconcentration step is included. Preconcentration

is a process whereby the ratio of the amount of a particular element is increased relative to that of the original matrix. The chemical techniques used in preconcentration not only provide enrichment factors but also, in many cases, analyte isolation which can increase the sensitivity of the instrumentation used.

## 1.2 METHODS OF PRECONCENTRATION

There are numerous methods of preconcentration techniques used today and these have been reviewed extensively by Minczewski (3), Leyden and Wegscheider (4) and Tolg et al (5).

Perhaps the simplest method of preconcentration of ions from solution is evaporation of the solvent. However, it does suffer from a number of disadvantages. Fractional crystallisation can lead to a microscopically inhomogeneous residue, matrix effects may be amplified rather than minimised, introduction of contamination throughout the procedure, possibility of the formation of acid-insoluble residues containing the desired trace elements, and the technique is very time consuming, especially if large preconcentration factors are required.

Precipitation is one of the oldest chemical techniques for the separation and concentration of ions. Precipitation methods are satisfactory for macro-separations although the precipitates are often contaminated with foreign ions.

One of the most widely used techniques of preconcentration is liquid-liquid

extraction. It is quick and can be highly specific with careful choice of chelating agents. There are practical limits however to the pre-concentration factors that can be reasonably achieved by batch extraction owing to the initial solubility of solvents in the aqueous phase. Also, significant portions of the organic solvent may adhere to the walls of the vessel, requiring repeated washings, thus decreasing the concentration factor attainable. There may also be the formation of emulsions which are difficult to separate.

Preconcentration onto ion-exchange resins is one of the most favourable methods. Ions of interest may be measured directly on a solid resin using X-ray spectrometry, neutron activation or isotopic dilution techniques, or by elution from the solid phase and analysis of eluent. Ion-exchange resins operate on an ion-association basis. They do not perform well in, for example, seawater, where sodium ions compete well compared to the less abundant transition metal ions, and so swamp the exchange sites. Chelating ion-exchange resins may be useful if alkali metal ions are not of interest. These resins contain functional groups that chelate with predominantly transition metal ions. For example, the commercially available Chelex-100 resin contains an iminodiacetic acid functional group, attached to an insoluble backbone. This resin has been used in seawater analysis (6,7) with success. However, the resin will not remove metals held in organic and inorganic colloids which can be present even after ultrafiltration. Also, there are samples such as seawater, or iron and calcium-rich freshwater in which major elements occupy the ion exchange sites thereby excluding the trace elements. To overcome this, masking agents or manipulation of pH must be applied.

Van Berkel et al, (8) have critically examined the use of Chelex-100 in the enrichment of artificial seawater for analyte preconcentration and matrix separation. They concluded that at a given liquid flow rate, pH, column washing conditions and amounts of resin are the most critical parameters and that these experimental conditions under which enrichment procedures have to be carried out, are much more important than had been generally assumed. They also noted that ionogenically bound trace elements are extremely susceptible to matrix effects. However, with careful optimisation they were able to quantitatively recover Cd, Co, Cu, Pb and Zn from artificial seawater.

The selective chelation of certain trace elements and essential exclusion of the alkali and alkaline earth elements can be achieved by varying the chelating agent upon the solid support. For example, chelating groups have been immobilised on siliceous surfaces to produce a variety of amine and dithiocarbamate-modified gels (9,10).

A major limitation to immobilised chelating materials is that generally they have a low exchange capacity. Also, there is some concern that leaching of the metal chelate from the support may occur, as it is not attached by a chemical bond. For a more detailed discussion, reviews by Murthy et al (11) and Marina et al (12), are recommended.

Activated carbon can be used as a collector material in trace analysis. Due to its special character, insoluble compounds, as well as soluble metal chelate complexes can be enriched (13).

## 1.3 ACTIVATED CARBON

Activated carbon is made by the carbonisation and activation of material rich in carbon, generally of vegetable origin. When the starting material is pyrolysed in the absence of air the majority of non-carbonaceous material is removed in the form of gaseous products. Following this, the activation process takes place which involves passing, usually, steam or carbon dioxide at 700-1100°C over the carbonised intermediate product. This removes tarry carbonisation products from the spaces between the elementary microcrystallites and causes their partial destruction.

This activation step may be eliminated if suitable substances, which restrict tar formation, are added to the starting material before carbonisation (14). The activation process increases the porosity and therefore surface area of the resulting carbon.

### 1.3.1 Mechanisms of adsorption

The sorption process is caused and influenced by various physical and chemical properties of the adsorbent and the substance adsorbed. It is these physical and chemical properties that have made activated carbon an ideal adsorbent.

The structure of activated carbon consists of elementary crystallites which is similar to graphite in two dimensions. These are composed of several planar layers formed by carbon hexagons. Unlike graphite, the planar layers are arranged at different angles to a perpendicular axis passing

through them and they overlap in an irregular manner. This is called a turbostratic structure (Figure 1.1). Between the spaces of the individual microcrystallites are pores. Pores in activated carbon are classified into three groups 1) Micropores (effective radii less than 1.8-2nm) 2) Mesopores (2-100nm) and 3) Macropores (100-2000nm).

Conventional types of activated carbon have a tridisperse structure, that is, consisting of all three classes of pores. Adsorbate molecules can penetrate into the pores of small dimensions located deep within the carbon sufficiently rapidly because of the presence of larger pores. The adsorption properties of conventional types of activated carbon exhibit practically no selectivity to the adsorbate molecules of different sizes. Activated carbon is therefore used as a universal adsorbent with a large capacity. The chemical structure of activated carbon can effect its selectivity. Certain atoms and functional groups present on the surface of activated carbon can contribute to the chemical adsorption of certain substances.

Work has shown that when appropriate chelating reagents are used with activated carbon, quantitative recovery rates can be obtained for a variety of elements, even in the presence of high electrolyte concentrations. Despite its wide use however, the mechanisms of adsorption onto activated carbon are not fully understood.

Conclusions on adsorption processes have been made by Piperaki et al (15). Their work on the adsorption of nickel and its amino acid complexes onto activated carbon resulted in the following suggestions:

FIGURE 1.1

SCHEMATIC REPRESENTATION OF NON-GRAPHITISING STRUCTURE OF ACTIVATED CARBON

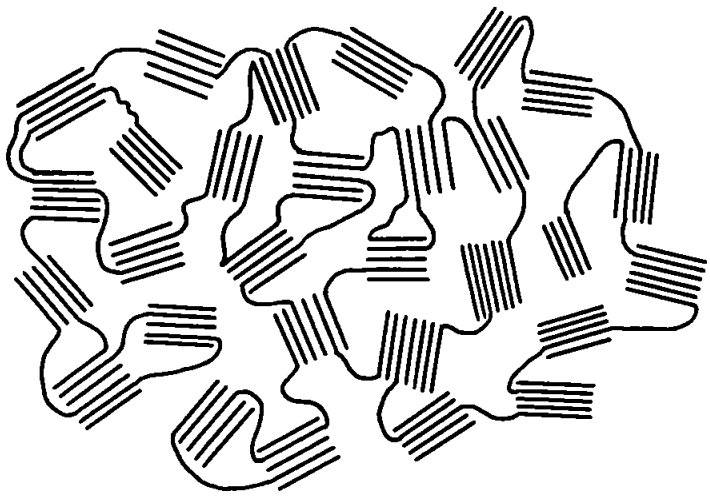

1) The sorption of metal chelates is affected by the complexing ligands. However, there are cases when the metal ion itself binds to the activated carbon without the presence of a complexing ligand. Some elements are reduced by the carbon out of the complex into their elemental state. Adsorbed gold is an example of this and cannot in general be separated from the carbon by simple elution with acid.

2) When the complexing agent has aromatic rings in its structure, Pi-orbital overlap interaction between the complexing agent and the activated carbon surface may occur. This has the effect of increasing the adsorption energy (16).

3) The sorption is affected by the presence of hydrophilic or hydrophobic groups in the complexing molecule. The more soluble the chelating reagent and its complexes the more the sorption capacity decreases. Hydrophobic properties, caused by, for example elongation of aaliphatic chain on the reagent resulted in an increase in sorption.

4) Quantitative adsorption on activated carbon can only be relied upon when the molecule of the chelating reagent is such that the centres for binding on carbon and those for binding the metal ion are so spatially separated that the orbitals have minimal mutual interaction. Piperaki et al cite Jackwerth (17) who found that in phenanthroline chelates the electrons of the nitrogen atoms which bind the metal ions during adsorption are affected to such an extent by the

interaction of the Pi-orbitals of the planar aromatic ring system with those of the carbon, that the chelate binding is disturbed and the metal ion is forced out of the complex when in an equilibrium situation.

Despite the findings of this work, there are still cases where water-soluble, charged complexes are adsorbed. Ryan and Murthy (18) found that in addition to Pi-electron interaction between graphitic planes and the ligand molecule, non-specific adsorption in the electrical double layer (whose nature depends upon the surface oxygen groups on the activated carbon and the nature of the electrolyte in solution) is at least partially responsible for the adsorption of charged complexes (11, 12, 14, 19).

A wide range of neutral chelates containing ligands such as dithizone (20, 21) sodium diethyldithiocarbomate (20, 22, 23) dithiophosphoric-acid-O, O-diethylester (24, 25), 8-hydroxyquinol (16, 26) and potassium xanthogenate (27) have been adsorbed onto activated carbon.

Work by Jones and Schwedt (28) has shown the chelating dye Chrome Azurol S (CAS) (Figure 1.2) gave a stable coating on resin material which was very resistant to oxidation and hydrolysis even in strong alkali solution. Recently, CAS metal complexes have been adsorbed onto activated carbon and analysed by flow injection ICP-AES-slurry atomisation (29) with quantitative recoveries.

FIGURE 1.2

STRUCTURE OF CAS MOLECULE

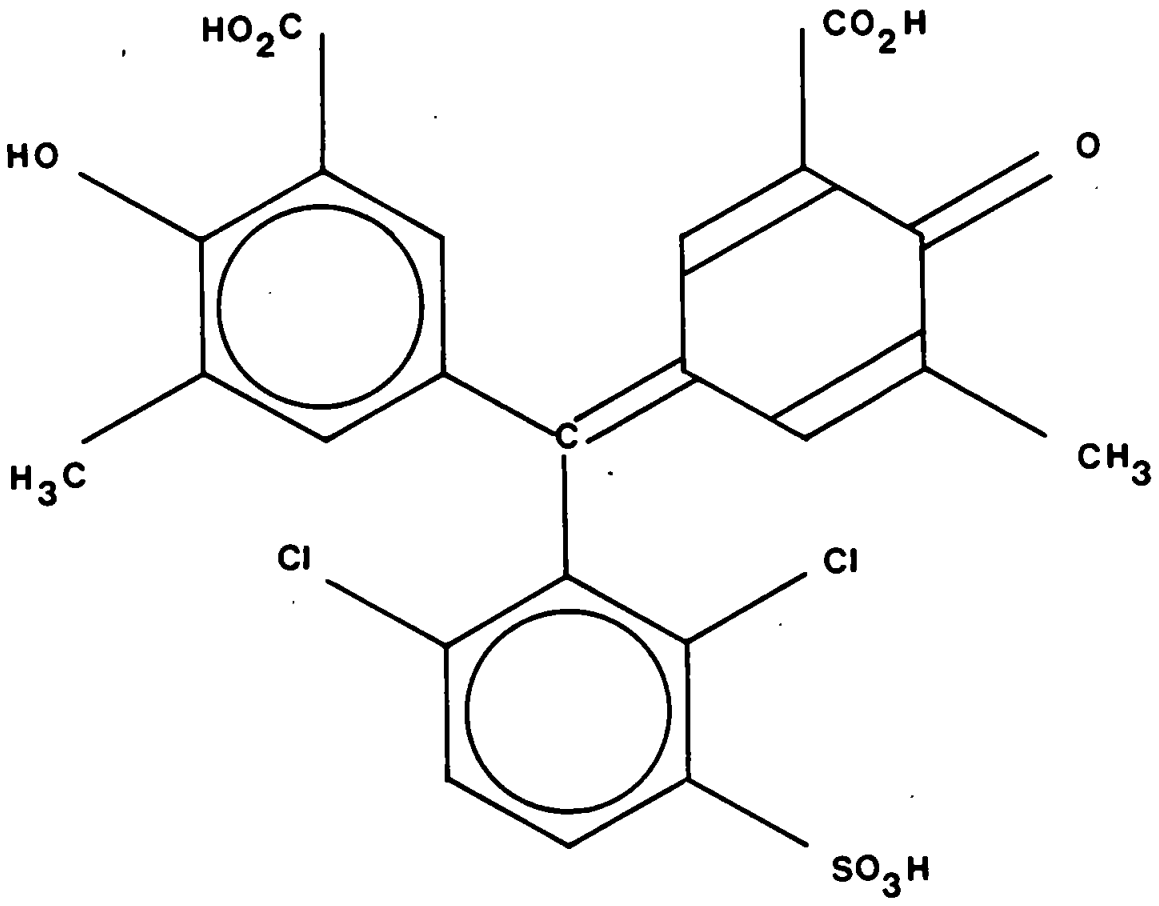


2", 6"- Dichloro-4'-hydroxy-3,3'-dimethyl-3"sulfo-fuchsone-5,5'-dicarboxylic acid (Chrome Azurol S)

## 1.4 ANALYSIS OF SORBENT

Generally the technique of sorption is performed either by filtration, column or batch mode. Filtration and column operation can sometimes be time consuming, especially when treating a large volume of sample. It is vital for maximum trace recoveries that sufficiently slow flow rates are used, or the filtration step repeated until the sorption equilibrium is established. Batch extraction offers the attraction that large sample volumes may be used.

In all of the above methods the sorbent may be desorbed with an appropriate eluent. This can however introduce contamination via the reagents used. As mentioned earlier, some elements are reduced to their elemental form and so cannot be desorbed by commonly available eluents and are therefore not detected in the final determination.

Direct analysis of the sorbent overcomes these problems. The material may be analysed using techniques such as neutron activation analysis (NAA) (16, 30) and X-ray fluorescence spectrometry (XRF) (16).

The direct introduction of solid materials into an atomizer is another approach. Gilbert (31) reported the first experiments on the direct atomisation of solids by flame photometry. Using a soil suspension in 1:1 glycerol-isoprenol he observed emission lines for the major elements. Investigations into the advantages and possibilities of direct analysis of solids has been reviewed by Langmyhr (32). He concluded that the problems of sample inhomogeneity, repetition of microweighings and slow

rates of analysis prevented the technique from being widely used. Van Loon (33) in another review dealt with direct trace elemental analysis of solids by atomic emission, atomic fluorescence and atomic absorption.

In recent years the technique of "slurry atomisation" has received much attention. Slurry atomisation involves the introduction of aqueous suspensions of solid particles into an atom source. It has been applied to several techniques, including flame atomic absorption spectrometry (34 - 41) electrothermal spectrometry (ETAS) (37, 42-50), direct current plasma emission spectrometry (DCP-AES) (51-53) inductively coupled plasma atomic emission spectrometry (ICP-AES) (37, 54-64) and inductively coupled plasma mass spectrometry (ICP-MS) (65, 66). Introducing slurries into the ICP was first suggested by Greenfield et al (67). Fuller et al, (37) showed that for successful slurry atomisation in the ICP it is necessary to have a high solids nebuliser and that atomisation efficiency is dependent upon sample transport efficiency, particle size of slurry, atomisation temperature and sample matrix. More recently work has shown that injector tube diameter has a major influence upon the particle size reaching the plasma; smaller diameter injector tubes exclude larger particles and thereby lower the signal obtained (68).

In the past few years, the role of sample introduction into the plasma has come under scrutiny and has been recognised as being the "Achilles heel" of the ICP (69). Analytical precision is determined by the stability of the analyte signal which is affected by the stability of the aerosol transport rates, and the sensitivity of the system by the transport efficiency. Therefore, it is desirable that the sample introduction system, consisting

conventionally of a nebuliser to produce an aerosol and a spray chamber to remove the larger droplets which cause instability of the plasma, produces a stable aerosol stream of small droplets and a high efficiency (70). Sharp (71, 72) has reviewed the mechanisms of operation and operating characteristics of pneumatic nebulisers and spray chambers used for analytical atomic spectrometry for solution analysis. Based on findings in the literature he has suggested new designs for sample introduction systems. Using the simplex optimisation routine, originally described by Spendley et al (73), torches (74, 75) and nebulisers (76) have been designed and optimised for solution analysis (77). This optimisation method has also been successfully applied to the determination of trace metals in coal slurries (57, 58) and it was thought that simplex optimisation may help in developing sample introduction systems for slurries.

## 1.5 DISCRETE SAMPLING METHODS

The conventional method of sample introduction for ICP-AES is based upon the continuous nebulisation of a flowing carrier stream which produces a steady state signal. By the very nature of preconcentration, often only a small volume of sample is available for analysis. Obviously, run on a continuous mode, the sample would be consumed very quickly and sequential multi-element analysis would not be possible. Hence there is a need for methods of sample introduction that do not depend upon large volumes of sample. A number of potentially suitable sampling techniques may be used. For example, the direct sample insertion device (DSID) whereby a graphite rod is inserted into the tip of a conventional sample

introduction tube in the centre of an ICP torch (78-82). Electrothermal vaporisation ICP-AES (83) is another microsampling approach that has been used. Laser ablation has become more frequently applied recently and has been used to volatilise micro-samples for subsequent analysis by ICP-AES (84, 85).

One of the most promising techniques of discrete sample introduction is by flow injection, with nearly 1000 papers (86) published since its inception in 1975 by Ruzicka and Hansen (87). Flow injection (FI) involves a range of techniques whereby a discrete sample volume is injected into a continuously flowing carrier stream. The sample is dispersed in the carrier stream to some extent and this is a function of volume injected, tube dimensions and flow rate. Applications to atomic spectrometry represent a fraction of FI papers and this particular field has been reviewed by Tyson (88). Surprisingly few of these publications refer to plasma spectrometry, although such application has been demonstrated (86, 89-92). Many discrete sampling techniques used in ICP-AES cause air entrainment, which results in instability of the plasma. Flow injection is particularly useful as entrainment does not occur when using this technique.

Flow injection is generally used as a solution based technique. However, success has been found in introducing slurries by flow injection. Indeed, more favourable dispersion characteristics of slurries may be advantageous compared with flow injection of solutions (64).

## 1.6 OBJECTIVES OF THIS WORK

The initial aim of this work was to preconcentrate trace metals from solutions of analytical grade reagents onto ion-exchange resins and analyse these by direct slurry atomisation - ICP-AES.

A number of parameters were studied as contributory to the optimal performance of the technique. Of utmost importance was the choice of ion-exchange material. It was thought that conventional ion-exchange resins would have limited use in preconcentrating trace metals from electrolytic solutions, owing to swamping of exchange sites. Therefore, use of the chelating resin, Chelex-100, was investigated.

Owing to its extraordinary adsorptive properties, activated carbon appeared to be a promising material for preconcentration. The effectiveness of activated carbon in adsorbing trace metals, is greatly enhanced by the presence of a chelating agent. The use of activated carbon, in conjunction with Chrome Azurol S chelating dye, was evaluated and optimal conditions and mode of preconcentration researched.

Conventionally, prior to analysis, the preconcentrated trace metal ions must either be eluted from the resin or the resin digested in strong acid. This is time consuming and liable to introduce contamination *via* the reagents used. Watson and Moore (54) preconcentrated traces of noble metals onto ion-exchange resin and analysed the loaded material by direct slurry atomisation - ICP-AES. An objective of this work was to further their research. Owing to the importance of particle size of slurry, careful

attention was paid to preparation of slurries, including methods of grinding, grinding time, and dispersal of slurry.

It was envisaged that only small sample volumes would be generated by the preconcentration technique. If the sample is continuously nebulised at normal uptake rates, at best, only single element determination is possible. It was clear that discrete sampling of small volumes was required. Flow injection (FI) of microvolumes of slurries was therefore performed. Optimal conditions were investigated including carrier stream flow rate and sample volume.

The volume of the spray chamber has an effect upon the signal of the sample. A large chamber, for example a Scott double-pass, causes excessive dilution of the small volume of sample. Different designs and sizes of spray chamber were investigated, using simplex optimisation where appropriate.

Real samples were analysed, comparing results obtained from FI (using sequential ICP) and continuous nebulisation (using simultaneous ICP). For continuous slurry nebulisation, internal standardisation was used to compensate for instrumental drift and viscosity effects arising from high concentrations of slurry.

# CHAPTER 2

## SORPTION EXPERIMENTS

### 2.1 INTRODUCTION

The obligation to determine concentrations of analytes below instrumental detection limits has made preconcentration procedures indispensible in present day analytical chemistry. Ion exchange is a mature preconcentration and separation technique applied in analytical chemistry. Conventional ion-exchange resins, formed from cross-linked styrene, divinyl benzene or other matrices containing inorganic functional groups are often used. One of the major disadvantages of these, however, is in the poor selectivity for heavy metals in solutions containing an excess of alkali or alkaline earth elements. The problem of concentrating a trace of one ion in the presence of a large concentration of another, requires the use of a resin with an abnormally high selectivity coefficient for the trace ion with respect to the bulk constituent. Chelating resins are well suited to the problem, provided that the trace element forms a chelate and the bulk ion does not. Chelex-100 is the commercial name of a frequently used chelating resin with an iminodiacetic acid function. There are numerous publications (e.g. 6, 7) reporting the analytical applications of the resin, the majority of which are concerned with the preconcentration of transition metals and a number of additional elements, from solutions of alkali and alkaline earth metals.

Other absorbent phases have been investigated, some without any or with little chemical functionality on the surface. Activated carbon has been used in this capacity, as detailed in Chapter 1.

Organic compounds are generally more effectively adsorbed onto activated carbon than inorganic solutes. The use of a chelate-forming reagent in solution enhances the efficiency and selectivity of activated carbon. A number of complexing agents have been used, but in this work Chrome Azurol S was investigated as a suitable reagent.

### 2.1.1 Chrome Azurol S

In analytical chemistry Chrome Azurol S (CAS) has been applied as a metal indicator and as a reagent for the photometric determination of metals. It has been used by Willard and Horton (93) as an indicator in the titration of fluoride with thorium. Theis (94) and Musil and Theis (95) employed the reagent in the chelatometric determination of aluminium, copper and zinc and for the detection of beryllium in weakly acidic solutions. Srivastava et al (96), observed that CAS formed very stable coloured chelates in aqueous solution with copper (II), beryllium (II), magnesium (II), cadmium (II), aluminium (III), lanthanum (III), cerium (IV), titanium (IV), zirconium (IV), uranium (VI), iron (III), cobalt (II), nickel (II) and palladium (II) under specific experimental conditions. Figure 2.1 shows the probable structures for CAS in acid, neutral and alkaline media.

FIGURE 2.1

STRUCTURES OF CAS IN ACIDIC, NEUTRAL AND ALKALINE MEDIA

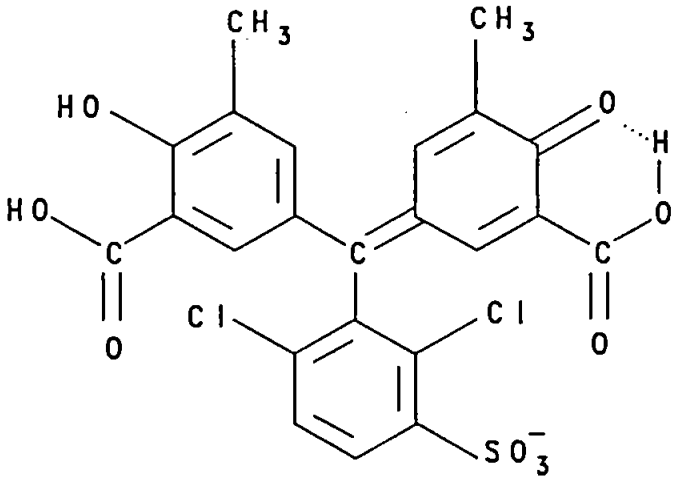

(i) Acidic medium

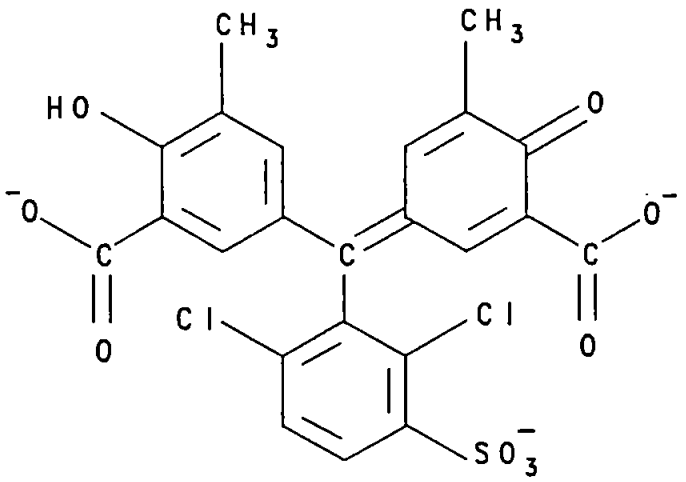

(ii) Neutral medium

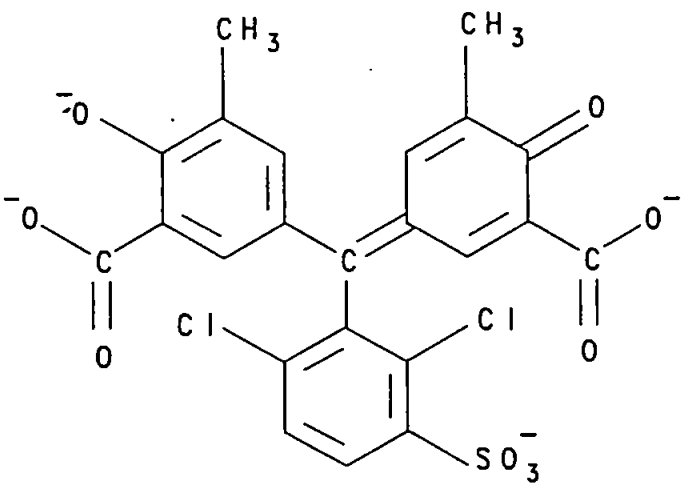

(iii) Alkaline medium

Owing to the comparatively long distance between the two bidentate groups it is considered improbable that both would be involved in complex formation. There is little information on the type of complex CAS forms with metals. However, iron (III) forms a 1:1 chelate (97, 98), as does thorium (96). Nickel forms a 1:2 chelate (99).

Following on from the work of Watson and Moore (54), whereby traces of noble metals were batch extracted onto ion-exchange resin and determined by direct injection of the loaded resin into an ICP, it was thought that this technique could be applied to the determination of trace metals in analytical grade reagents. To evaluate fully trace metal preconcentration by adsorption, three very different sorbent phases were investigated:- 1) ion-exchange resin 2) chelating resin and 3) activated carbon with CAS.

## 2.2 EXPERIMENTAL

Initial adsorption experiments were monitored using a flame atomic absorption spectrometer (IL 151, Thermo-Electron, Warrington, UK) and an air/acetylene flame. Table 2.1 shows the instrumental conditions that were used for each element determined.

## 2.3 ADSORPTION OF COPPER ONTO CONVENTIONAL ION-EXCHANGE RESIN

TABLE 2.1
ATOMIC ABSORPTION SPECTROMETER OPERATING CONDITIONS

| ELEMENT | WAVELENGTH (nm) | BANDPASS (nm) | LAMP CURRENT (mA) |
|---|---|---|---|
| CALCIUM | 422.7 | 1 | 7 |
| COPPER | 324.7 | 1 | 5 |
| IRON | 248.3 | 0.3 | 8 |
| MAGNESIUM | 285.2 | 1 | 3 |
| NICKEL | 232 | 0.15 | 10 |
| MANGANESE | 279.5 | 0.5 | 5 |

Flame conditions:air–acetylene,fuel lean,blue

### 2.3.1 Chemical reagents

Dowex 50W-X8 (100-200 mesh) ion exchange resin (BDH Ltd. Poole, U.K.) in $H^+$ form was used throughout all the uptake experiments.

All reagents used were of Aristar reagent grade (BDH Ltd. Poole, U.K.) and all solutions were prepared with doubly distilled, deionised water.

### 2.3.2 Stock Standard Solutions

Stock 10,000 mg $L^{-1}$ copper solution was prepared by the addition of copper metal (1.000g) to nitric acid (5ml) with heating until dissolution was complete. After dilution with water to 100ml, the solution was stored in an acid-washed polyethylene bottle.

### 2.3.3 Sample preparation

Four test solutions were prepared :20% (m/v) sucrose solution; 30% (m/v) glucose solution; 10% (m/v) potassium nitrate solution and water. These were made up to 250ml in volume and spiked so that the overall solution contained 1 $\mu g ml^{-1}$ copper. Each solution was adjusted to pH 5.5 using dilute ammonia and nitric acid solutions. Standards containing 1 $\mu g ml^{-1}$ copper in each of the test solutions were prepared for calibration. To each of the sample solutions, resin (1g) was added and agitated with a magnetic stirrer. At varying time intervals an aliquot

was drawn off and filtered through a 10ml syringe fitted with a filter pad. The filtrate was analysed using AAS. The reduction in the copper concentration was recorded and ratioed to the standard, to correct for instrumental drift.

### 2.3.4 Results and discussion

Figure 2.2 a - d shows the copper adsorption profiles for each of the test elements. Adsorption of copper from sucrose, glucose and water was virtually complete and equilibrium took about thirty minutes, although this was reached more quickly in water. The relatively slow rate of exchange was probably due to the particle size of the resin. Small particle size favours rapid exchange because of a greater specific surface and hence more diffusion occurs per unit time per unit quantity of resin.

Adsorption of copper onto the resin from potassium nitrate resulted in only 13% being exchanged. This was attributed to the large excess of potassium ions competing with the less abundant copper ions in solution. Owing to the more selective ability of chelating resins to preconcentrate trace metal ions from solutions of alkali and alkaline earth metals, experiments using Chelex-100 were performed. Copper and magnesium were chosen as test elements as they represented strong and weakly chelated metals respectively.

FIGURE 2.2
EXCHANGE OF 1µg/ml COPPER ONTO DOWEX 50W–X8 RESIN

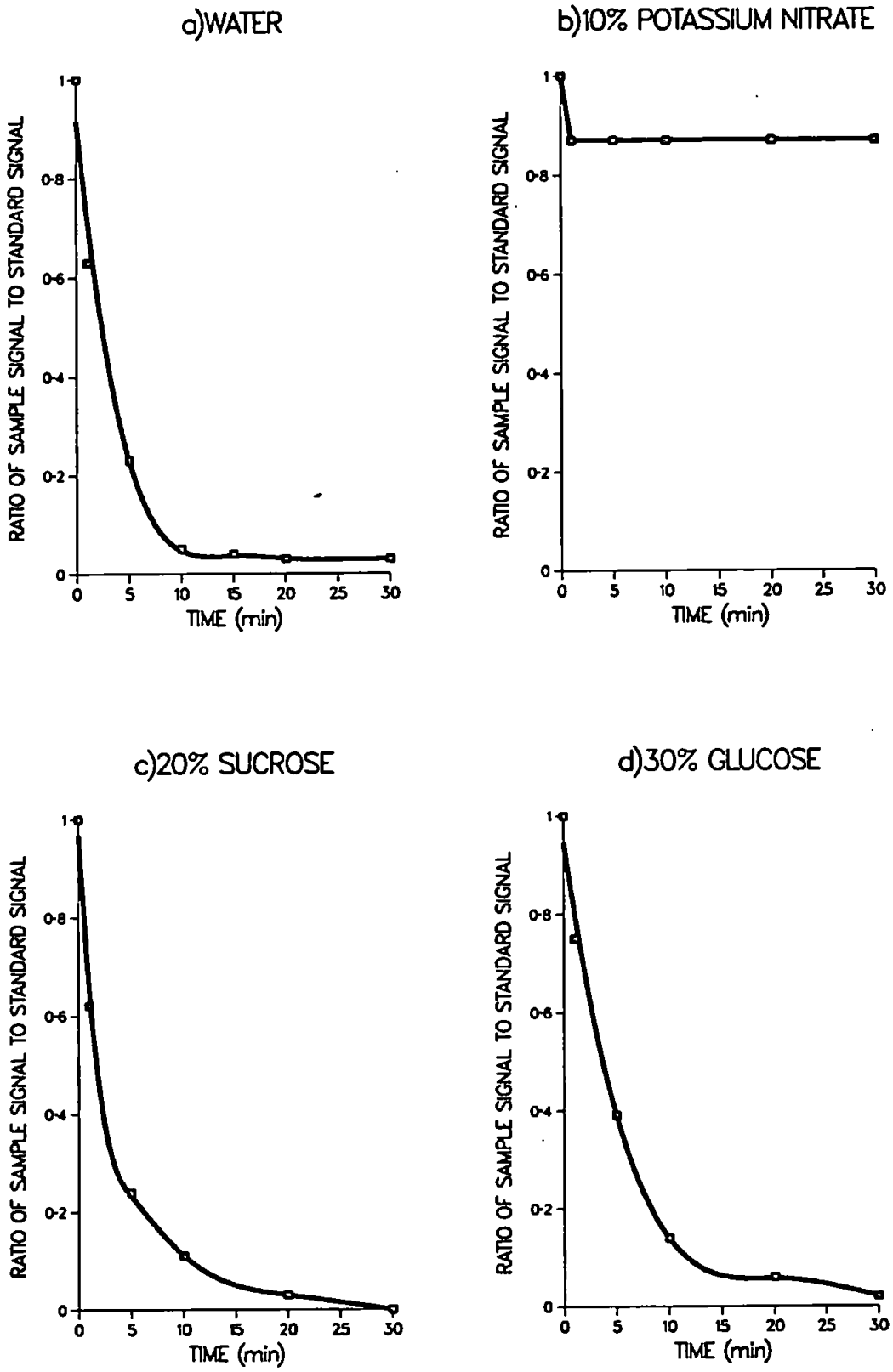

## 2.4 ADSORPTION OF COPPER AND MAGNESIUM ONTO CHELEX-100 RESIN.

### 2.4.1 Chemical reagents

Chelex-100 chelating resin (Biorad Laboratories, Richmond, VA, USA) was used throughout all adsorption experiments. All reagents used were of Aristar reagent grade (BDH Ltd., Poole, UK) and all solutions were prepared with doubly distilled, deionised water.

### 2.4.2 Stock Standards

Copper standard as 2.3.2 was used.

Magnesium standard (10,000 $mgL^{-1}$) was prepared by weighing out the equivalent of 1.000 g of magnesium or high purity MgO and transferred to a 100 ml volumetric flask. Deionised water (5 ml) and $HNO_3$ (2.5 ml) were added and warmed until dissolution was complete. The solution was cooled and diluted to 100 ml with deionised water. This was stored in an acid-washed polyethylene bottle.

### 2.4.3 Sample preparation

Two sets of four test solutions were prepared, as detailed in section 2.3.3. One set was spiked with 1$\mu gml^{-1}$ copper and the other with

$1\mu gml^{-1}$ magnesium. The solutions spiked with copper were adjusted to pH 5.5 and those with magnesium to pH 10.0 using dilute ammonia. To each of the solutions Chelex-100 (1 g) in the $H^+$ form, was added and stirred with a magnetic stirrer. As before, aliquots were drawn off, filtered and analysed by AAS, recording the reduction in signal for copper and magnesium.

### 2.4.4 Results and discussion

Figures 2.3 a-d show the copper adsorption and 2.4 a-d the magnesium adsorption profiles for each of the test solutions.

Both copper and magnesium were adsorbed from all the solutions, including the potassium nitrate, with equlibrium being attained after 10-20 minutes. The pH chosen for each element was dependent upon their ability to form chelates. For magnesium (a weakly chelated element) the pH had to be taken up to pH 10 for full adsorption to occur. This was so that the iminodiacetic acid function was sufficiently ionised to complex the magnesium. Copper on the other hand is strongly complexed by Chelex-100 and so the degree of ionisation required is less.

The ultimate aim of the project was to preconcentrate trace metals from solutions onto a solid phase and analyse this by slurry atomisation FI-ICP-AES. Although Chelex-100 looked promising as regards preconcentration, problems were encountered in introducing the loaded

FIGURE 2.3
ADSORPTION OF 1µg/ml COPPER ONTO CHELEX-100 RESIN

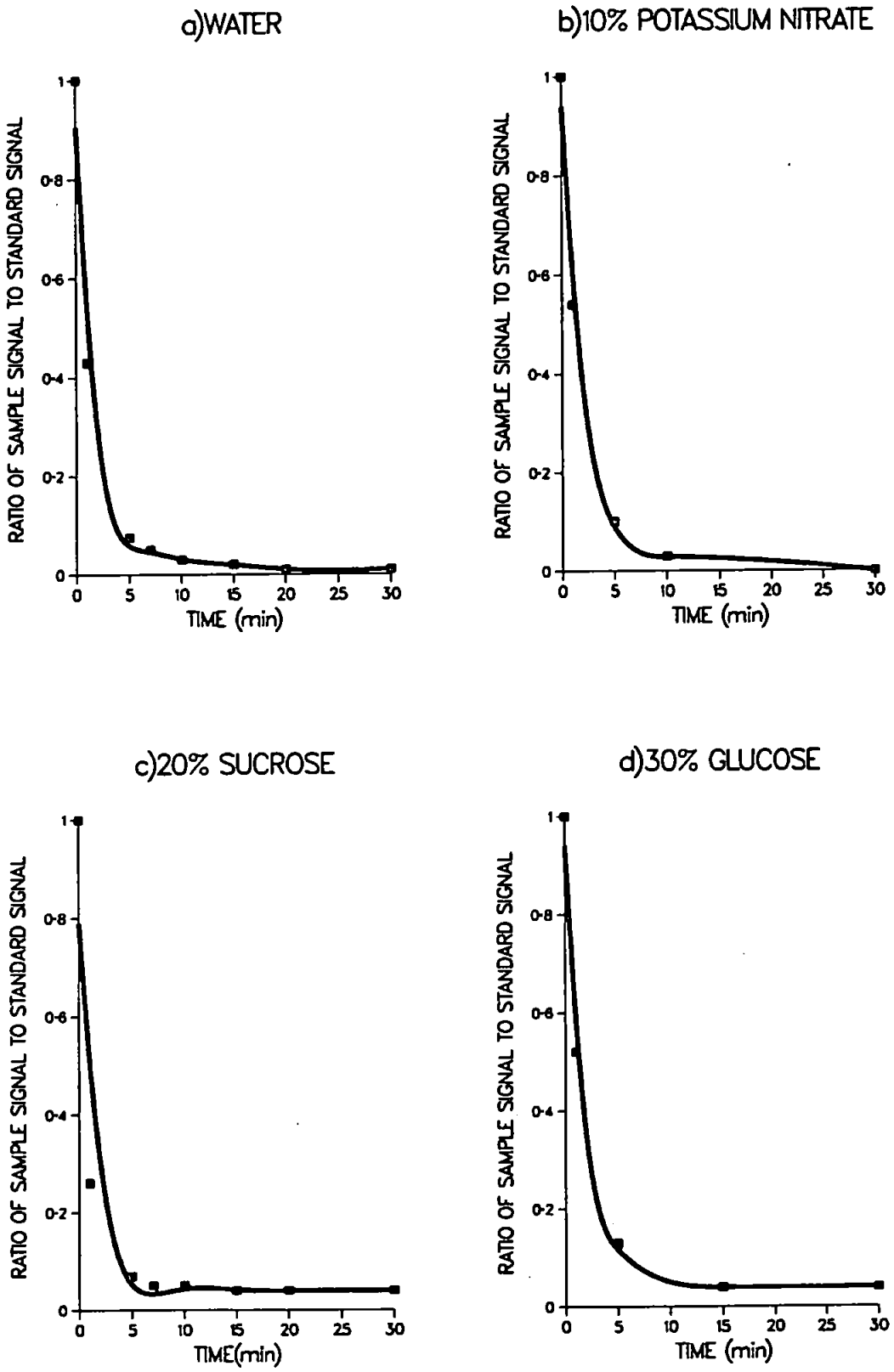

FIGURE 2.4
ADSORPTION OF 1µg/ml MAGNESIUM ONTO CHELEX–100 RESIN

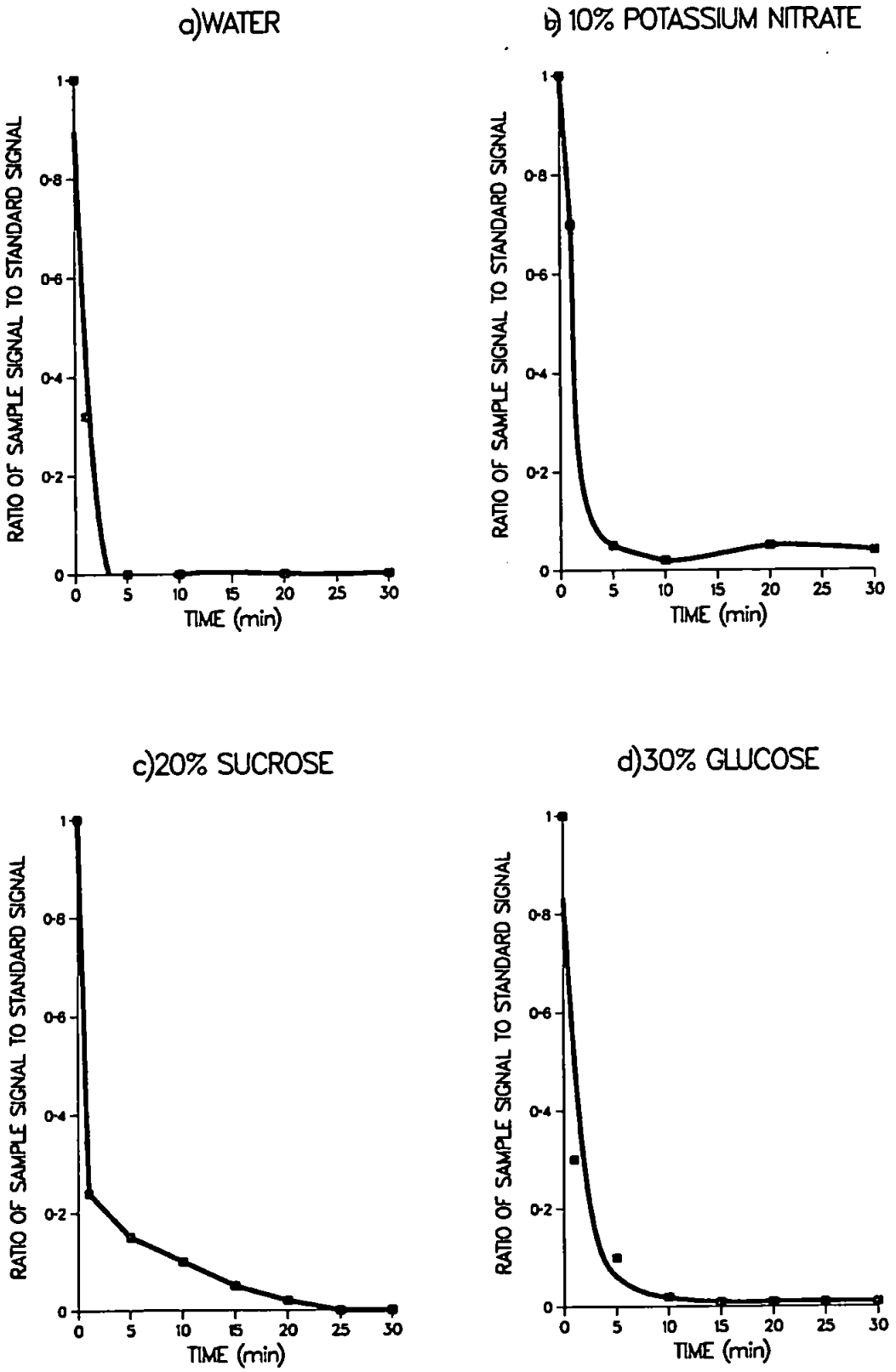

resin slurry into the ICP by FI, owing to blocking of FI valve. The slurry was not very stable and flocculated badly.

As a result of this, attention was turned to the use of activated carbon because it is easily ground and has excellent adsorptive properties as described earlier. Initial experiments were carried out using CAS-coated activated carbon beads.

## 2.5 ADSORPTION OF METALS ONTO ACTIVATED CARBON COATED WITH CAS

### 2.5.1 Chemical reagents

Activated carbon beads (0.25 - 0.6mm diameter) (BDH Ltd., Poole, UK) were used. Chrome Azurol S was obtained from Eastman Kodak Company (Rochester, New York, USA). All other reagents were of analytical grade (BDH Ltd., Poole, UK) and all solutions were prepared with doubly distilled water.

### 2.5.2 Coating procedure (100)

About 50g of activated carbon was batch washed with five washings each of acetone and methanol, then thoroughly washed with deionised water. CAS (500mg) was dissolved in 80:20 water:methanol and IM $HNO_3$ (15ml) was added. This was agitated constantly until the CAS was adsorbed onto

the surface of the carbon which took approximately 10 minutes. The carbon was washed with a small amount of 1M $HNO_3$, to remove metal ions, then stored in dilute acetic acid at pH3.0. To exploit fully the chelating power of CAS, fairly alkaline conditions are necessary. As such, it was important to prevent metal hydroxide formation. To prevent this an auxiliary complexing agent may be added to the sample before pH adjustment. However, the auxiliary complexing agent should be weaker than the CAS so that when the coated carbon is added to the solution, it competes successfully with the complexing agent and adsorbs the metals. Four auxiliary complexing agents were examined:- citric acid, tartaric acid, triethanolamine and lactic acid. Copper was used as a test element.

### 2.5.3 Sample preparation

To check that the activated carbon did not adsorb copper or reduce it to its elemental state on the surface of the carbon, two sets of water samples were spiked with 1 $\mu g ml^{-1}$ of copper and adjusted to various pHs. To one set of solutions, uncoated activated carbon was added and to the other, CAS-coated activated carbon. These were agitated as before and the decrease in copper signal was recorded.

Similar experiments were performed with the auxiliary complexing agents. Two sets of water samples were made up so that they contained an overall concentration of 0.01M auxiliary complexing agent and 1 $\mu g ml^{-1}$ copper. To one set, coated carbon was added and to the other, uncoated carbon.

All solutions were stirred and aliquots taken at fixed-time intervals, filtered and analysed for copper depletion.

### 2.5.4 Results and discussion

Figure 2.5a shows the adsorption profile of copper in solution without the presence of an auxiliary complexing agent onto uncoated carbon. At pH 2.9 and 5.25 there is no adsorption, although at pH 9.0, the copper is beginning to adsorb to a slight extent. There appears to be a pH dependence upon the sorption of copper. As there was no adsorption in acid solutions, it seems that it is not the hydrate $Cu^{2+}$ cation, but rather the hydrolysed or partially hydrolysed product that is adsorbed onto activated carbon but only to a small extent. Figure 2.5b shows that copper is adsorbed onto the CAS-coated carbon to a much greater extent, with the optimum pH being at 5.25. There is little adsorption in very acidic and none in very alkaline conditions suggesting the CAS-Cu complex becomes weaker than the hydrolysed copper at higher pHs.

Figure 2.6a shows the adsorption of copper from a solution containing 0.01M citric acid, onto CAS-coated carbon. The copper is not adsorbed to any great extent. It would appear that the citric acid complex is too strong a competitor for the copper compared to the CAS and so little copper is adsorbed from solution. However, the extent of adsorption of the copper-citrate complex onto the carbon is not great, only 15% after 1 hour (Figure 2.6b).

FIGURE 2.5a
ADSORPTION OF 1µg/ml COPPER ONTO UNCOATED ACTIVATED CARBON BEADS

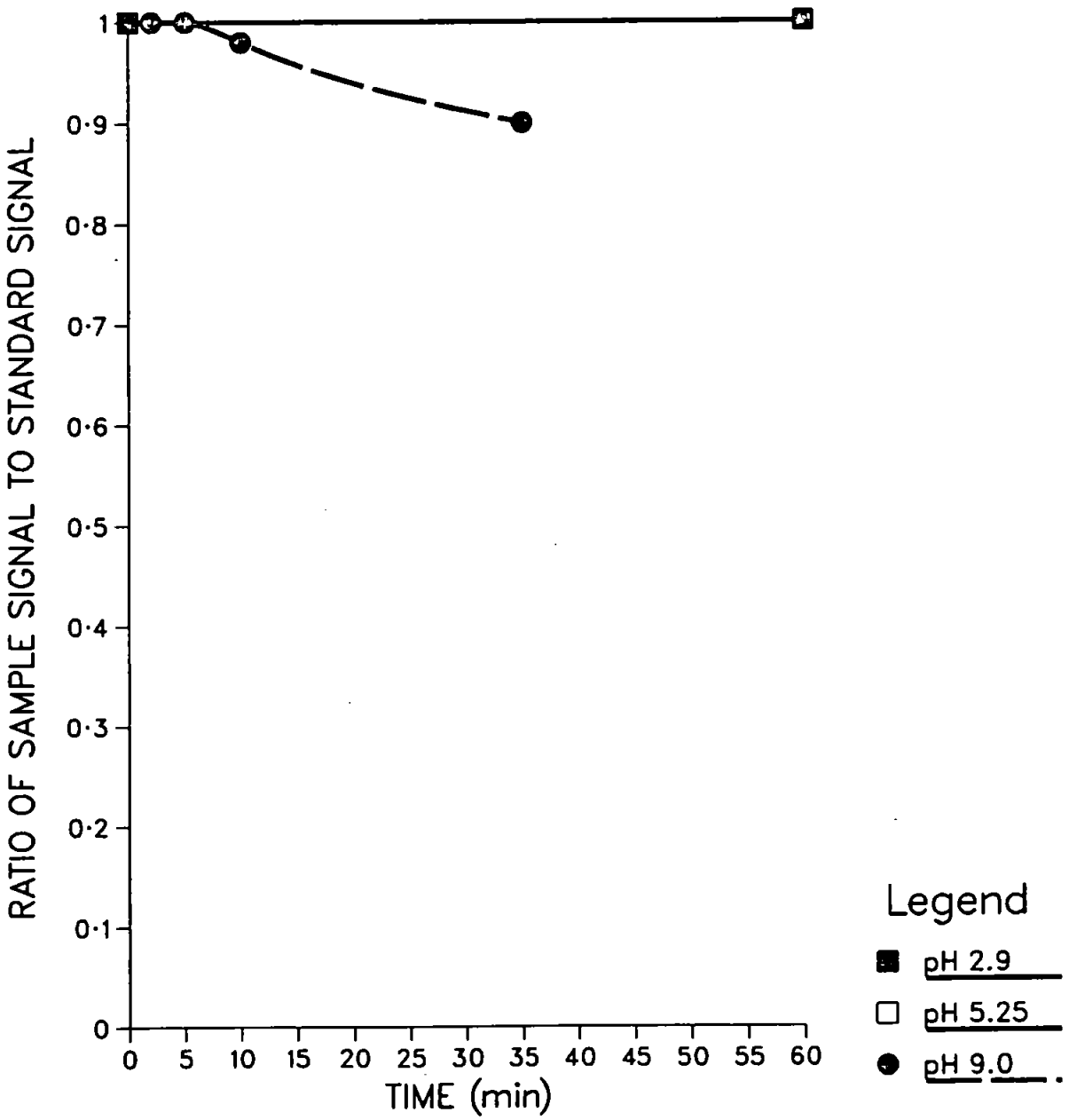

FIGURE 2.5b
ADSORPTION OF 1µg/ml COPPER ONTO CAS–COATED ACTIVATED CARBON BEADS

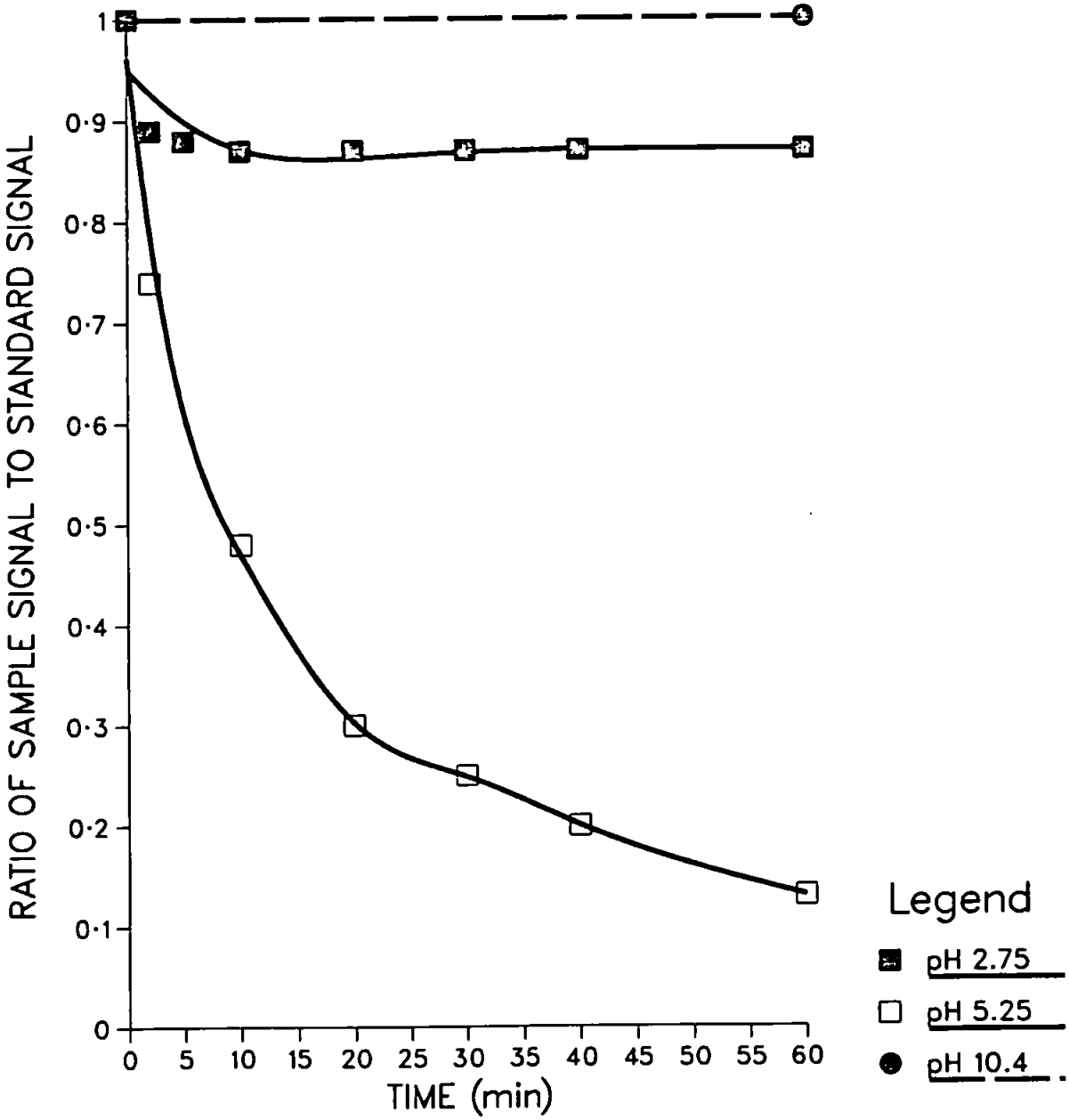

FIGURE 2.6a
ADSORPTION OF 1µg/ml COPPER ONTO CAS–COATED ACTIVATED CARBON BEADS FROM A 0.01M CITRIC ACID SOLUTION

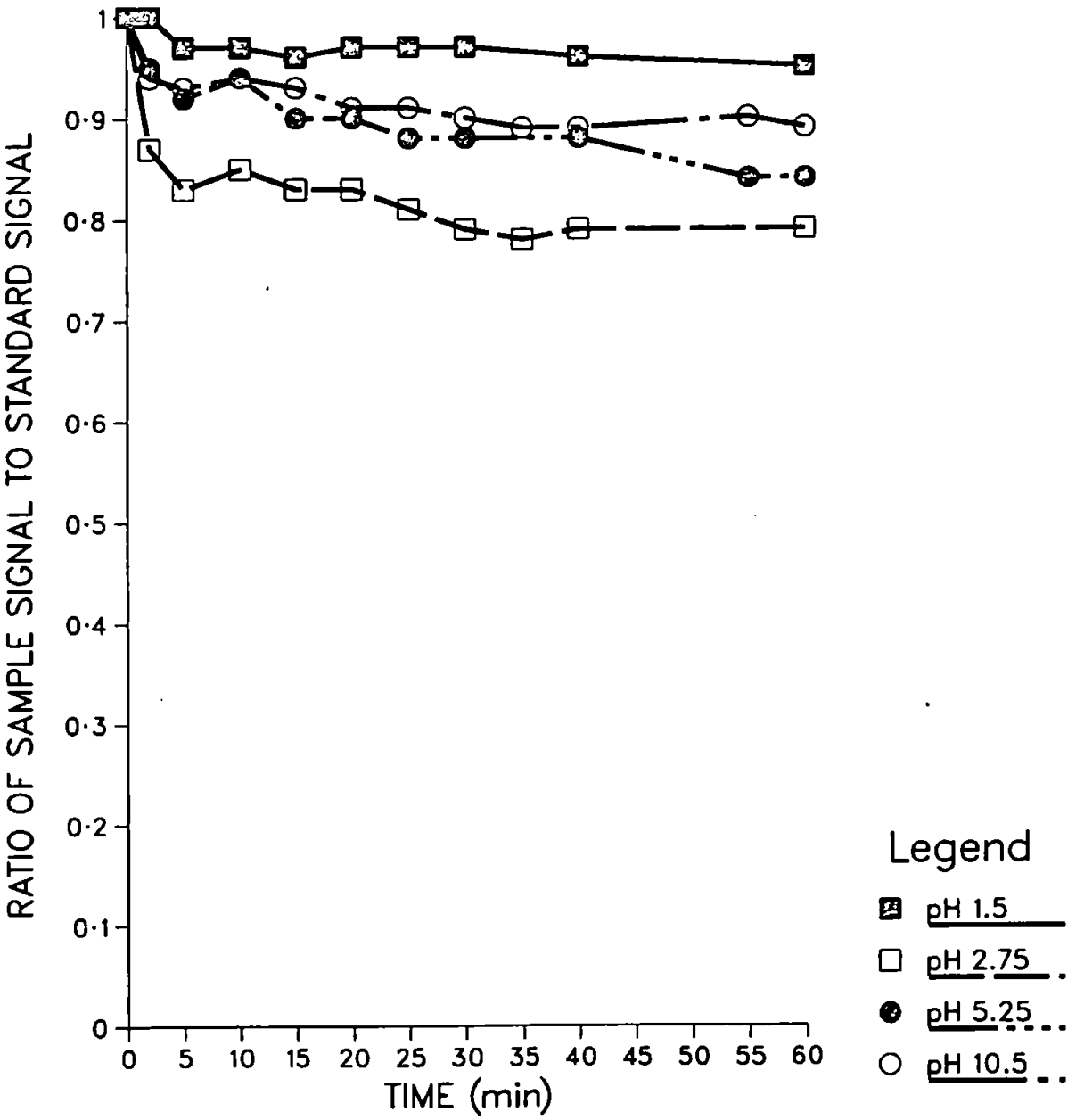

FIGURE 2.6b
ADSORPTION OF 1µg/ml COPPER ONTO UNCOATED ACTIVATED CARBON BEADS FROM A 0.01M CITRIC ACID SOLUTION

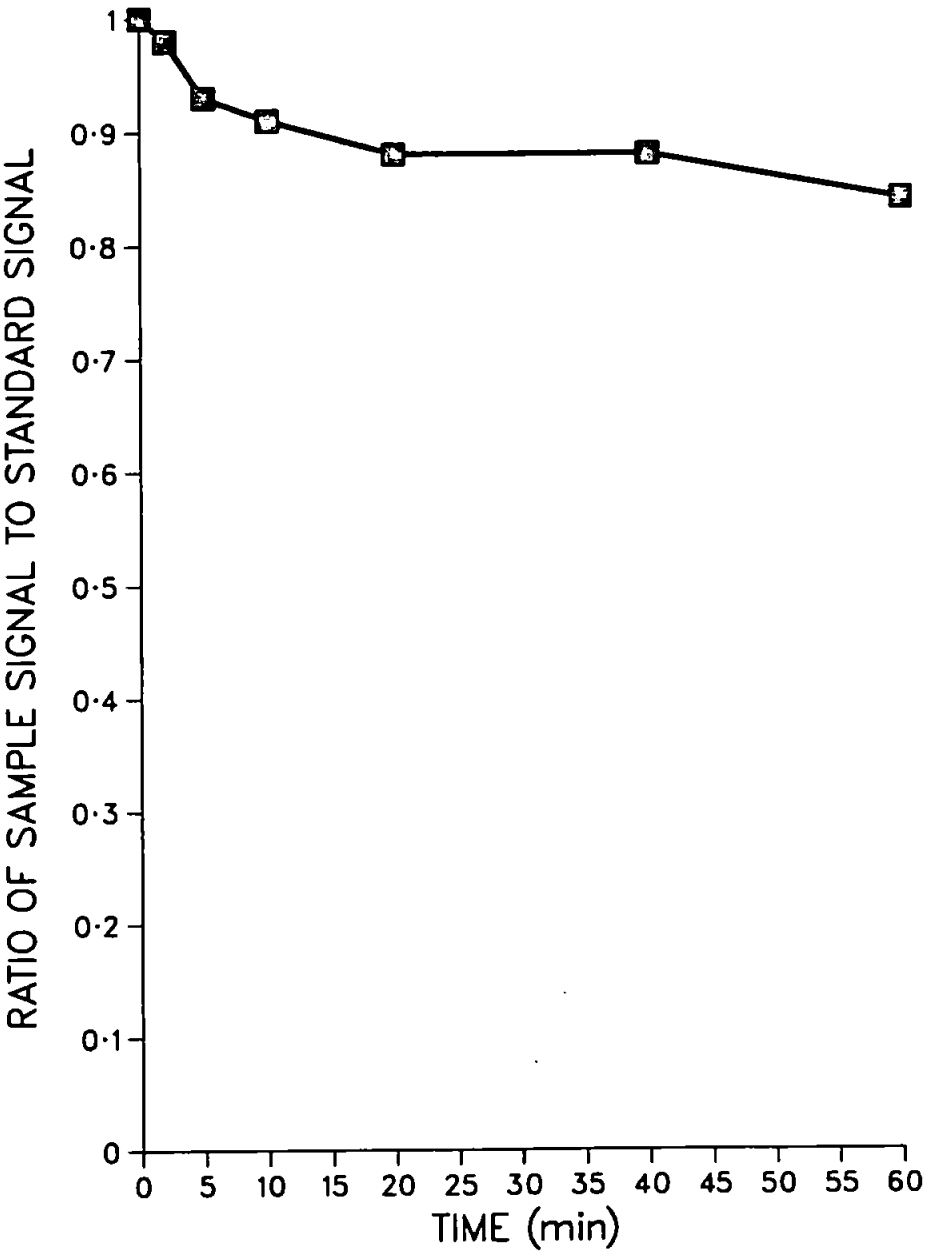

The amount adsorbed at a given temperature and concentration of the bulk phase, depends upon the nature of the adsorbent and all the components of the solution (solutes and solvent). Of most significance for this is the mutual affinity of substances with similar polarity. One would expect activated carbon, being a non-polar adsorbent, to have the greatest affinity for non-polar substances as opposed to polar ones. Abiding by this rule, the competitive adsorption of the solvent will be more marked the less its polarity and therefore, the optimum condition for adsorption on activated carbon is the adsorption of non-polar solutes from polar solvents, for example, water. In view of the adsorption profile of the citric acid-copper complex this would seem a plausible explanation, owing to the polar nature of the complex. However, the CAS-copper complex is also polar and can be adsorbed onto the carbon.

One possible explanation for the difference in adsorption of the CAS-copper complex (Figure 2.5b) and the citrate-copper complex (Figure 2.6b) onto the carbon, could be due to the microporous nature of the carbon acting as a filter, i.e. only allowing certain sized molecules to be adsorbed. Work carried out on the adsorption of dyes onto XAD-resin (100), found a similar phenomenon whereby only certain dyes were adsorbed by the resin, which has a microporous nature. Size of molecules was thought to be the reason for the different adsorbances observed. If this explanation is correct then it would be expected that the other auxiliary complexing agents would also be adsorbed to different extents depending upon the size of molecule.

Figure 2.7a shows the adsorption of copper onto uncoated carbon from a 0.01M lactic acid solution. The CAS complexes the copper more strongly than the lactic acid at pH 5.25 and 10.5. At pH 1.6, no adsorption is observed and this is probably due to the CAS molecule not being in its active form. Figure 2.7b shows the adsorption of the lactic acid-copper complex onto the carbon with 80% being adsorbed in 1 hour.

The adsorption of copper onto CAS-coated carbon in the presence of 0.01M tartaric acid is shown in Figure 2.8a. Again, the CAS-copper complex is stronger than the tartrate complex at pH 5.25 and pH 10.5, although full adsorption was not attained, suggesting that there is some interference in the presence of tartaric acid. The tartaric acid-copper complex is adsorbed by the activated carbon (Figure 2.8b), leaving about 20% of copper in solution after 1 hour.

Triethanolamine (TEA) was also investigated. The adsorption profile of copper onto CAS-coated carbon from a 0.01M TEA solution is illustrated in Figure 2.9a. The CAS-copper complex is stronger than the TEA-copper complex and so is adsorbed by the carbon. TEA-copper complexes are adsorbed onto carbon in the absence of CAS (Figure 2.9b), although about 50% remains in solution.

As a conclusion to these experiments, the adsorption of copper from solutions containing various auxiliary complexing agents onto CAS-coated activated carbon can be explained by the magnitude of their stability

FIGURE 2.7a
ADSORPTION OF 1µg/ml COPPER ONTO CAS–COATED ACTIVATED CARBON BEADS FROM A 0.01M LACTIC ACID SOLUTION

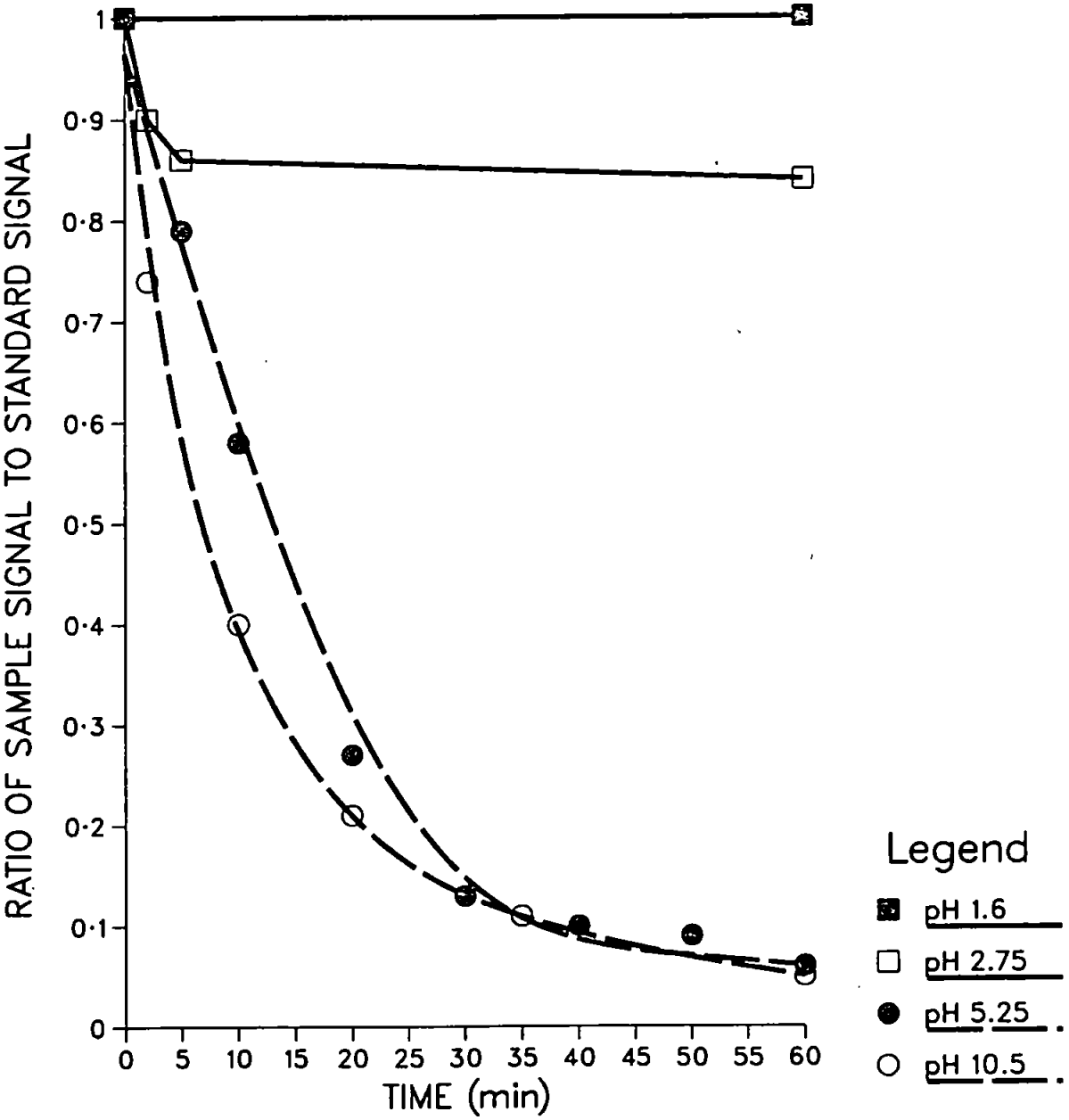

FIGURE 2.7b
ADSORPTION OF 1µg/ml COPPER ONTO UNCOATED ACTIVATED CARBON BEADS FROM 0.01M LACTIC ACID SOLUTION

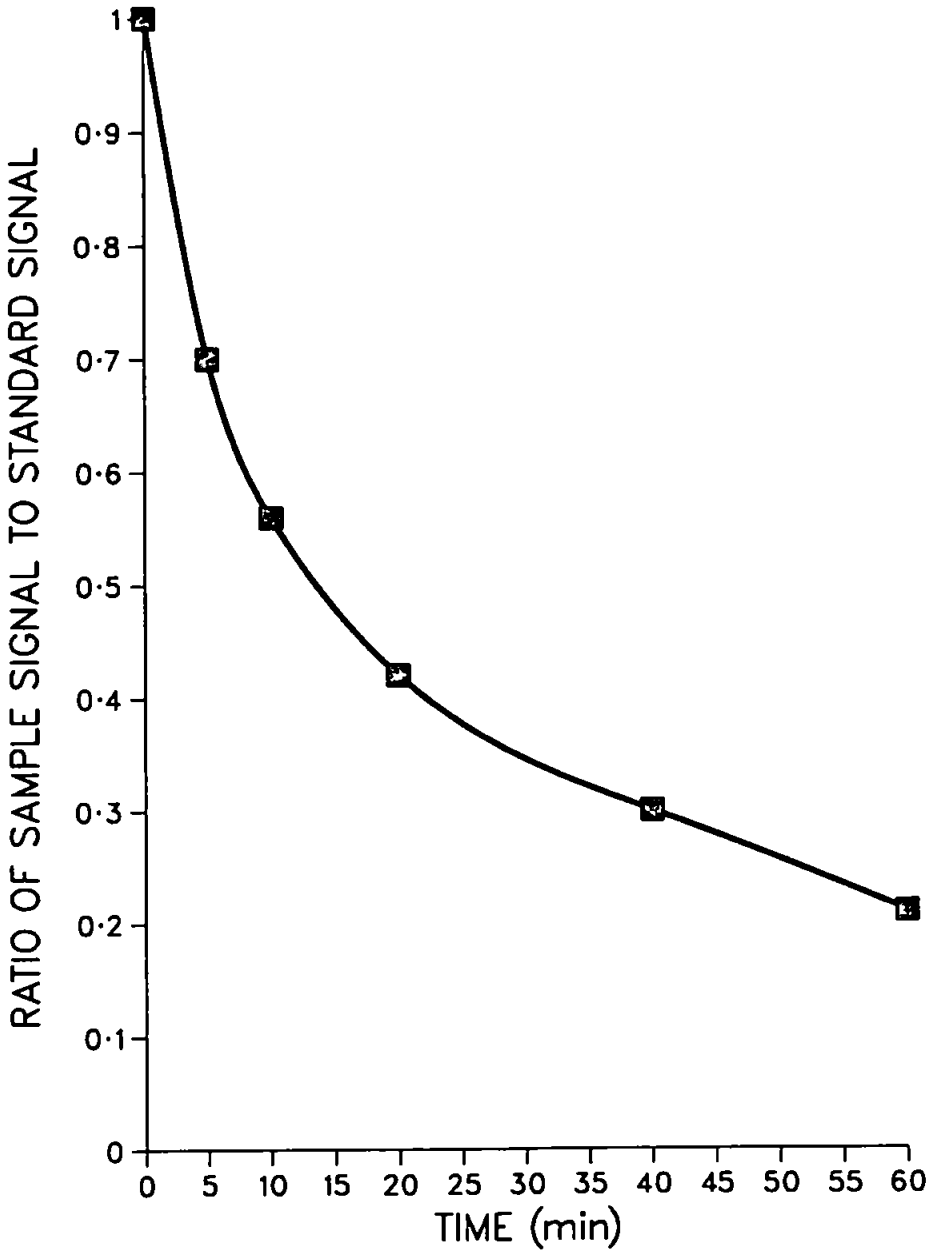

FIGURE 2.8a
ADSORPTION OF 1µg/ml COPPER ONTO CAS–COATED ACTIVATED CARBON BEADS FROM 0.01M TARTARIC ACID SOLUTION

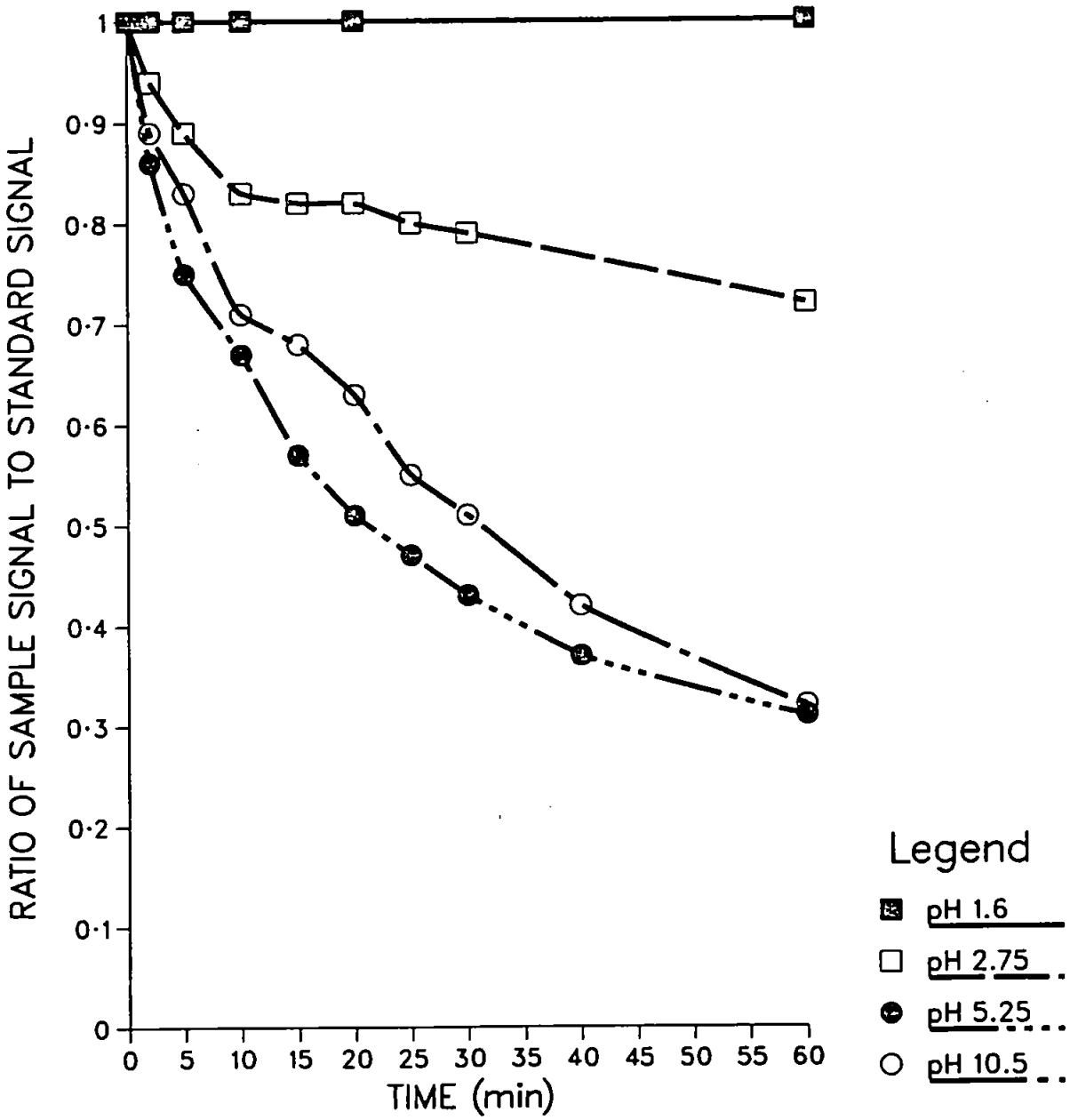

FIGURE 2.8b
ADSORPTION OF 1µg/ml COPPER ONTO UNCOATED ACTIVATED CARBON BEADS
FROM A 0.01M TARTARIC ACID SOLUTION

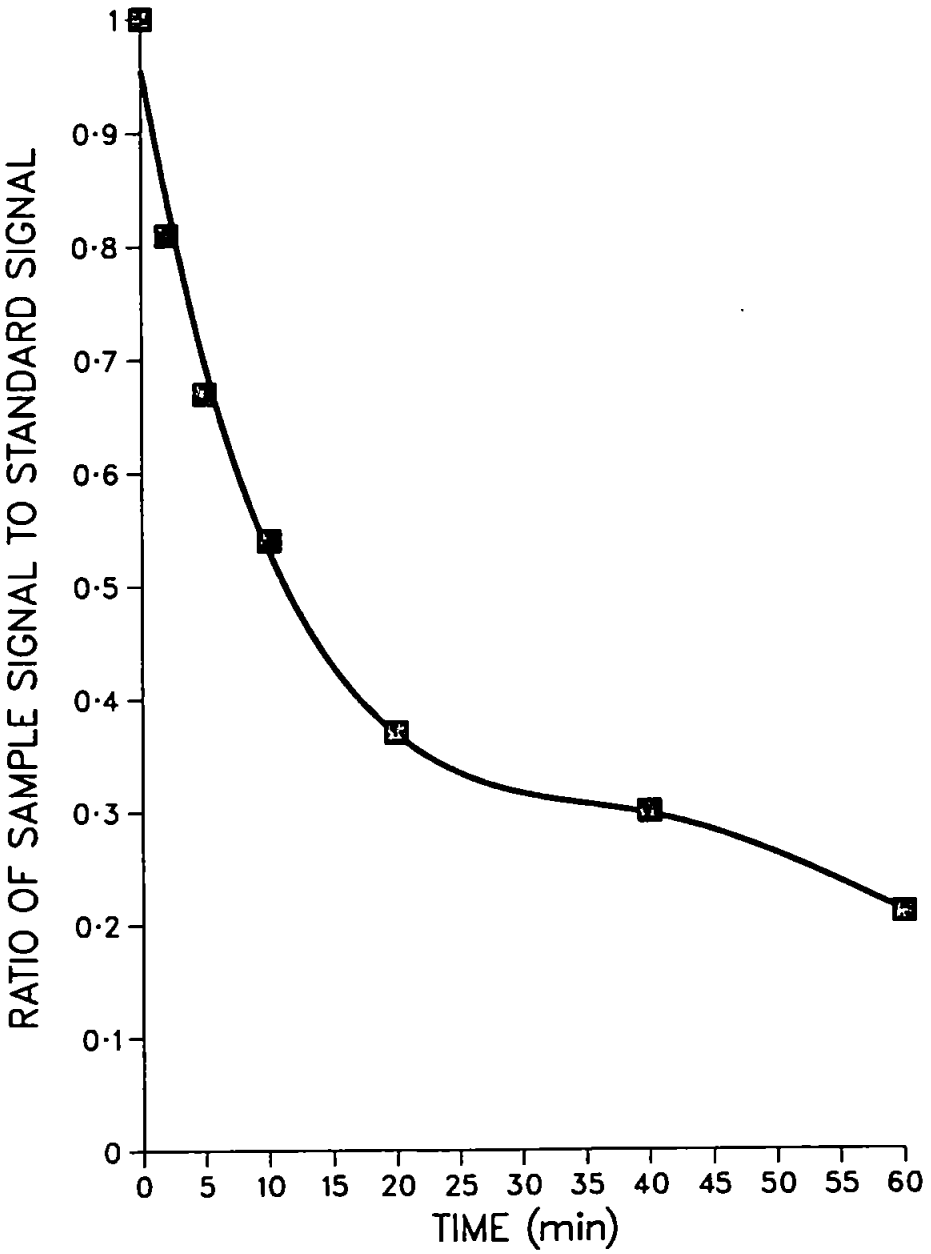

FIGURE 2.9a
ADSORPTION OF 1µg/ml COPPER ONTO CAS–COATED ACTIVATED CARBON BEADS FROM A 0.01M TEA SOLUTION

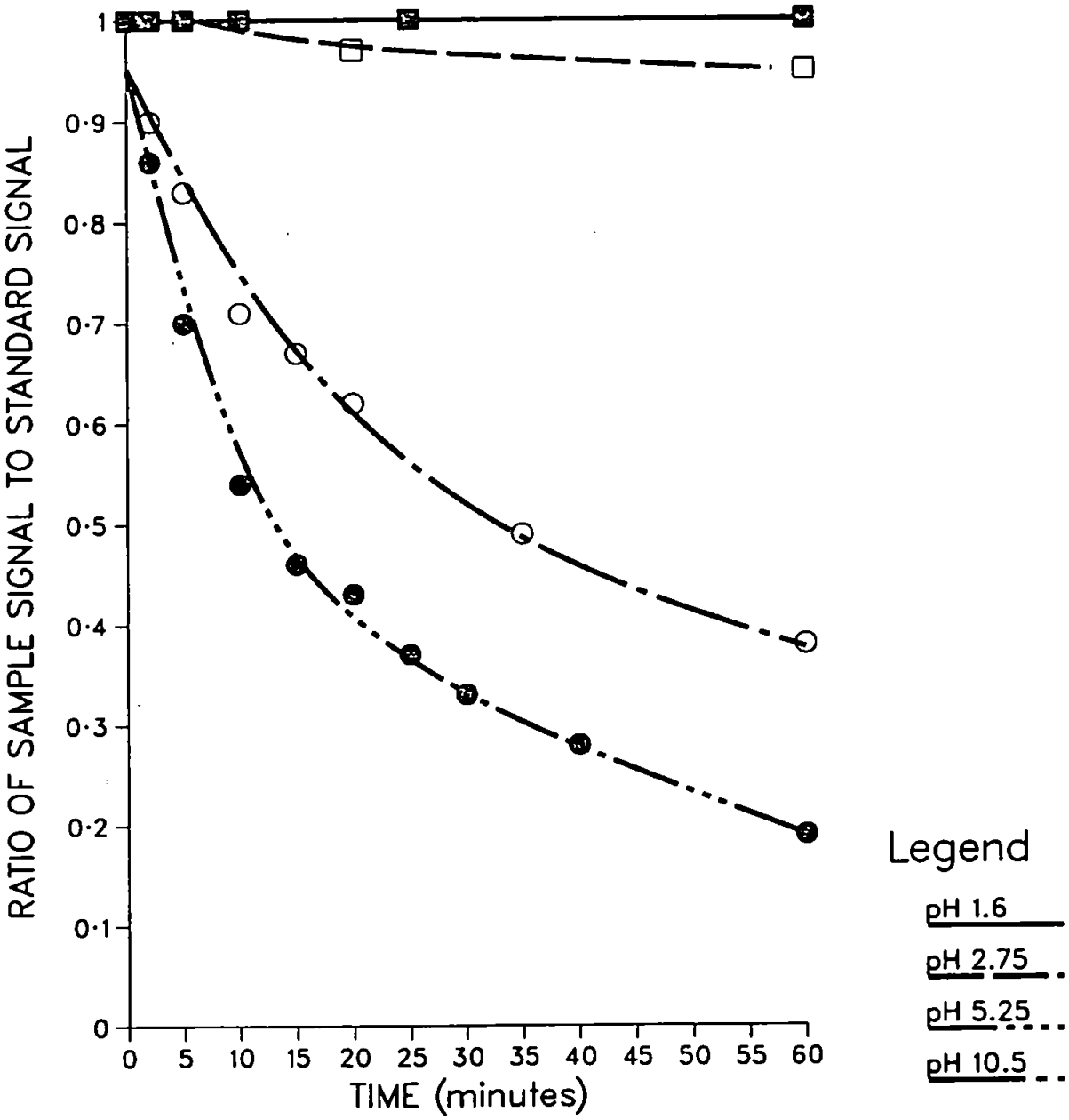

FIGURE 2.9b
ADSORPTION OF 1µg/ml COPPER ONTO UNCOATED ACTIVATED CARBON BEADS
FROM 0.01M TRIETHANOLAMINE SOLUTION

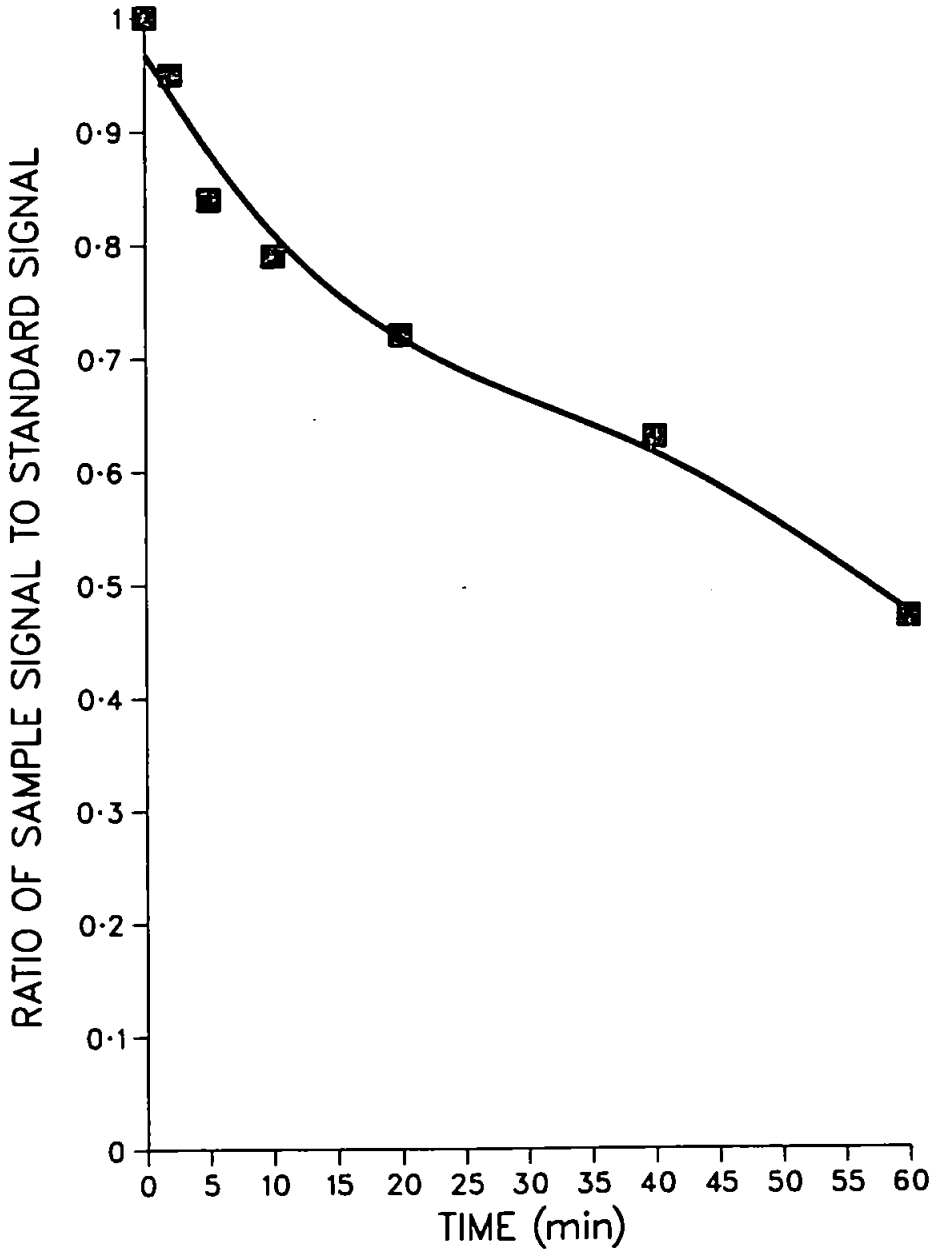

constants.

When a complex is formed by the reaction

$$M + L \longrightarrow ML \qquad \ldots\ldots \quad 2.1$$

The equilibrium of the above reaction is defined by the expression

$$K_{ML} = \frac{[ML]}{[M]\,[L]} \qquad \ldots\ldots \quad 2.2$$

where $K_{ML}$ is the formation constant. In order to keep the equilibrium equations in a simple form, although consideration must be taken of the influence of all side reactions in which M and L take place, a new constant is defined

$$K' = K_{M'L'} = \frac{[ML]}{[M']\,[L']} \qquad \ldots\ldots \quad 2.3$$

The expression [M'] denotes the concentration not only of the free metal ion but also of all the metal in solution that has not reacted with the complexing agent. The term [L'] correspondingly, represents the

concentration of the free ligand as well as the concentrations of all species of the complexing agent not bound to the metal. K' is known as the conditional stability constant. It is often convenient not to prime the constant itself, but its qualifying subscripts. Thus, $K_{MT..}$ indicates that the side reactions of the ligand, but not the side reactions of the metal ion have been taken into account. $K_{MT..}$ indicates that the side reactions of the metal and the ligand have been taken into account.

The conditional constant gives the relationship between the concentration of product formed [ML]; the total concentration of uncomplexed metal [M'] and the total concentration of the uncomplexed reagent [L']. Table 2.2 shows the stability constants for copper citrate, lactate, tartrate, TEA and CAS complexes. (101) In this work, the strongest copper complex was formed by citric acid and the weakest by TEA. This was shown in the adsorption profiles whereby the citric acid complex bound the copper more strongly than the CAS and thus prevented full adsorption of the CAS-copper complex onto the carbon. However, CAS competed more successfully than TEA for the copper and so the CAS-copper complex was preferentially adsorbed. From the results, it would appear that the order of increasing ability to complex copper in the presence of CAS is

citrate > tartrate > TEA > lactate

CAS is less strongly complexing than the citrate, but more so than the tartrate. These results fit in well with the equilibrium constants where the citric acid-copper complex has a $pK_1$ value of 18.0 which is higher

**TABLE 2.2**

**LOG EQUILIBRIUM CONSTANTS FOR COPPER COMPLEXES** (101)

| | Temp | Medium | Log equilibrium constant $K_1$ |
|---|---|---|---|
| Citric Acid | 20 | 0.1M $NaClO_4$ | 18 |
| CAS | 25 | 0.1 | 4.02 |
| TEA | 25 | 0.1 | 3.9 |
| Tartaric Acid | 20 | 0.1 $NaClO_4$ | 3.2 |
| Lactic Acid | 31 | 0.1 | 2.55 |

than any of the other complexing agents studied. The weakest complexing agent examined was the lactic acid and this has the lowest $pK_1$ value.

More difficult to explain was the variation of adsorption of copper with different complexing agents without the competing presence of CAS. Size of molecule is a possible answer, although without further information or actual size and configuration of molecules, no definite conclusions can be drawn.

## 2.6 ADSORPTION OF CAS-METAL COMPLEXES ONTO POWDERED ACTIVATED CARBON

One of the major disadvantages of adsorbing metals onto the surface of CAS-coated activated carbon was the time required to reach equilibrium. As with ion-exchange, small particle size enhances adsorption owing to the increase in specific surface. The particle size of the carbon beads was about 0.5mm diameter. It was thought that equilibrium could be reached more rapidly by using activated carbon powder, whose particle size is below 100μm.

Owing to the difficulties of competing auxiliary complexing ligands in the previous experiments, advantage could be seen in adding CAS to the solutions, then adsorbing the preformed CAS-complexes onto the activated carbon.

### 2.6.1 Chemical reagents

Activated carbon Darco G-60 (Aldrich Chemical Co., Gillingham, Dorset, UK), was used throughout the experiments.

### 2.6.2 Stock Standard Solutions

Stock copper and magnesium standards as in 2.3.2 and 2.4.1 were used.

Stock calcium standard (10,000 $\mu g ml^{-1}$) was prepared by weighing the equivalent of 1.000g of calcium as high purity $CaCO_3$ and transferring it to a 100ml volumetric flask. Deionised water (5ml) and concentrated $HNO_3$ (5ml) were added carefully. After dissolution, the solution was diluted to 100ml with deionised water and stored in an acid washed polyethylene bottle.

Stock iron standard (10,000 $\mu g ml^{-1}$) was prepared by weighing out 1.000g of high purity iron sponge. This was transferred to a beaker and concentrated HCl (5ml) was added and heated to boiling until the sponge had dissolved. This was cooled and transferred to a 100ml volumetric flask, diluted with deionised water to 100ml and stored in a polyethylene bottle.

Stock manganese (10,000$\mu m l^{-1}$) was prepared by weighing out the equivalent of 1.000g of manganese as high purity MnO, concentrated $HNO_3$

(5mls) was added and after dissolution the solution transferred to a 100ml volumetric flask and made up to 100ml with deionised water. The solution was stored in an acid washed polyethylene bottle.

Nickel standard ($10,000\mu gml^{-1}$) was prepared by weighing out 1.000g of high purity nickel powder. This was transferred to a 100ml volumetric flask where concentrated $HNO_3$ (2ml) was added and the solution warmed until dissolution was complete. The solution was cooled and diluted to 100ml with deionised water and stored in an acid-washed polyethylene bottle.

### 2.6.3 Sample preparation

Six water samples (250mls) were spiked with $1\mu gml^{-1}$ of each of the test elements (Ca, Cu, Fe, Mg, Mn and Ni). CAS (10mg) was added and the pH of the solutions were adjusted according to predetermined optimum pH conditions. Activated carbon (0.5g) was added and stirred, taking aliquots at time intervals, filtered and the filtrate analysed by AAS. Reduction in element signal was again recorded. Two sets of glucose (30%), sucrose (20%) and potassium nitrate (10%) solutions were prepared and spiked with Cu and Mg ($1\ \mu gml^{-1}$). As above, CAS (10mg) was added to form the complexes in solution, activated carbon was introduced and stirred and filtered aliquots of the solution drawn off and analysed by AAS.

### 2.6.4 **Results and discussion**

Figure 2.10 a-f show the adsorption of test elements from water onto the carbon. The most striking feature is rapidity of adsorption, with equilibrium being reached in 2-5 minutes or quicker. It was found in a later experiment, that the presence of CAS was not required to effect copper adsorption onto the carbon. That this was not seen earlier in the experiments using activated carbon beads, suggested that a) the particle size of the carbon is critical - the smaller the size the higher the adsorbability resulting from the larger specific surface, and b) the surface chemistry of the carbon is important. The beads were spherical and hard and it was believed that they were of polymeric origin. The powder was manufactured from animal and plant material. The different origins of the carbon could have affected the surface chemistry, thus adsorbabilities. There is evidence to support the theory that $Cu^{2+}$ is reduced by the carbon to $Cu^{0}$ which plates onto the surface. Adsorption of copper from glucose, sucrose, and potassium nitrate solutions is shown in Figure 2.11, a-c. Adsorption is very rapid, even in sucrose, which at 20% is quite viscous. The adsorption of magnesium from the test solutions can be seen from Figure 2.12, a-c. It is interesting to note that before the addition of extra CAS and activated carbon, the degree of adsorption in each solution is similar. This suggests that the CAS was not complexing the magnesium, but rather the ion-exchange group in the CAS molecule was exerting an effect. This was seen when an extra 10mg of CAS was added to the solutions. In all cases, the adsorption of copper

FIGURE 2.10
ADSORPTION OF METALS ONTO POWDERED ACTIVATED CARBON USING CAS CHELATING DYE

a)CALCIUM (pH10)

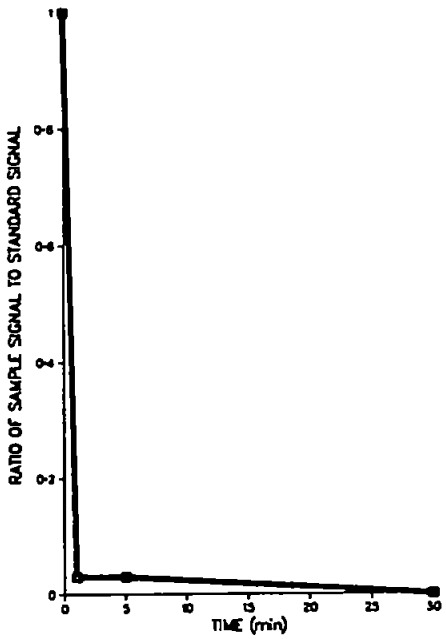


b)MAGNESIUM (pH10)

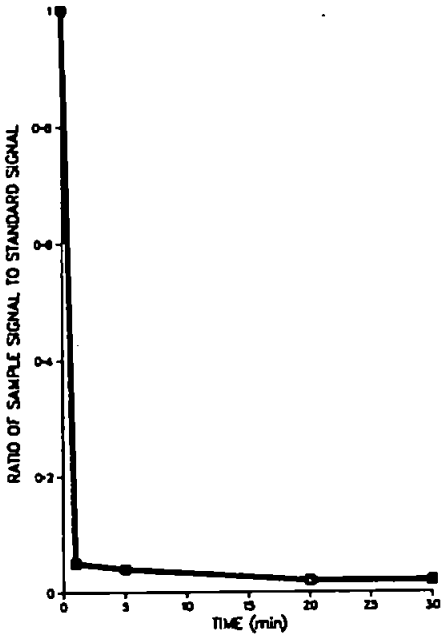


c)MANGANESE (pH5.8)

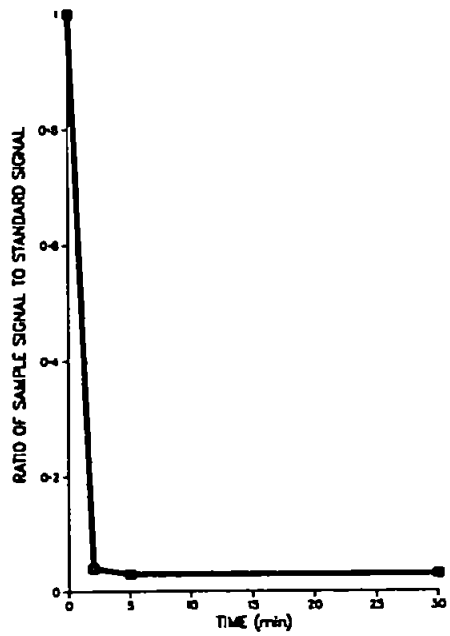


d)IRON III (pH2.4)

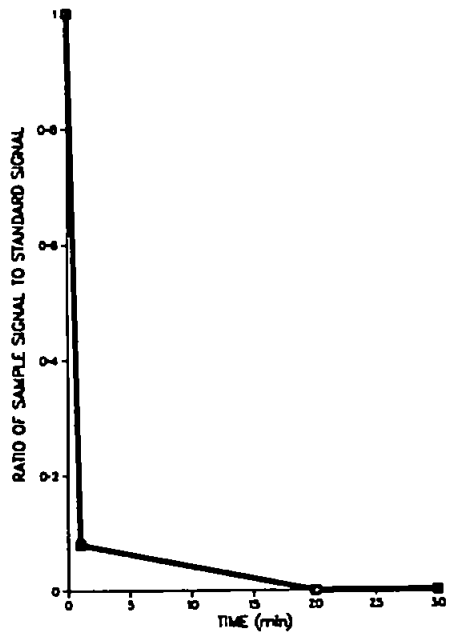

FIGURE 2.10 cont.

e)NICKEL (pH 6.5)

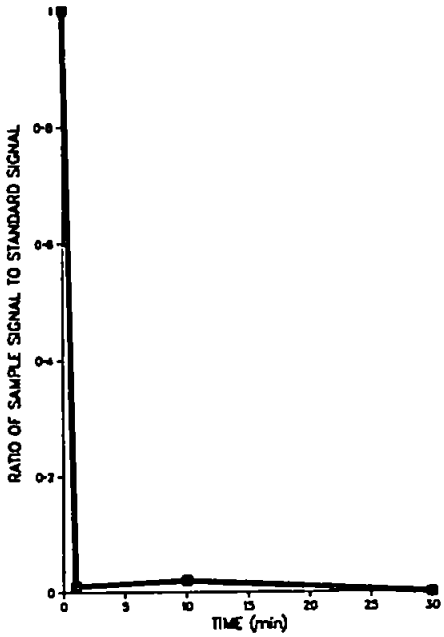


f)COPPER (pH5.6)

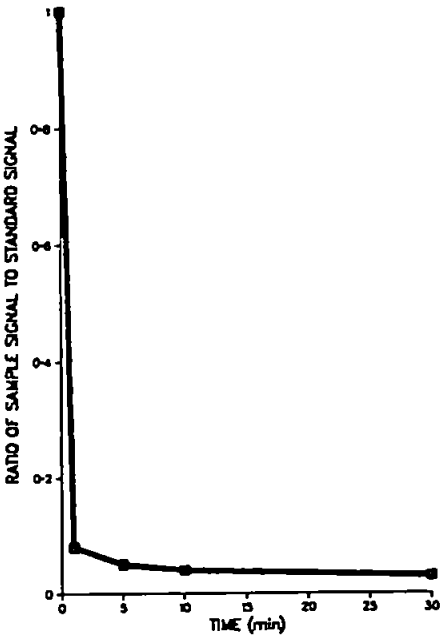

FIGURE 2.11
ADSORPTION OF 1µg/ml COPPER ONTO ACTIVATED CARBON USING CAS CHELATING DYE

a)10% POTASSIUM NITRATE

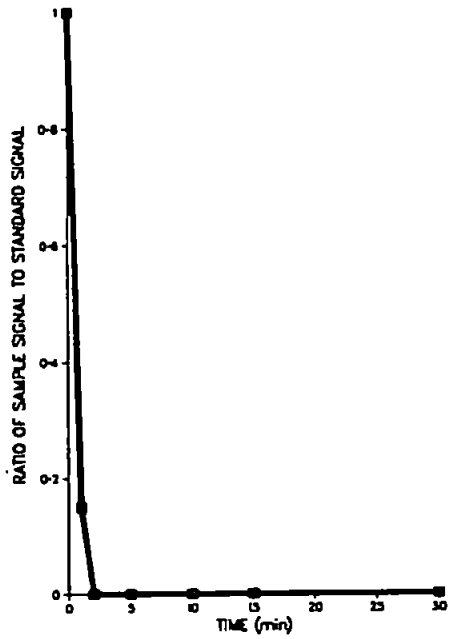


b)20% SUCROSE

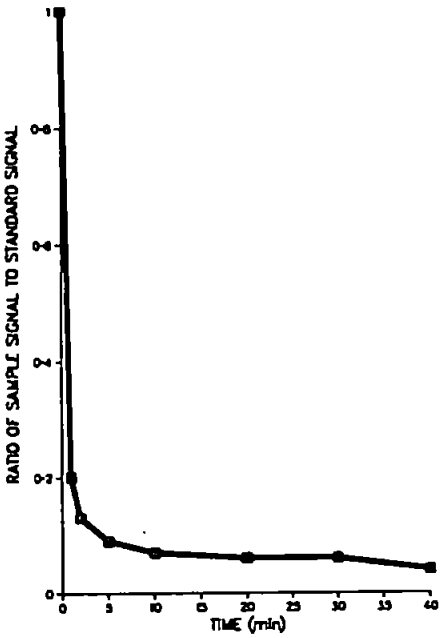


c)30% GLUCOSE

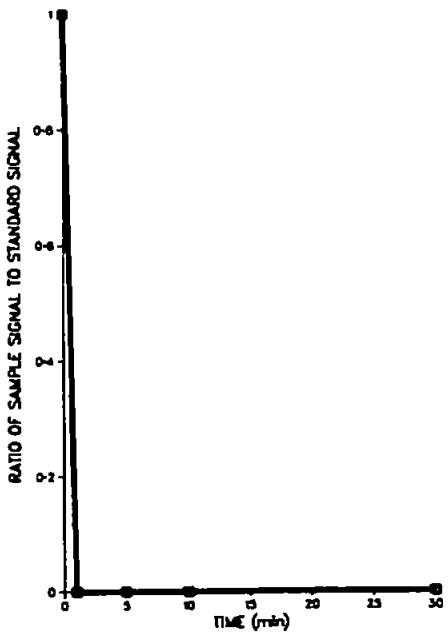

FIGURE 2.12
ADSORPTION OF 1µg/ml MAGNESIUM ONTO ACTIVATED CARBON USING CAS CHELATING DYE

a)10% POTASSIUM NITRATE (pH11)

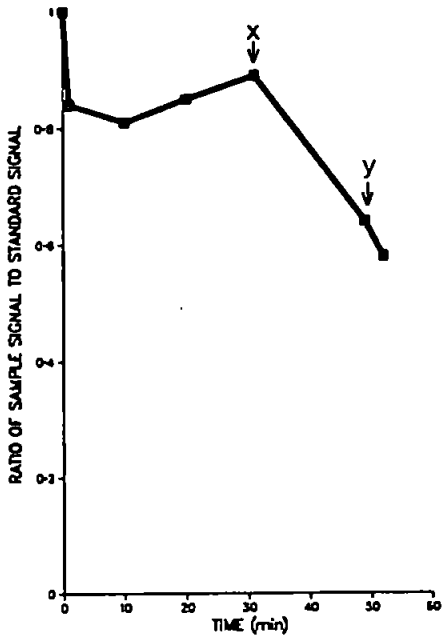


b)20% SUCROSE (pH11)

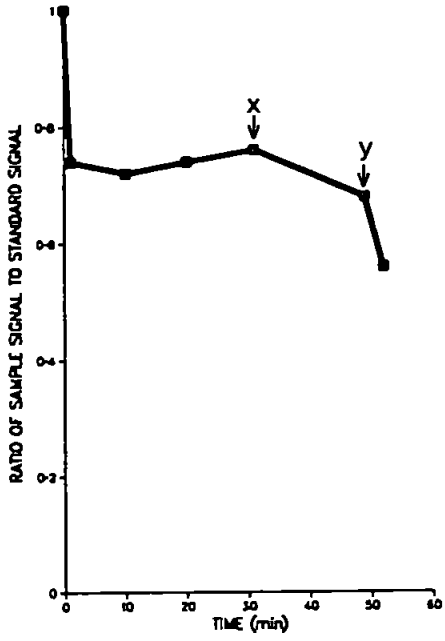


c)30% GLUCOSE (pH11).

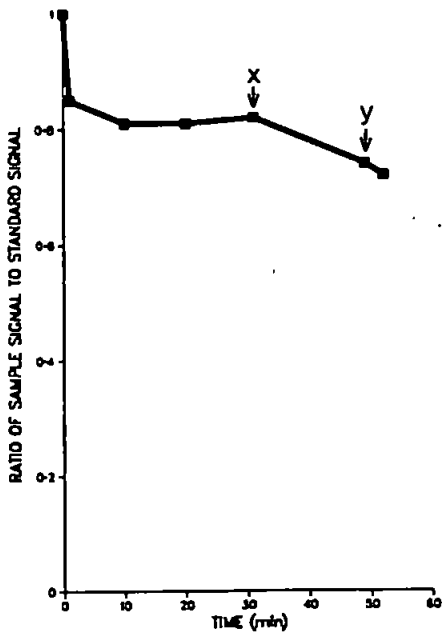


x= addition of further 10mg cas

y.= addition of further 0.5g activated carbon

increased. Addition of more activated carbon also increased the adsorption of magnesium. A possible explanation of this was that the surface of the carbon was saturated and could not physically adsorb any more magnesium. With the use of a more appropriate complexing agent it is thought that adsorption of magnesium onto activated carbon could be achieved.

## 2.7 CONCLUSIONS

This chapter has shown the feasibility of adsorbing metal ions from solution onto a solid support. The use of conventional ion-exchange resins is limited in this work owing to an inability to exchange metal ions, such as copper, in the presence of an excess of alkali or alkaline earth metals. One of the main aims of the work was to preconcentrate metal ions from electrolytic solutions and so ion-exchange resins would be of little use in this area.

The chelating resin, Chelex-100, was able to adsorb both copper and magnesium from 10% potassium nitrate. However, problems with sample introduction into the ICP curtailed its use.

Powdered activated carbon, in the presence of CAS chelating dye was found to be the most promising material. The high adsorbability of activated carbon gave impressive equilibration times. Ca, Cu, Fe, Mg, Mn and Ni were all adsorbed successfully in aqueous solutions, although

magnesium in concentrated sucrose, glucose and potassium nitrate solutions was not. In order to adsorb magnesium, a different chelating reagent would need to be used.

# CHAPTER 3

# DEVELOPMENT OF OPTIMISATION STUDIES FOR FLOW INJECTION - SLURRY ATOMISATION

## 3.1 INTRODUCTION

Inductively coupled plasma atomic emission spectrometry (ICP-AES) has become a valuable tool for the determination of major and minor constituents in a range of samples. This plasma source provides a wide dynamic working concentration range and is relatively free from chemical interferences. These attributes combine to enhance the scope and versatility of the technique with respect to the number of analytes that can be measured and the number of sample matrices that can be analysed.

### 3.1.2 Sample introduction into the ICP

The first stage in ICP analysis is the introduction of the sample into the plasma. In principle, the sample can be in the solid, liquid or gaseous state. Liquid samples are generally preferred, owing to homogeneity, standardisation and handling considerations. However, many samples occur naturally in the solid form and practical advantages can be realised if solid samples are introduced directly into the plasma, without pre-treatment or conversion to a liquid. For example, samples may be analysed in their natural state; contamination from reagents is minimised; dilution errors are reduced; sample transfer losses arising from extra sampling handling steps are avoided and reagent and manpower costs are

reduced. A number of methods may be used to introduce solids directly into the ICP. However, many of these for example, mechanical agitation of powders (67, 102, 103), fluidised bed chambers (104), and direct insertion into the plasma on a graphite rod (78), suffer problems arising from density differences of components within the sample, leading to segregation and inhomogeneity. For a more detailed discussion on various solid sample introduction methods, references 105 and 106 are recommended.

### 3.1.3 Slurry sample introduction into the ICP

This work introduced solid samples into the ICP in the form of slurries. Work has shown (see Chapter 1) that the particle size distribution of the slurry is a vital factor. If the distribution includes a significant fraction over 8μm in diameter, atomisation/transport efficiency is greatly affected. Therefore, it was necessary to reduce the particle size to below 8μm, and preferably lower, by a suitable grinding procedure. Effective dispersal of the slurry is an equally important criterion in slurry atomisation. A slurry incorporates a solid, generally a powder, into a liquid medium. The powder becomes difficult to disperse if its surface is lyophobic. A dispersing agent is added therefore, to wet the surface of the lyophobic material, thus rendering it lyophilic.

### 3.1.4 Aerosol generation

Having prepared a slurry with particle size below 8μm, the next stage in the analysis is its introduction into the plasma source as an aerosol. This

is effected by the use of a nebuliser which converts a solution or slurry, into a fine mist. The Babington-type nebuliser is the preferred device for slurry nebulisation. The nebuliser used in this work, the so called 'Ebdon Nebuliser', (Figure 3.1) reported by Ebdon and Cave (76), is a V-groove variant of the geometry of the Babington-type. Unlike the Meinhard nebuliser which is susceptible to blocking, the Ebdon nebuliser is completely unblockable. The nebuliser is constructed in Kel-F or PTFE and has two channels drilled along its length ending in orifi. The sample is pumped along the upper channel (1.2mm diameter) and gas through the lower one. As the sample emerges from the nebuliser block, it runs down the V-groove and over the gas orifice (0.2mm diameter). The high velocity gas shatters the sample into droplets, which are then carried through the spray chamber and into the plasma.

All pneumatic nebulisers produce primary aerosols with broad droplet size distributions. If these large droplets reached the plasma it would cause instability and so it is necessary to remove these using a spray chamber as a separator or filtering device. It is important to note that the final state of the aerosol as it enters the plasma, is not just a function of the spray chamber, but also of the torch injector and aerosol delivery tube.

The addition of a spray chamber aerosol delivery system to the nebuliser, has a number of effects:

(i) the aerosol particle size distribution is modified;

(ii) the aerosol concentration is decreased;

(iii) the phase equilibrium of the aerosol is modified towards the establishment of thermal equilibrium;

## FIGURE 3.1
## SCHEMATIC DIAGRAM OF EBDON NEBULISER

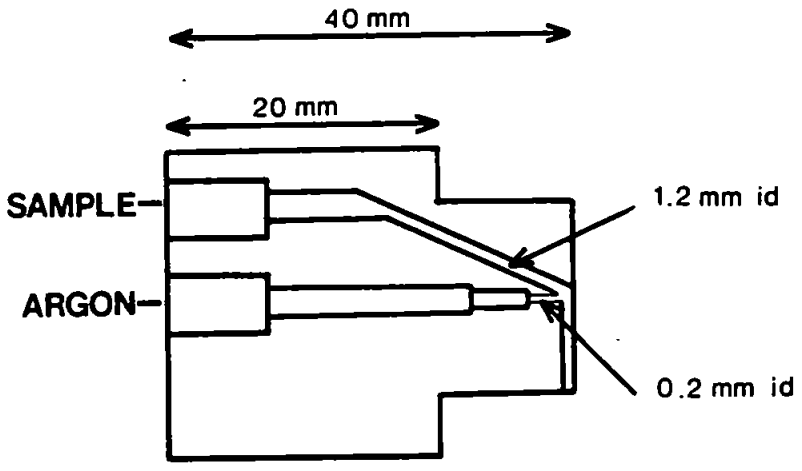

(iv) the charge equilibrium is modified;

(v) the turbulence that is associated with the nebulisation process, and conversion of the inertial energy into heat, is reduced. These effects are accounted for by a number of processes, for example, recombination, inertial impaction, evaporation, charging/discharging and the decay of turbulence and these processes are greatly affected by the geometry of the spray chamber. For continuous, steady state nebulisation of typical nebuliser uptake rates (1-2 $mlmin^{-1}$), and injector gas flow rates (0.5 - 1.5 $Lmin^{-1}$), the transport efficiency of nebulisation is about 1-2%. This means that only 10-40$\mu lmin^{-1}$ of actual analyte, gets to the plasma. In flow injection (FI) sample volumes of for example 200-300µl are injected into a flowing carrier stream. At the transport efficiency rate specified above, only 2-6µl reaches the plasma (107), it is evident therefore, that the power of detection achievable with such nebulisation systems is limited.

The aim of this study was to introduce small volumes of slurries (<500µl) into the ICP by FI. It was thought that this would be most successfully achieved by reduction of the spray chamber volume, hence dispersion of sample, and therefore yielding better sensitivity. It was important however, with this aim, that the overall objective of the spray chamber, of producing a stable aerosol stream of small droplets, with a narrow particle size distribution, was maintained.

## 3.2 EXPERIMENTAL

The plasma emission spectrometer used was a sequential computer-

controlled, fully integrated ICP (Plasmakon S35, Kontron Spektralanalytik, Eching, FRG). The plasma operating conditions were as follows: power (net forward), 1.5kW; carrier gas flow rate, 1.5Lmin$^{-1}$; outer gas flow rate, 15Lmin$^{-1}$; and intermediate gas flow rate, 0.4Lmin$^{-1}$. This instrument incorporates a data acquisition system which does not have a direct analogue to digital converter (ADC) between the photomultiplier tube (PMT) and the computer. Instead, a system of voltage to frequency conversion is used whereby the PMT is gated (time base regulated) by the computer. Such a system offers clear advantages for FI as this more rapid data reading facility, compared with normal ADC, means that sampling rate problems associated with ADCs used in FI work are not encountered.

A Minipuls peristaltic pump, (Gilson, Luton, Beds. UK) together with a six-port switching valve (P.S. Analytical, Sevenoaks, Kent, UK) and 0.8mm i.d PTFE tubing formed the basis of the FI manifold. A variety of PTFE injection loops (100-500µl) and connecting tube lengths were used. The sample was supplied to the nebuliser via the peristaltic pump. The sample was introduced into the plasma in the form of an aerosol which was produced by a high-solids PTFE nebuliser (Ebdon nebuliser P.S. Analytical). The aerosol was carried into a spray chamber. Initial studies, performed with a conventional Scott double-pass spray chamber, were disappointing. Presumably the large volume of this spray chamber caused excessive dilution of microlitre-sized samples with the carrier stream. An in-house designed spray chamber (Figure 3.2) was examined for use in FI.

**FIGURE 3.2**

**DIAGRAM OF BULBOUS-ENDED SPRAY CHAMBER**

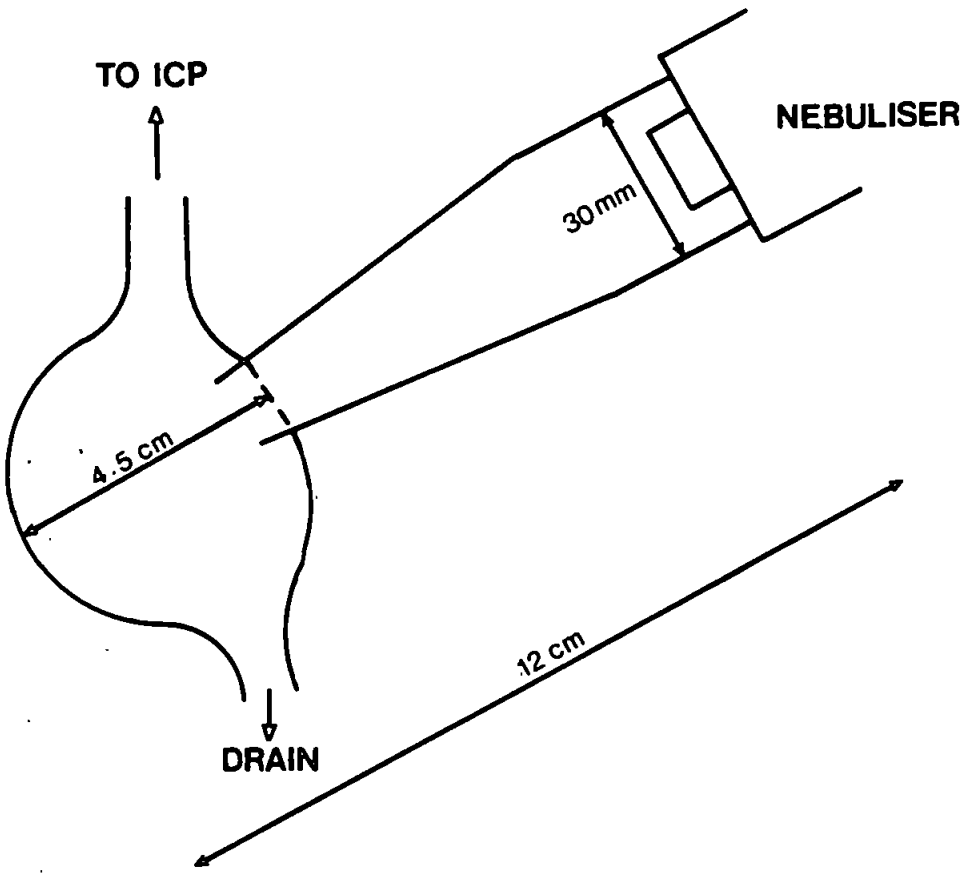

Particle size distributions were measured using a Coulter Counter TA II multi-channel particle analyser (Coulter Electronic Ltd., Luton, Beds., UK). The instrument can measure electronically, the volume of particles in the size range from 0.6-800μm. This is achieved by measuring the change in potential difference as particles suspended in an electrolyte, are sucked through a small orifice. This is possible, since as the particle traverses the orifice, it alters the resistance of the flow of current across the section. The instrument operates at constant current, hence the change in potential is also proportional to volume. Coulter electrolyte (Isoton II) was used for particle size measurements and a 140μm orifice tube for all the determinations.

### 3.2.1 Reagents

For preliminary experiments, Dowex 50W-X8 (100-200 mesh) ion-exchange resin (BDH Ltd., Poole, Dorset, UK) was used. Validation experiments were carried out using two Certified Reference Material (CRM) soils, S01 and S02 (CANMET, Ottawa, Ontario, Canada).

All reagents were of analytical grade (BDH Ltd.) and all solutions prepared with doubly distilled, deionised water.

### 3.2.2 Sample preparation

#### 3.2.2.1 Ion-exchange resin slurry preparation

Ion-exchange resin (1g) was weighed into a polypropylene screw-topped

bottle and 10g of polyacrylic spheres (Glen Creston, Stanmore, Middlesex, UK) were added. This was shaken for a period until the particle size of the slurry was below 8μm, typically 2-4 hours. The slurry and grinding medium were separated and washed through a Buchner funnel, into a calibrated flask. Copper was then added to a total concentration of $20\mu g ml^{-1}$.

An aqueous $20\mu l ml^{-1}$ copper solution was also prepared.

### 3.2.2.2 Certified Reference Material preparation

The comminution method chosen involved shaking a known amount of reference soil with tetrasodium pyrophosphate dispersant solution (overall concentration of dispersant 1% m/v) and zirconia grinding medium (in the ratio of 1:10 sample:grinding medium (108) in a sealed polypropylene bottle for 3 hours (53). The spheres were washed and removed from the solution and made up to the required volume. Particle size distributions are shown in Figures 3.3 and 3.4.

## 3.3 RESULTS AND DISCUSSION

Before any analyses were performed, the controlling parameters were investigated. Variables studied included spray chamber design, sample injection volume and carrier stream flow rate.

FIGURE 3.3
PARTICLE SIZE DISTRIBUTION OF SO1 AFTER GRINDING

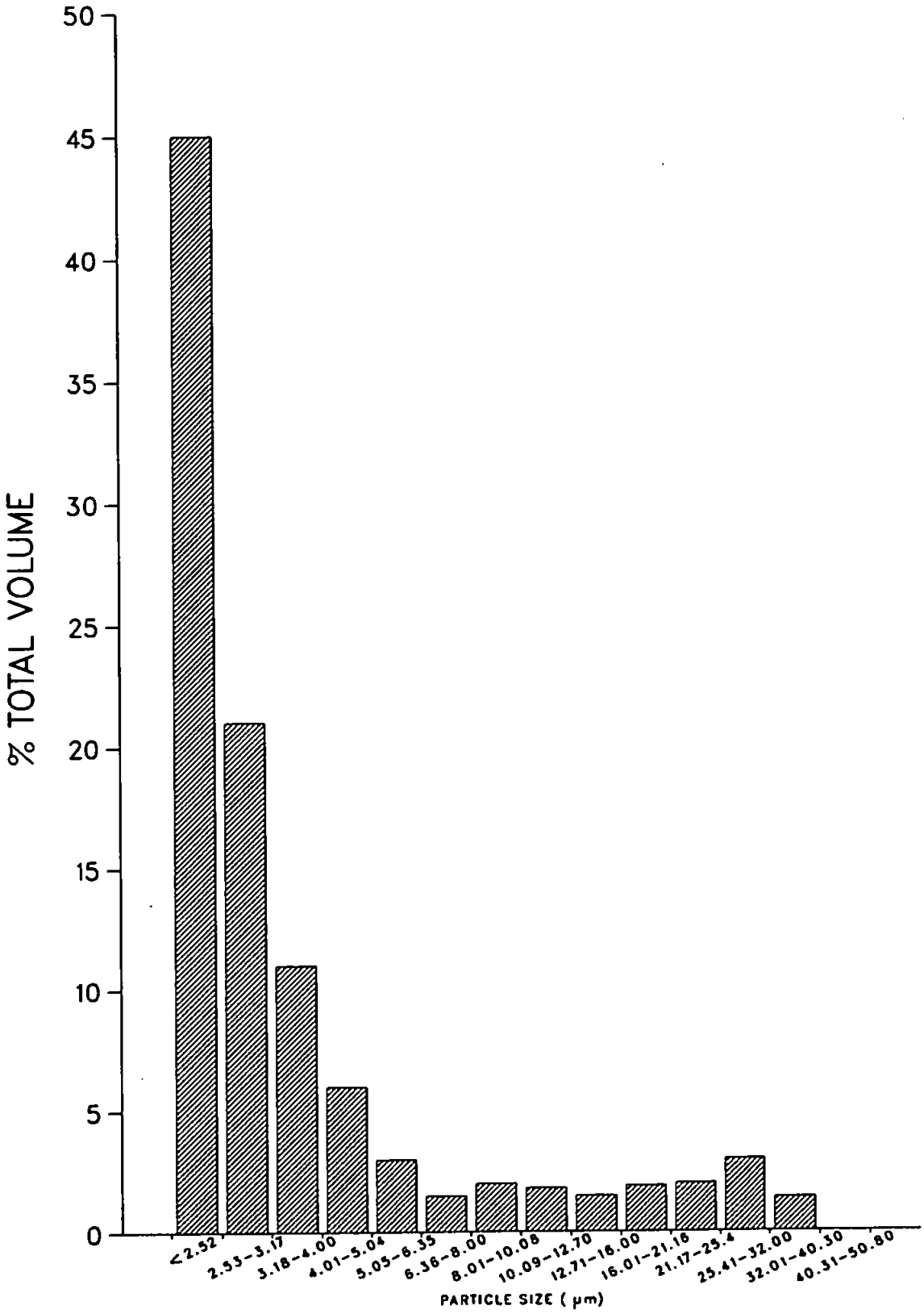

FIGURE 3.4
PARTICLE SIZE DISTRIBUTION OF SO2 AFTER GRINDING

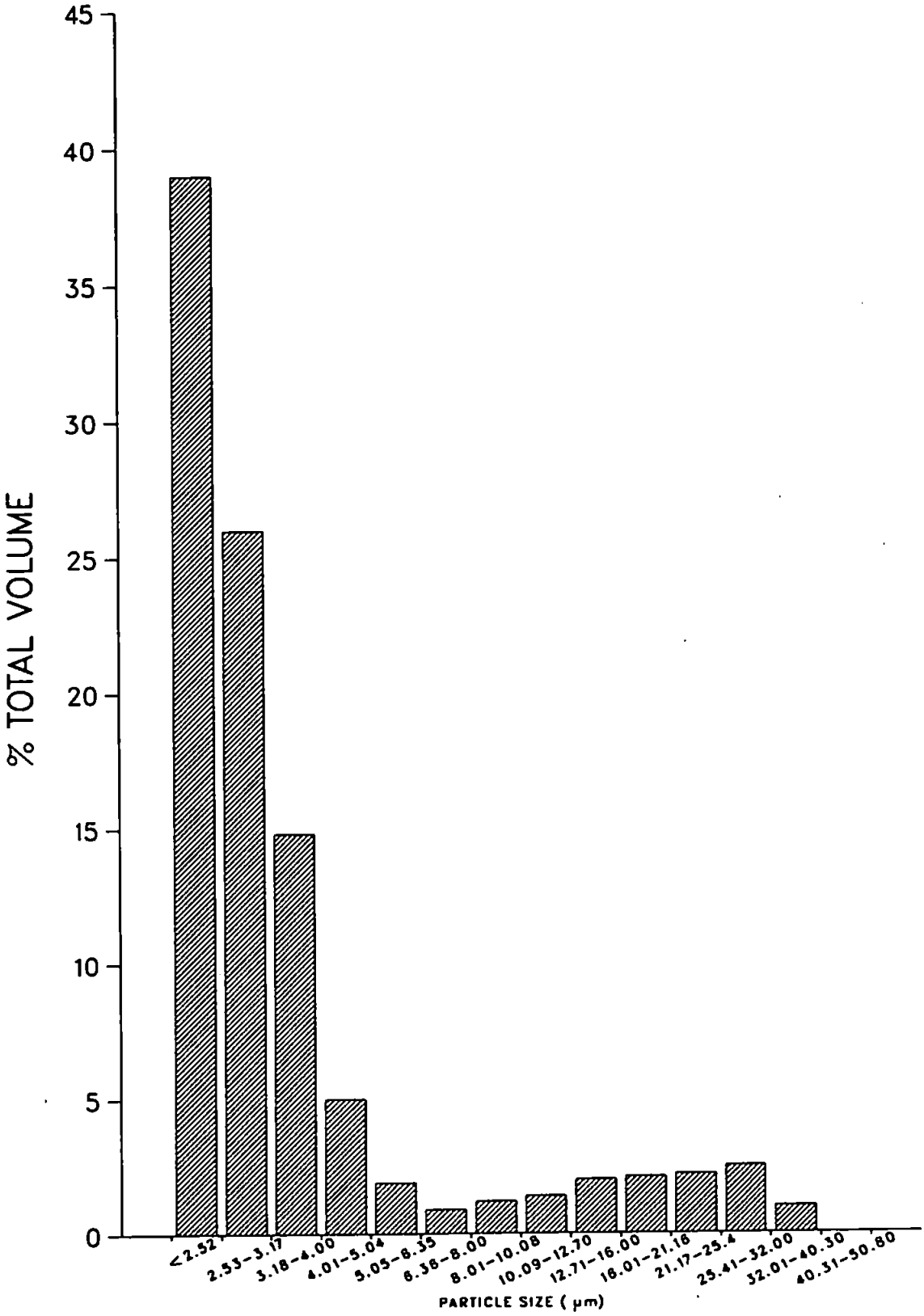

### 3.3.1 Spray chamber design

Preliminary experiments were performed using a conventional Scott double-pass spray chamber (SDPSC). However, as mentioned earlier this caused excessive dispersion. The spray chamber was replaced by a single-pass design (SPSC). Problems were encountered with the formation of condensation at the base of the injector tube, causing instability of the plasma.

The spray chamber that was chosen (Figure 3.2) was the bulbous-ended spray chamber (BESC) which was longer than the straight through variety. As the slurry emerged from the nebuliser some of the larger particles impacted on the adjacent glass surfaces. The larger particles should be eliminated by the bends in the chamber and go to drain. In the SDPSC, particles that have negotiated the reverse direction between the inner and outer tubes travel back along the spray chamber, where gravitational forces and impaction may cause more particles to drop out. With the spray chamber shown in Figure 3.2, the particles do not have to travel along a second chamber but enter directly into the injector tube. Although the volume of the BESC was slightly higher than the SDPSC, 120 and 110ml respectively, the BESC offered an easier route for the particles to travel, hence the 50% increase in sensitivity observed.

### 3.3.2 Sample injection volume

An ion-exchange resin (10% m/v) spiked with 20 $\mu g ml^{-1}$ of copper was used in this experiment. Figure 3.5 compares the response for the copper

FIGURE 3.5
EFFECT OF VARYING INJECTION VOLUME ON SIGNAL FOR A 20µgml$^{-1}$ COPPER SOLUTION AND A RESIN SLURRY SPIKED WITH THE SAME CONCENTRATION OF COPPER

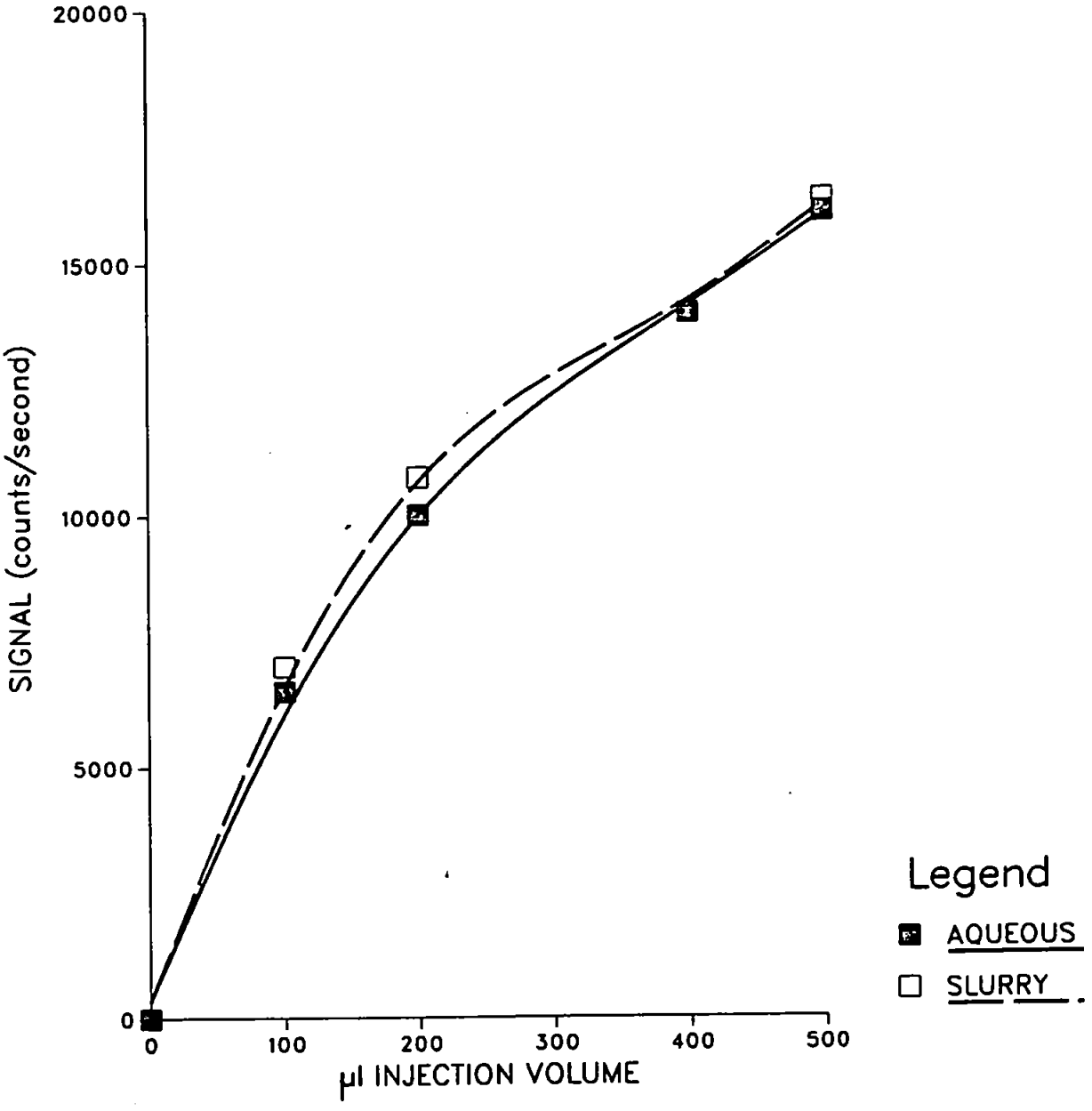

-spiked ground resin and an aqueous sample with the same concentration, with increasing injection volume. The slurry signal tended to be slightly higher than the aqueous response and it is thought that this was due to the slurry being a two phase system, thereby reducing dispersion. As can be seen from the graph, the signal increased with increasing injection volume. This was not unexpected because dispersion at smaller volumes is increased and so the sample is more 'dilute' when it reaches the plasma.

Previous work showed that with a Scott double-pass spray chamber a 500µl injection volume gave a response 75% of that obtained by continuous nebulisation. The bulbous-ended spray chamber alleviated this problem, so that signals from continuous and discrete nebulisation were comparable at sample volumes of 500µl and above. This was particularly advantageous as it meant that standards could be either nebulised continuously or introduced by FI.

### 3.3.3 **Carrier stream flow rate**

The carrier stream used in this experiment was doubly-distilled, deionised water. The flow rate was controlled by a peristaltic pump with variable speed settings. The effect of increasing the pump flow rate on the signal was to sharpen up the peak characteristics. Peak height was not affected greatly in either spray chamber. A flow rate of 5.5mlmin$^{-1}$ was chosen as this gave a peak with good sensitivity and symmetry. The high carrier stream flow rate also increases sample throughput.

### 3.3.4 Analysis of slurries of Certified Reference Materials

To validate the FI slurry atomisation ICP-AES technique two slurries of CRM soils S02 and S02 were prepared, 0.1% m/v for minor element determinations and 5% m/v for trace elements. Results obtained by FI slurry atomisation using conventional aqueous standards for calibration are shown in Table 3.1. It can be seen that the technique offered excellent agreement with certified values for all six elements studied. Typically the precision was around the 2% (relative) level, which is similar to that obtained with this instrumentation for aqueous solutions.

In conclusion to this set of experiments, FI-slurry atomisation ICP-AES has proved to be a viable analytical technique. A new design of spray chamber offering excellent characteristics for FI-ICP-AES has been developed. Overall, the technique combines many of the advantages of FI with the greater sample throughput and other advantages of slurry atomisation. The application of FI to slurries is as convenient as to solutions and no major instrumental modifications are required. Indeed, the more favourable dispersion characteristics of slurries may be advantageous compared with FI of solutions.

From the results it appeared that reduction of spray chamber volume led to an increase in sensitivity. However, it was not clear as to whether this was due to a reduction in dispersion of the sample in the carrier stream, or to the different geometric design of the chamber, which may have altered the emergent particle size distribution and transport efficiency of the system. Thus a need was identified to investigate the

**TABLE 3.1**

DETERMINATION OF ELEMENTS IN CRM SOILS S02 AND S02 USING FI SLURRY ATOMISATION ICP-AES

| Soil | Element/ Concentration Units | Experimental result* | Certified Value |
|---|---|---|---|
| S01 | Ca/% | 1.75 ± 0.02 | 1.8 ± 0.07 |
| | Fe/% | 5.9 ± 0.13 | 6.0 ± 0.13 |
| | Mg/% | 2.25 ± 0.17 | 2.31 ± 0.003 |
| | Mn/% | 0.089 ± 0.001 | 0.089 ± 0.003 |
| | Cu/$\mu gg^{-1}$ | 59.0 ± 0.1 | 61.0 ± 3.0 |
| | V/$\mu gg^{-1}$ | 132.0 ± 5.0 | 139.0 ± 8.0 |
| S02 | Ca/% | 1.95 ± 0.11 | 1.96 ± 0.1 |
| | Fe/% | 5.3 ± 0.16 | 5.56 ± 0.16 |
| | Mg/% | 0.54 ± 0.02 | 0.54 ± 0.03 |
| | Mn/% | 0.068 ± 0.012 | 0.072 ± 0.002 |
| | Cu/$\mu gg^{-1}$ | 8.0 ± 0.1 | 7.0 ± 1.0 |
| | V/$\mu gg^{-1}$ | 60.0 ± 5.0 | 64.0 ± 10.0 |

* Means of six replicate determinations ± 2 standard deviations

effect of spray chamber design upon analytical performance. The performance of various nebuliser/spray chamber configurations may be partially assessed by measurement of the particle size distribution of the emergent sample and the transport efficiency of the system.

Four spray chambers were assessed for their emergent particle size distributions and transport efficiencies:- a Scott double-pass spray chamber (SDPSC), a single-pass (SPSC), the bulbous ended chamber (BESC) used in the previous experiments, and a smaller version of the BESC, the reduced volume spray chamber (RVSC) and are shown in Figure 3.6, 3.7 and 3.8 respectively. The BESC is illustrated in Figure 3.2. Numerous techniques have been employed to trap aqueous aerosols, such as momentum transfer methods (110, 111), collection on membrane filters (112-114) or on U-tubes packed with silica gel for aqueous sprays and activated carbon for organic sprays (115). Cascade impaction is another method that may be used (113, 116, 117) and this approach was used in this study, for the collection of aerosol particles and calculation of transport efficiency.

## 3.4 EXPERIMENTAL

The cascade impactor used in this work was of the Andersen stack sampler type (Figure 3.9). A mark III Andersen stack sampler (Andersen Samplers Inc., Atlanta, Georgia, USA) was positioned above the exit point of a 1.8mm i.d. capillary injector, which was connected to each of the spray chambers under investigation. Slurries (500mls) of 1% m/v activated carbon were used in all experiments, having been previously

## FIGURE 3.6

## DIAGRAM OF SCOTT DOUBLE-PASS SPRAY CHAMBER

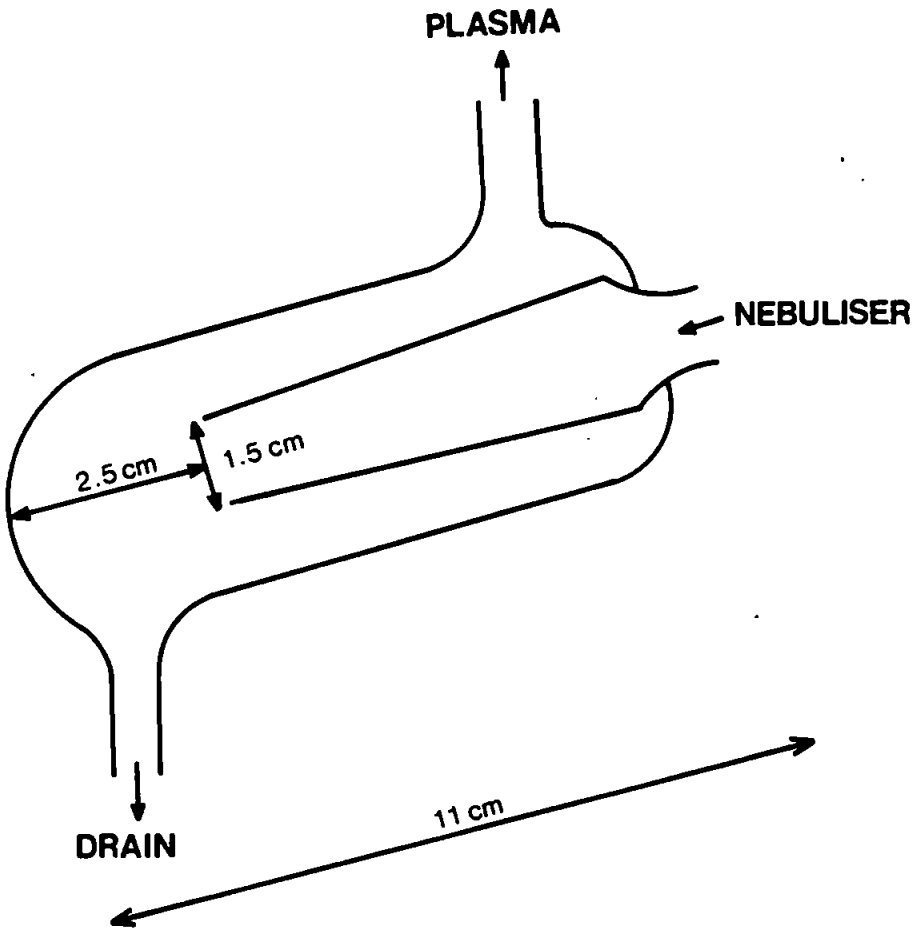

**FIGURE 3.7**

**DIAGRAM OF SINGLE-PASS SPRAY CHAMBER**

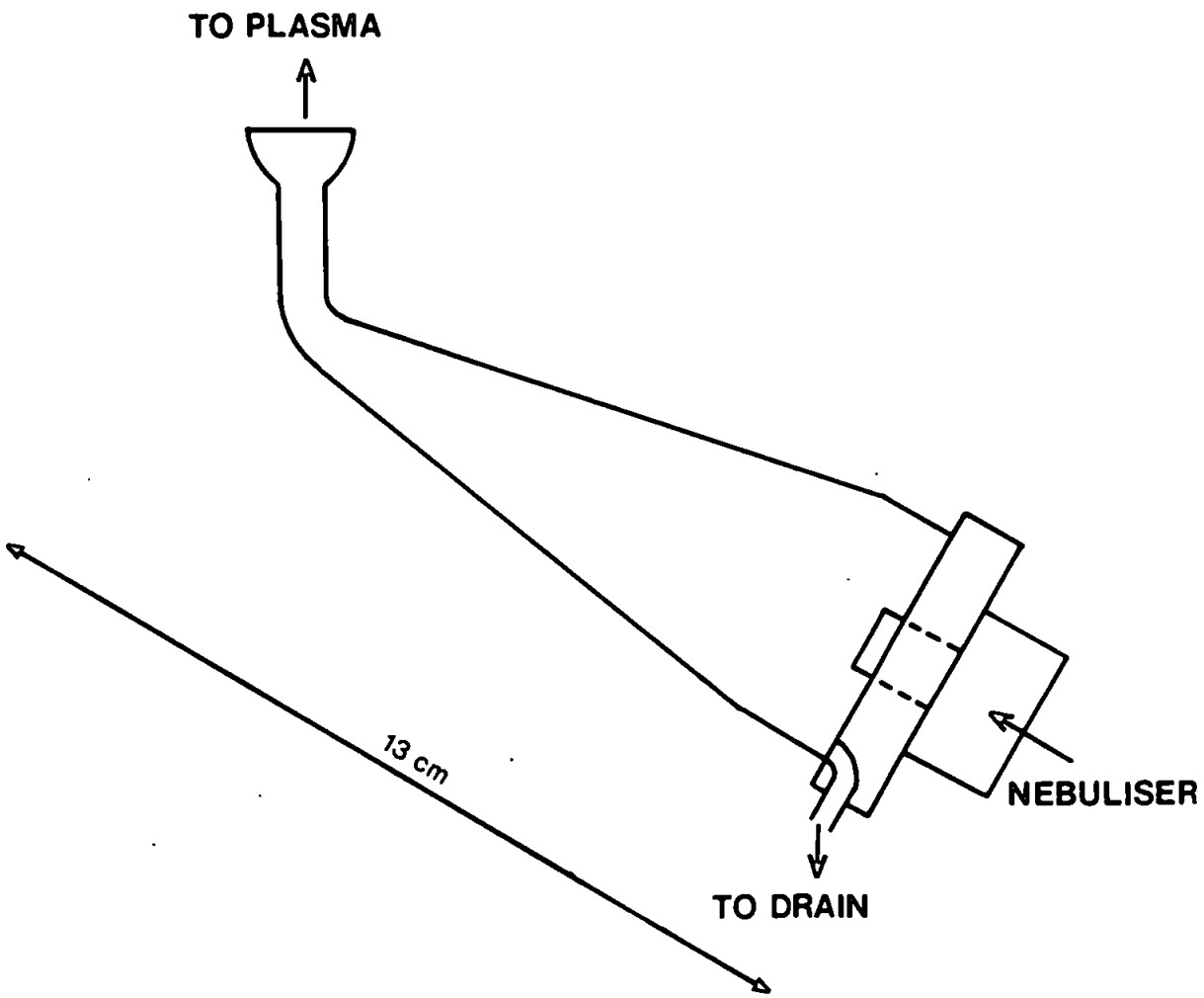

**FIGURE 3.8**
**DIAGRAM OF REDUCED-VOLUME SPRAY CHAMBER**

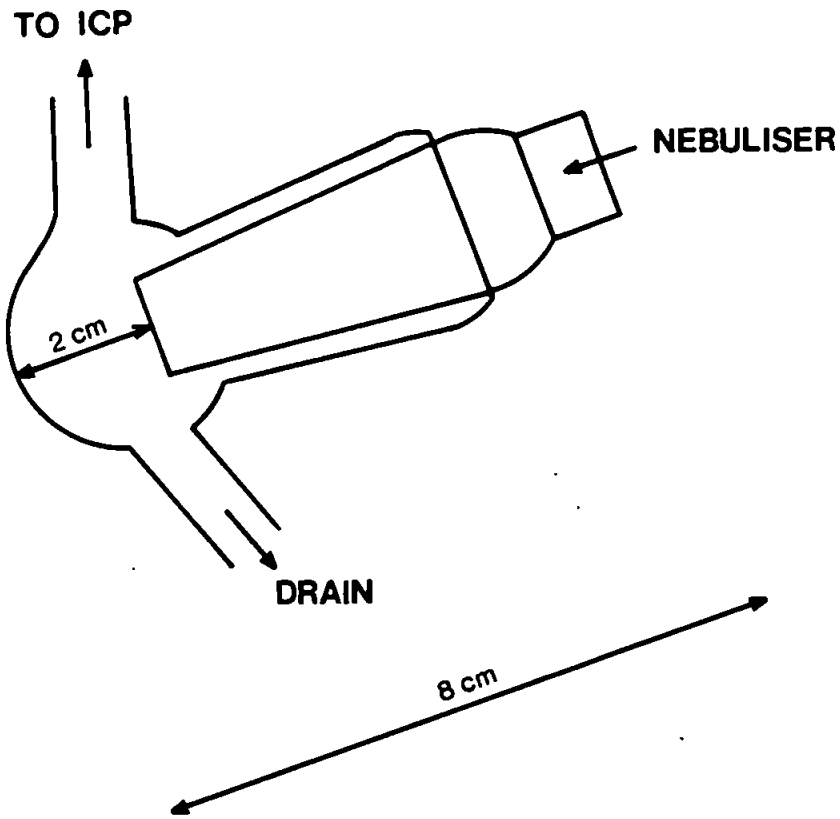

**FIGURE 3.9**
**THE ANDERSEN STACK SAMPLER**

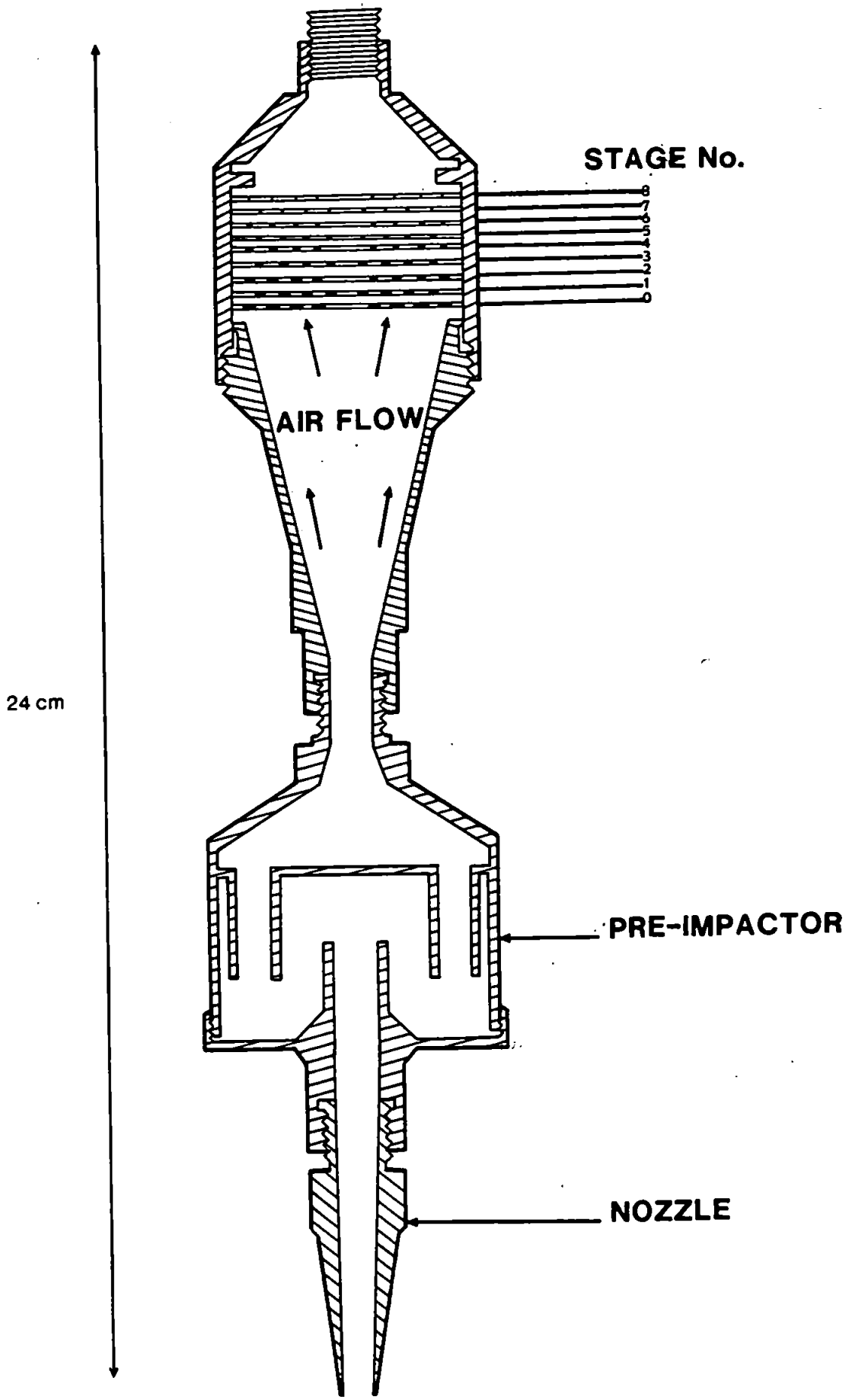

ground by the bottle and bead method described earlier. All slurries were dispersed in 1% Triton-X100 (BDH Ltd., Poole, Dorset, UK). These were supplied to a 'mini-Ebdon' nebuliser (Figure 3.10) (P.S. Analytical) via a peristaltic pump at $2 ml min^{-1}$. In order to evaluate the SPSC and the RVSC, it was necessary to reduce the size of the Ebdon nebuliser, which was physically too large to fit. The nebuliser and gas flow rate was $0.6 L min^{-1}$ and isokinetic sampling was performed according to the following equation:

$$Q_o = Q_i \, d_o^2 / d_i^2 \quad ..... \quad 3.1$$

where $Q_o$. is the rate at which the aerosol is drawn into the stack ($L min^{-1}$), $Q_i$, the rate of the gas carrying the sample ($L min^{-1}$), $d_o$, the diameter of the cascade impactor inlet nozzle (mm) and $d_i$, the diameter of the injector tube from which the sample is issued (mm). All the solid material collected after consumption of all the sample, was weighed and transport efficiencies were calculated by the summation of the slurry masses obtained from each of the impactor stages, ratioing to the slurry starting weights, pre-nebulisation and multiplying by 100. Particle size distributions of the total post-nebulisation slurry were carried out using a Coulter Counter.

A $3.7 \times 10^{-2}$W laboratory compressor fitted with an in-line calibrated flow meter was used to draw air through the cascade impactor.

## FIGURE 3.10
## SCHEMATIC DIAGRAM OF MINI-EBDON NEBULISER

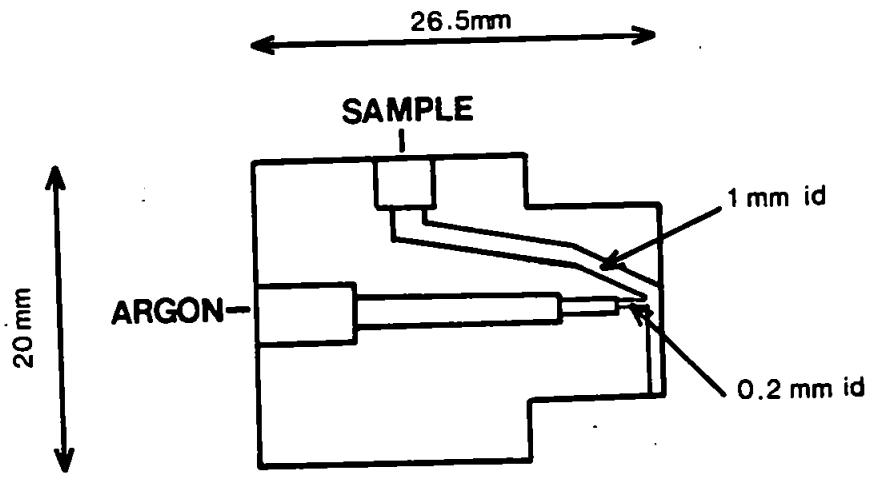

## 3.5 RESULTS AND DISCUSSION

The particle size distributions of 1% activated carbon slurries, emerging from four different spray chamber arrangements are shown in Figure 3.11. At first glance, it would appear that large particles are transported through the nebuliser system in the cases of the SDPSC and RVSC. In the case of the SDPSC, the whole of the distribution is not shown, and perhaps only half has been represented. The Coulter Counter measures the percentage of total volume within each size band. The tube used in this experiment was 140μm, whose lower limit is 2.52μm. It calculates % Total volume as though the whole distribution, above 2.52μm, is shown. The larger particles therefore are more pronounced than they would have been had the full distribution been observed.

Larger particles were observed with the RVSC. In this case, more of the whole distribution was viewed and so it is probable that some larger particles did reach the exit of the injector tube. This was not unexpected as the volume of the chamber was only 30ml.

The SPSC chamber was effective at filtering out the larger particles with the distribution being below about 5μm. With the chamber being small, and only single pass, one would have expected the facilitation of large particle transfer. However, the constriction in the structure before it enters the injector tube causes the larger particles to impact on the surface.

The BESC had a particle size cut-off of 8μm. This chamber was just a

FIGURE 3.11
EFFECT OF SPRAY CHAMBER DESIGN UPON PARTICLE SIZE DISTRIBUTION OF A 1% ACTIVATED CARBON SLURRY EMERGING FROM A 1.8mm ID INJECTOR TUBE (Carrier gas flow rate: 0.63Lmin$^{-1}$;Sample uptake rate: 2mlmin$^{-1}$)

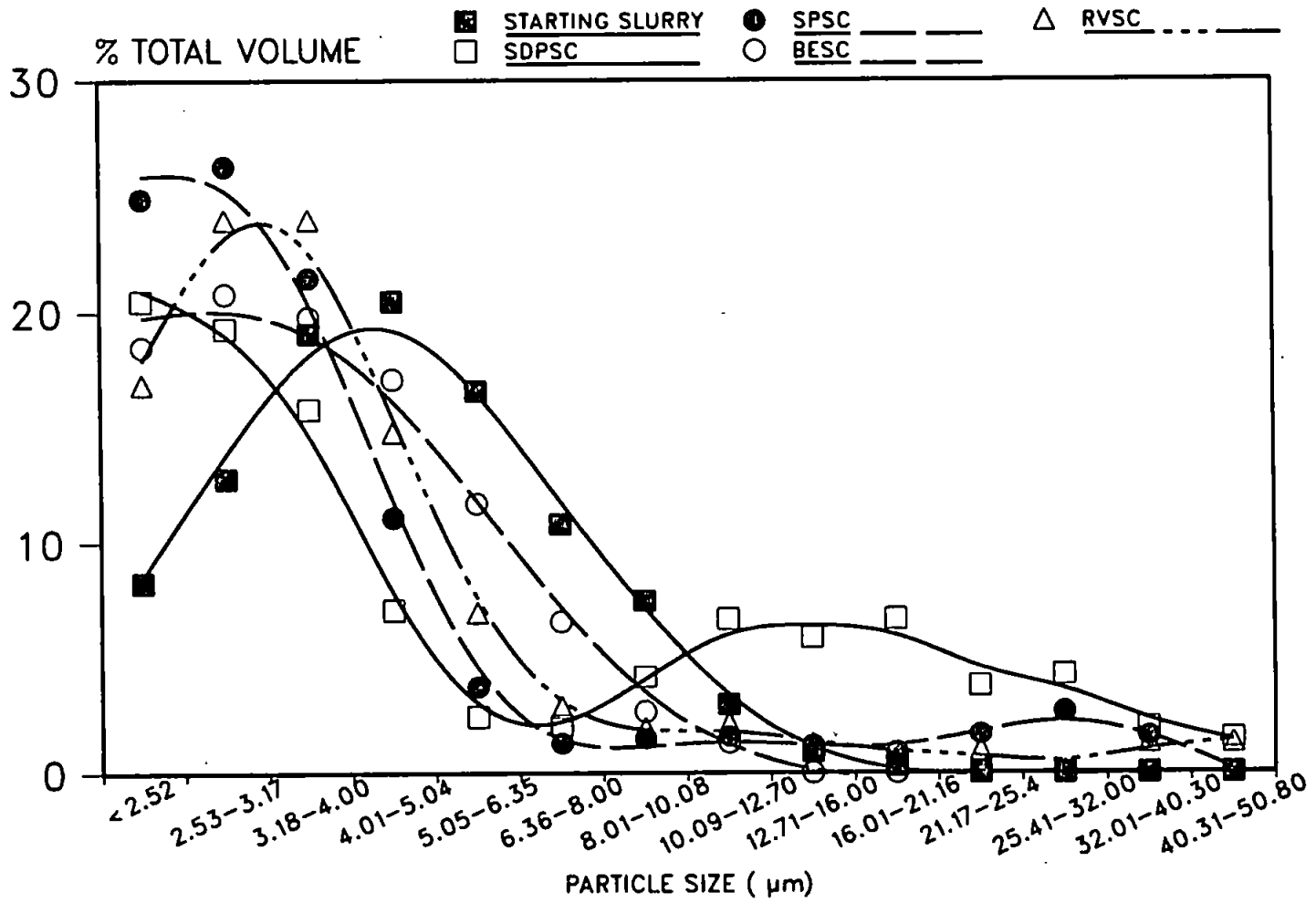

larger version of the RVSC, but this obviously had a profound effect upon particle size distribution.

Mass transport efficiencies were calculated and the results are shown in Table 3.2. The most effective spray chamber at transporting mass was the RVSC. This was encouraging, as it was thought that its small volume hence reduced dispersion of sample, would be ideal for use in FI. However, from Figure 3.11, it appeared that the chamber did not remove the larger droplets which would cause instability in the plasma. At the other extreme, the SDPSC and SPSC were efficient at removing such droplets and this was reflected by the low transport efficiencies of 0.42 and 0.45% respectively. Smaller particles obviously have less mass than larger particles, and so, in order to achieve higher transport efficiencies, proportionally more particles have to be collected. It is for this reason that the RVSC was so efficient, at 0.91% - larger particles having more mass, were collected.

Earlier in the chapter it was stated that the ideal spray chamber would produce a stable aerosol stream of small droplets with narrow particle size distribution, as well as increasing the mass transport efficiency. The BESC most closely fulfilled these criteria. The mass transfer efficiency was higher than the SDPSC and SPSC, at 0.66%. The emergent particle size distribution was less than 8μm, unlike that of the RVSC, whose high efficiency was, in part, a result of large emergent particles. The BESC appeared to have conditioned the aerosol adequately, i.e. removal of larger droplets, as well as increasing the efficiency over the SDPSC and SPSC. From observation of the BESC nebulisation system, the aerosol

TABLE 3.2
TRANSPORT EFFICIENCIES FOR DIFFERENT SPRAY CHAMBERS

| SPRAY CHAMBER TYPE | %TRANSPORT EFFICIENCY |
|---|---|
| SDPSC | 0.42 |
| SPSC | 0.45 |
| BESC | 0.66 |
| RVSC | 0.91 |

$$\%\text{TRANSPORT EFFICIENCY} = \frac{\text{Total mass of slurry (solid) collected in impactor}}{\text{Total mass of slurry (solid) entering the nebuliser}} \times 100$$

underwent recirculation in the bulbous-end in a cyclonic manner. The larger particles went to drain, whilst the smaller particles remained in the argon stream and thence were transported to the plasma.

## 3.6 CONCLUSIONS

The aim of this work was to introduce small volumes of slurries into the ICP by FI. Previously, FI had only been applied to aqueous samples. This work showed that FI of slurries is a viable analytical technique. Excellent results were obtained from Certified Reference Material soils, S01 and S02, thus validating the technique.

The objective of the project was to preconcentrate trace metals from analytical grade reagents, whose levels are generally, below $10ngml^{-1}$. As well as using a powerful preconcentration technique, the determination step needs to be sensitive. Using the SDPSC sensitivity for FI was not very good, owing to the excessive dispersion of sample in the carrier stream and also poor transport efficiency. Of the four spray chambers examined, the BESC was the most effective at producing a stable aerosol stream of small droplets and reducing dispersion, whilst increasing the overall transport efficiency of the system. Thus it was seen that geometry of spray chamber has a marked effect upon emergent particle size distribution and mass transport efficiency.

# CHAPTER 4

## SIMPLEX OPTIMISATION OF SPRAY CHAMBERS

### 4.1 INTRODUCTION

Optimisation is concerned with adjusting the controllable variables in a given situation, so as to achieve the best possible result.

There are a number of optimisation methods that may be used, many of which involve computation (118). One such method is that of simplex optimisation which optimises all the operating parameters simultaneously.

A simplex is a geometric figure defined by a number of points equal to one more than the number of dimensions of the space. A simplex in two dimensions is a triangle, in three, a tetrahedron. The series can be extended to higher dimensions, but these simplexes are not easily visualised.

Spendley et al (73), first developed the method which was then improved by Nelder and Mead (119) to include a variable step-size, thereby accelerating optimisation, improving precision and correct identification of optima. Yarbro and Deming (120) advocated the use of a large initial simplex, in order that factor space be thoroughly explored. The figure of merit used for this investigation was that of net signal to background (SBR), identified by Greenfield and Burns (121) as the criterion with which different plasmas would be directly comparable independently of the

spectrometer used. SBR is regarded as a function of five interrelated variables: power, height of observation, and flows of outer, intermediate and injector gases. The most significant effects on an analyte signal are produced by variations in forward power, observation height and injector gas flow rate. These three factors interact in a complex manner and their combined effects are different for different spectral lines. The outer and intermediate gas flows have relatively small effects on spectral line intensities and their influence can be understood and adjusted almost independently of the other factors.

Ebdon et al (77), were the first workers to apply the simplex routine for use in the ICP and since, has become a popular technique for ICP optimisation studies. The technique of simplex optimisation is clearly useful in the tuning-up of an instrument, but also has application in the design and testing of novel sample introduction systems, including torch configurations. A number of workers have used the simplex routine in this way (75, 122-124).

The aim of this work was to use the simplex routine for optimisation of the four spray chambers discussed in Chapter 3 and assess their usefulness for FI applications. In order to compare directly each spray chamber, with meaningful results, it is necessary that the operating conditions have been optimised. If one set of running conditions were set for all the spray chambers, direct comparison would not be valid, as it is unlikely that each system would be running at the maximum of its capabilities.

It was hoped that the conditions given by the simplex for each spray

chamber might provide information on spray chamber design. This was achieved by Ebdon and Cave (76), who compared two spray chambers, a Scott double-pass and a cyclone with the same nebuliser and torch assembly for both. The results showed that the cyclone chamber required a much larger and powerful plasma at optimum conditions. From this, they concluded that the solvent loading was greater in the cyclone design, which caused cooling of the plasma and reduction in the atomisation and excitation properties. In order to maintain the SBR, greater power was required. The application of simplex optimisation in this diagnostic approach, is clearly of great benefit, especially in the development of novel sample introduction systems.

## 4.2 SIMPLEX OPTIMISATION OF SPRAY CHAMBERS

### 4.2.1 Experimental

The ICP used in this work was a Kontron Plasmakon S-35 (Kontron Spektralanalytik, Eching, West Germany). The sample was introduced to the plasma in the form of an aerosol which was produced by the 'Mini-Ebdon' nebuliser (P.S. Analytical), via a peristaltic pump. The aerosol was carried into the spray chamber under investigation and thence through a 3mm i.d. central injector tube of the torch and into the plasma. The ICP torch (of the larger Greenfield type) was mounted centrally in a four-turn copper induction coil, which was water-cooled. A radio frequency (rf) generator supplied power (maximum 3.5kW) to the coil. The generator was crystal-controlled and operated at a frequency of 27.12MHz.

The simplex program, based upon Nelder and Meads' modified version, was written in BASIC for the Apple IIe micro computer (125). The simplex program terminated when the responses of all the vertices of the current simplex were within an operator-determined relative standard deviation. The degree of precision on the response factor used in this study was 3%.

Net signal to background ratio (SBR) was used as the figure of merit. The influences of the rf power coupled into the plasma, the injector gas flow rate and the observation height on the intensities of various spectral lines are critical to SBR. These three parameters were optimised, whilst the nebuliser uptake rate, coolant and plasma gas flow rates were kept constant. Tables 4.1 and 4.2 show the plasma running conditions and the boundary conditions of the plasma respectively. Barnes (126) noted that emission intensities for ion lines are more susceptible to changes in power and injector gas flow rate and atom lines show greater variations in spatial distributions in emission signal above the rf coil. This can result in difficulties when best possible results are required for the simultaneous use of an ion and atom lines. It was for this reason that an ion Mn (257.60nm) and atom line (Cu 324.75nm) were chosen for optimisation procedures.

Optimisation studies were carried out on solutions containing $5\mu g ml^{-1}$ of copper or manganese.

The operating conditions for each spray chamber (Scott double-pass spray chamber [SDPSC], single pass spray chamber [SPSC]], Bulbous-ended

TABLE 4.1

PLASMA RUNNING CONDITIONS

| | |
|---|---|
| Outer gas flow rate ($Lmin^{-1}$) | 18 |
| Intermediate gas flow rate ($Lmin^{-1}$) | 0.5 |
| Nebuliser uptake rate ($mlmin^{-1}$) | 0.7 |

TABLE 4.2

BOUNDARY CONDITIONS FOR SIMPLEX OPTIMISATION

| | | | |
|---|---|---|---|
| Power* | (kW) | | 1 - 1.7 |
| Height** | (mm) | | 0 - 60 |
| Injector gas | | ($Lmin^{-1}$) | 0.5 - 1.5 |

* net forward power

** measured above the load coil

spray chamber [BESC] and reduced volume spray chamber [RVSC]), were optimised by the simplex procedure for Cu and Mn separately. Once the optimum conditions had been found, a set of univariate searches were performed, in which two of the optimised parameters were held constant and the third varied as SBR was measured. This confirmed whether the simplex had identified the optimal conditions and also gave insight on the influence of each parameter on the performance of the plasma.

### 4.2.2 Results and discussion

The optimum values obtained for the carrier gas flow rate, power and observation height above the load coil, are given in Tables 4.3 and 4.4 for copper and manganese respectively.

Figures 4.1 - 4.6 show separately the univariate searches for SBR versus carrier gas flow rate, power and observation height for each spray chamber for copper and manganese lines. Optimum conditions selected by the simplex are shown by the two parallel lines.

#### 4.2.2.1 Effect of different parameters

a) **Carrier Gas Flow rate**

For copper, the SBRs increased with a rise in carrier gas flow rate. The RVSC, SDPSC and BESC had best responses at the maximum working capacity of the nebuliser, i.e. $1.5 Lmin^{-1}$. It was found that the nebuliser was slightly blocked with PTFE swarf which prevented the flow rate further being increased. This was removed, and so it was possible,

**TABLE 4.3**

**EFFECT OF SPRAY CHAMBER TYPE UPON OPTIMUM OPERATING CONDITIONS FOR THE DETERMINATION OF COPPER USING THE 324.75nm ATOM LINE**

| PARAMETER | SPRAY CHAMBER TYPE | | | |
|---|---|---|---|---|
| | RVSC | SDPSC | SPSC | BESC |
| Injector gas flow/Lmin$^{-1}$ | 1.4 | 1.5 | 1.5 | 1.5 |
| Power/kW | 1.2 | 1.1 | 1.2 | 1.0 |
| Observation height above load coil/mm | 28 | 32 | 27 | 30 |
| Net signal C/S | 10324 | 7394 | 10333 | 8612 |
| Background C/S | 647 | 485 | 720 | 479 |
| SBR | 12.6 | 14.3 | 14.3 | 16.8 |

**TABLE 4.4**

**EFFECT OF SPRAY CHAMBER TYPE UPON OPTIMUM OPERATING CONDITIONS FOR THE DETERMINATION OF MANGANESE USING THE 257.6nm ION LINE**

| PARAMETER | SPRAY CHAMBER TYPE | | | |
|---|---|---|---|---|
| | RVSC | SDPSC | SPSC | BESC |
| Injector gas flow/Lmin$^{-1}$ | 1.0 | 1.0 | 1.1 | 1.0 |
| Power/kW | 1.1 | 1.0 | 1.1 | 1.1 |
| Observation height above load coil/mm | 13 | 15 | 16 | 14 |
| Net signal C/S | 43739 | 44825 | 44921 | 56281 |
| Background C/S | 1156 | 1452 | 1280 | 1752 |
| SBR | 36.8 | 30.3 | 34.6 | 31.2 |

FIGURE 4.1
UNIVARIATE SEARCH SHOWING EFFECT OF CARRIER GAS FLOW RATE UPON NORMALISED SBR USING THE Cu(I) 324.75nm LINE FOR:

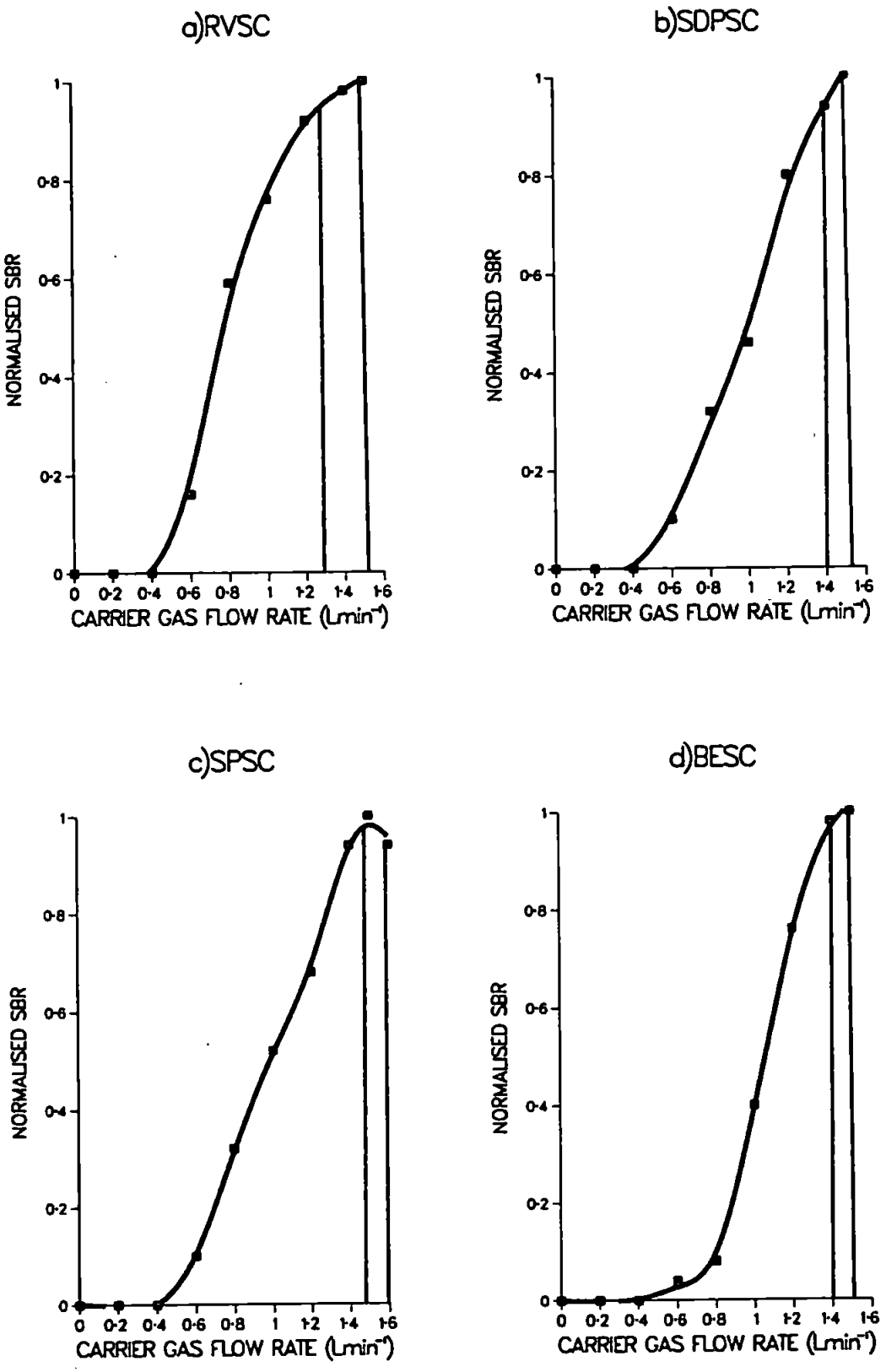

FIGURE 4.2
UNIVARIATE SEARCH SHOWING EFFECT OF POWER UPON NORMALISED SBR USING THE Cu(I) 324.75nm LINE FOR:

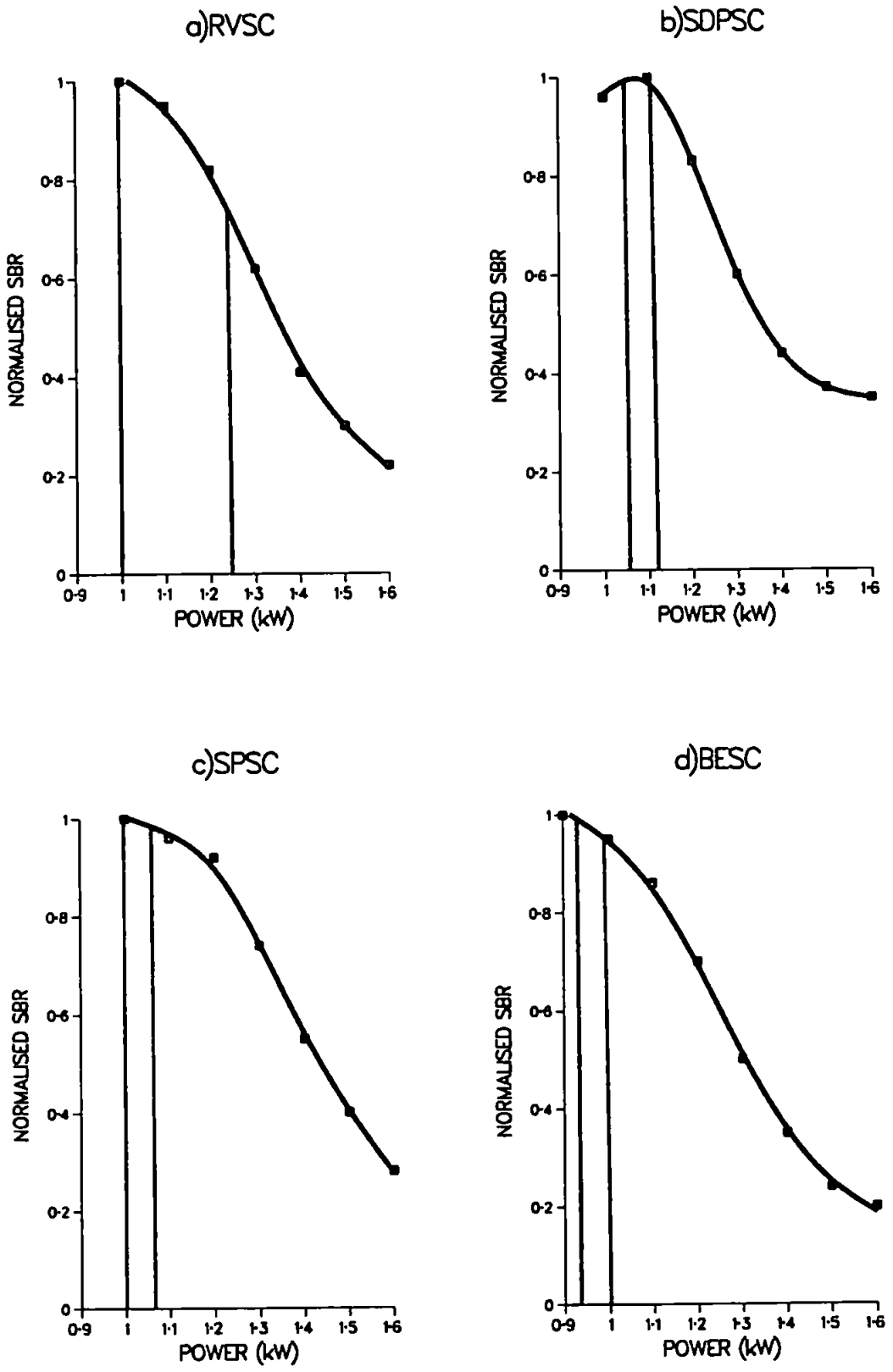

FIGURE 4.3
UNIVARIATE SEARCH SHOWING EFFECT OF OBSERVATION HEIGHT ABOVE LOAD COIL UPON NORMALISED SBR USING THE Cu(I) 324.75nm LINE FOR:

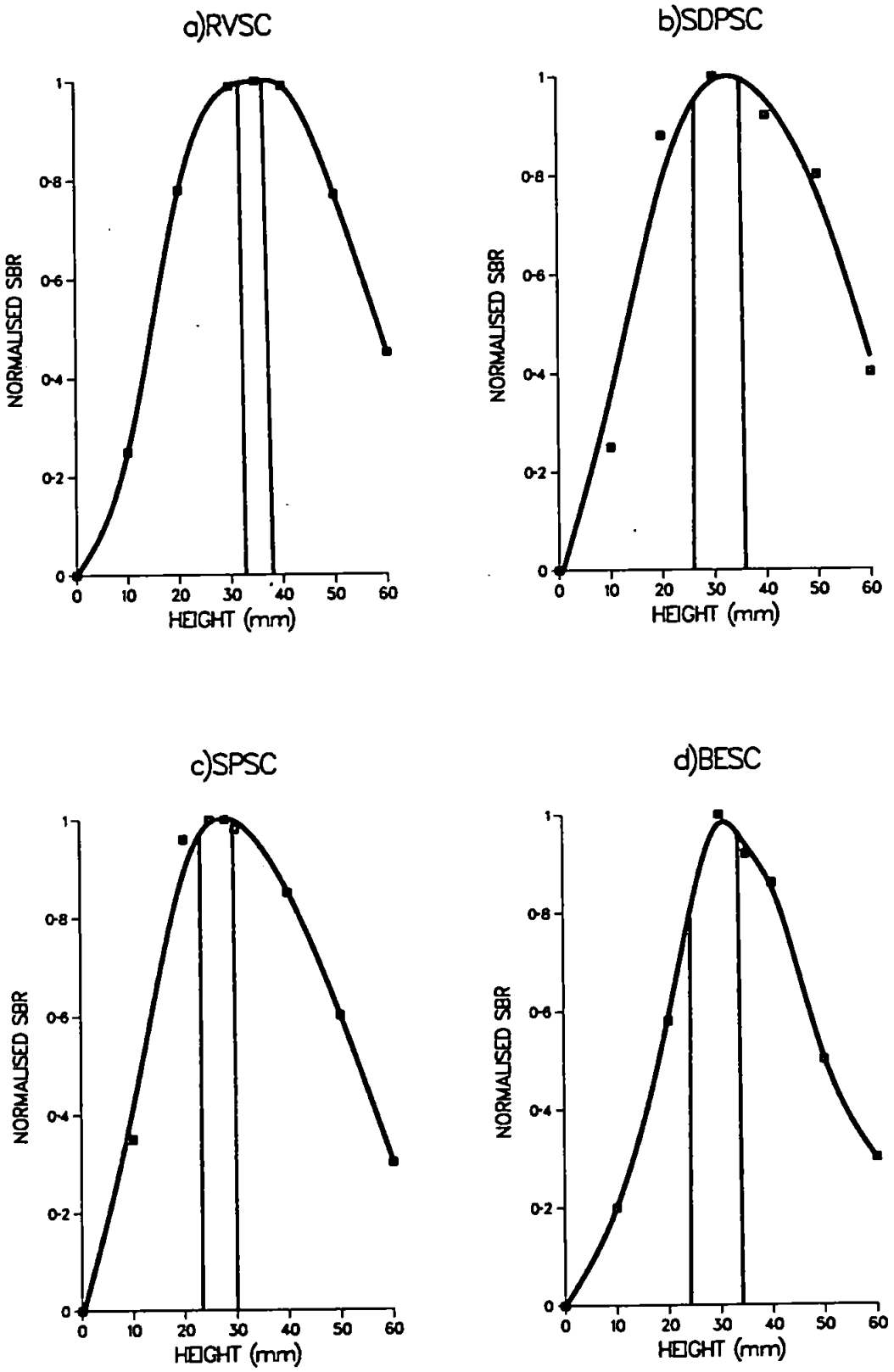

FIGURE 4.4
UNIVARIATE SEARCH SHOWING EFFECT OF CARRIER GAS FLOW RATE UPON NORMALISED SBR USING THE Mn(II) 257.60nm LINE FOR:

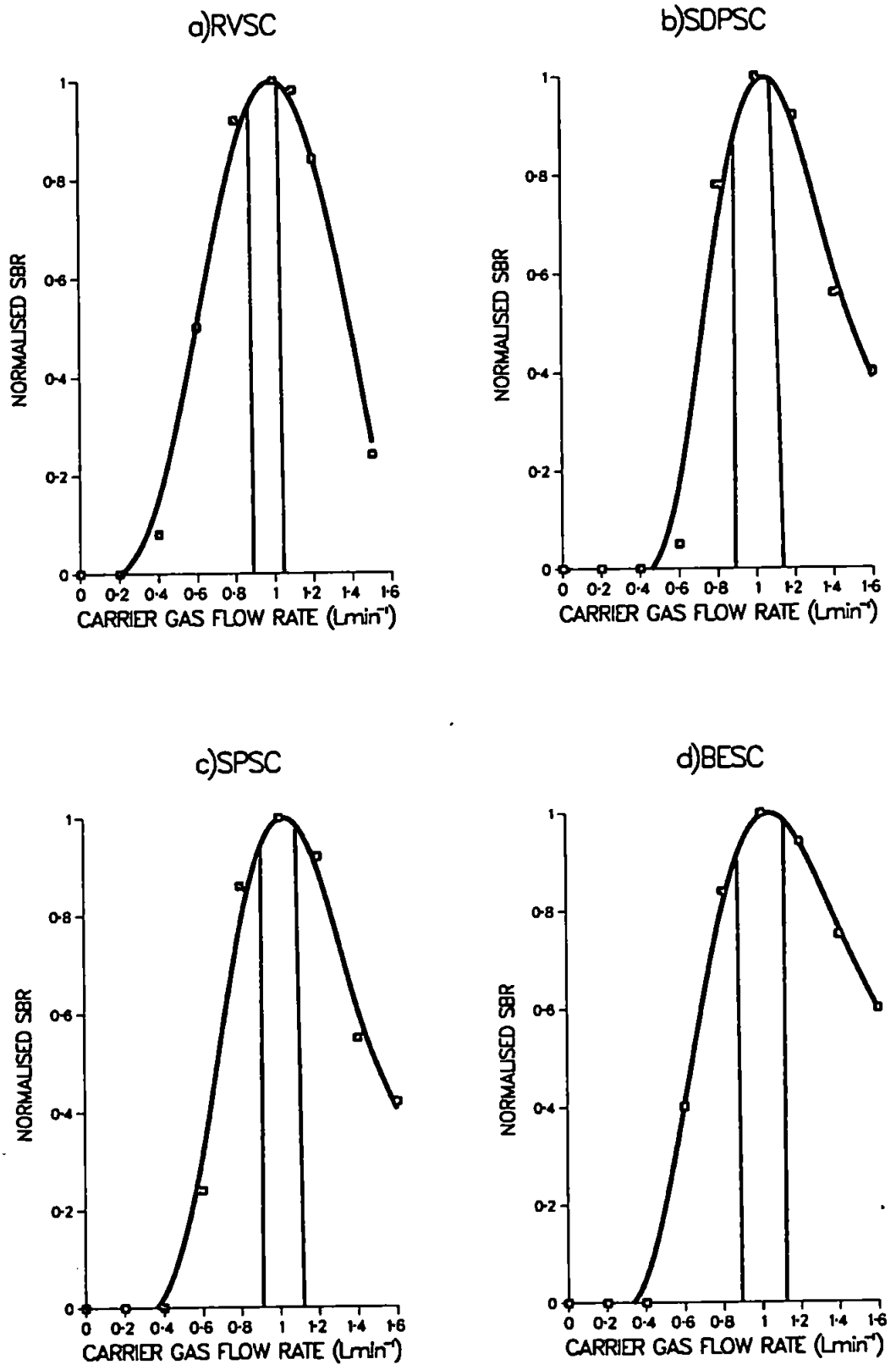

FIGURE 4.5
UNIVARIATE SEARCH SHOWING EFFECT OF POWER UPON NORMALISED SBR USING THE Mn(II) 257.60nm LINE FOR:

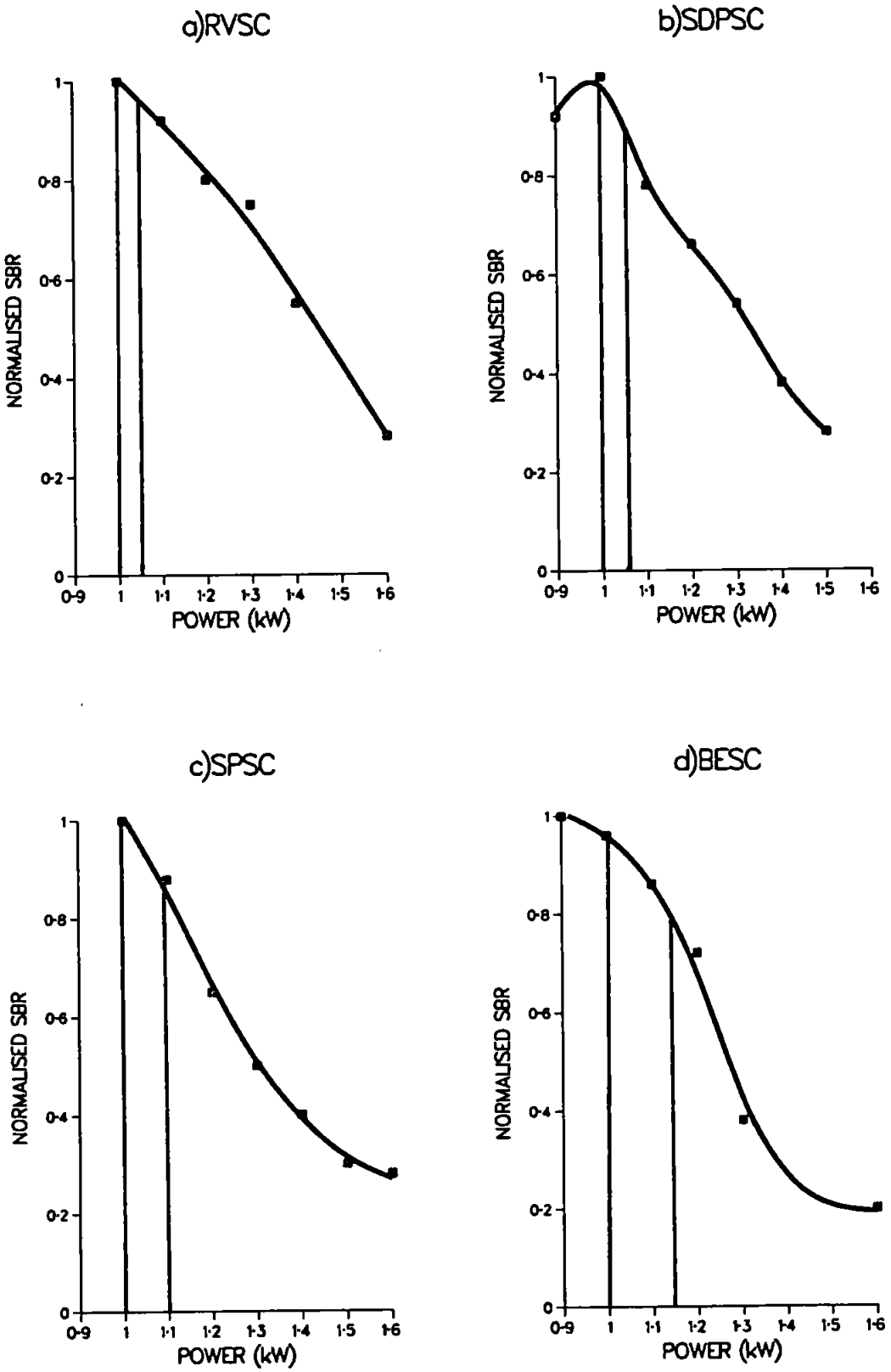

FIGURE 4.6
UNIVARIATE SEARCH SHOWING EFFECT OF OBSERVATION HEIGHT ABOVE LOAD COIL UPON NORMALISED SBR USING THE Mn(II) 257.60nm LINE FOR:

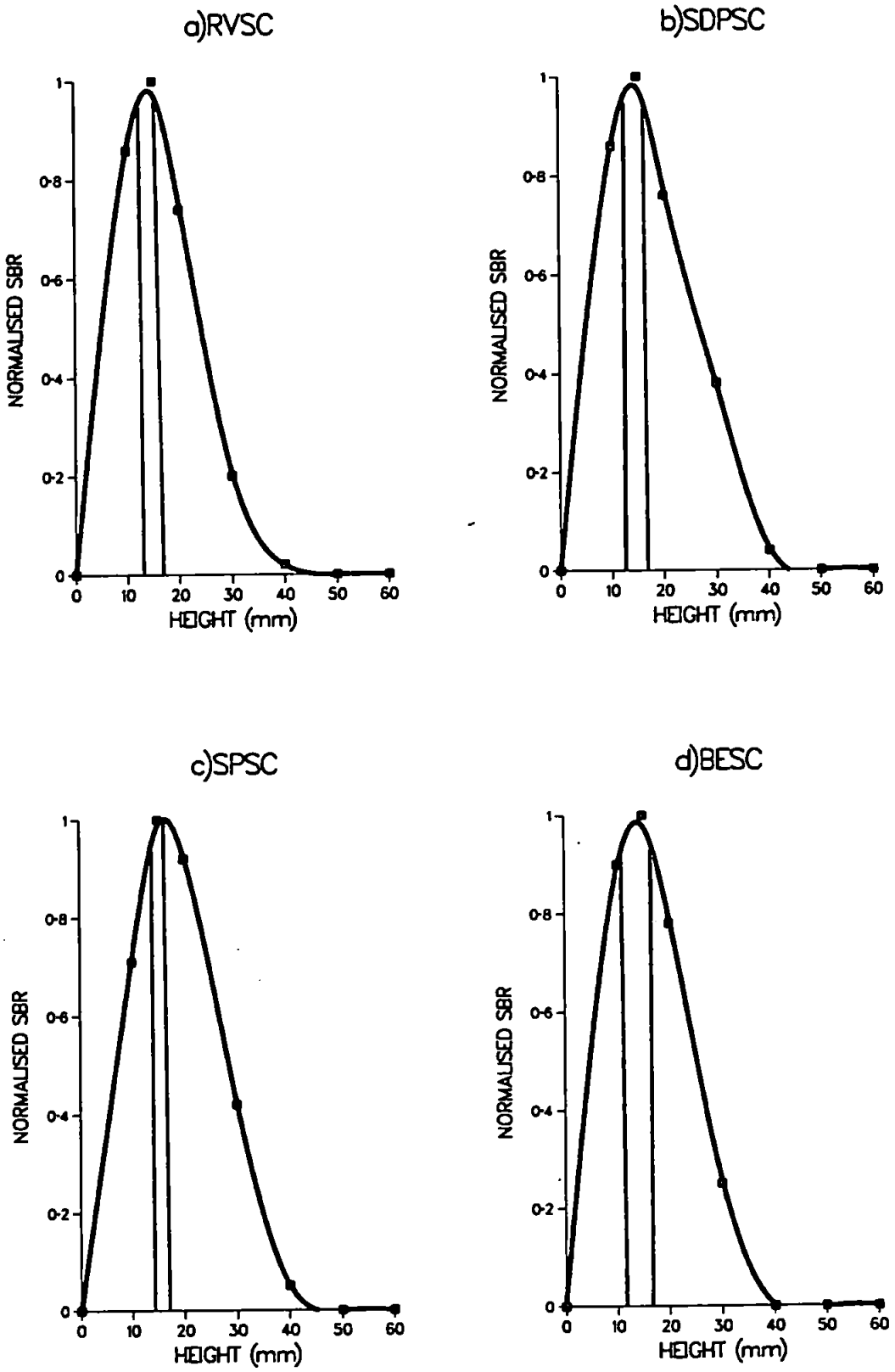

in the optimisation of the SPSC to increase the flow rate to $1.6Lmin^{-1}$. It was then possible to see the maximum for carrier gas flow-rate in the SPSC. For manganese, the flow rate was lower, at between 0.95 and $1.1Lmin^{-1}$ for all the chambers.

Very low carrier gas flow rates are inadequate to 'punch' the plasma and so the analyte does not penetrate the viewing zone. The effect of increasing the carrier gas flow rate results in a decrease of temperature in the observation zone and also markedly modifies the structure and appearance of the ICP, thus rendering excitation conditions unsuitable for analytical purposes. At high carrier gas flow rates, the initial radiation zone (IRZ) is pushed up into the normal analytical zone (NAZ) where there are serious effects from easily ionised elements (EIEs). This is what is seen when the spectral lines (both hard and soft) pass through a maxima, the latter being more affected.

b) **Power**

The simplex routine did not always identify the optimal power, for example the BESC with Mn. This was probably due to the simplex being on the edge of a plateau, with the optimum not well defined. It had been expected that the spray chambers with higher transport efficiencies would require higher power in order to maintain the SBRs, from a cooler plasma. This was not found, and in all cases, the simplex identified lower powers. This was because the background increased more rapidly with increased power than the net signal, therefore the highest SBRs were found at the lower end of the power range where the background was reduced. However, there was a lower practical limit, dictated by plasma stability.

This requirement for stability demands a small sacrifice from the SBRs. Adding more solvent to the plasma will require increasing the rf power so that the plasma does not extinguish. This is an important factor in the flow injection application. In order to increase sample throughput and improve peak shape, the carrier stream flow rate needs to be quite high (in this work 4-5.5mlmin$^{-1}$). It is evident therefore, that the power has to be increased to prevent plasma instability.

c) **Observation height**

There was some variation in observation height between the different spray chambers, although this was probably not significant, with the difference between average values only being 3 and 2mm for copper and manganese respectively. The average optimum height for the RVSC was slightly lower for copper at 28mm as opposed to the SDPSC which had the highest average value of 32mm. In general, the ranges of the simplex were fairly close to one another. However, the RVSC had a wide optimal range from 16 - 35mm above the load coil for copper. For the vertex having an observation height of 16mm, the power was lower than the other vertices. The background was very much reduced, hence giving the higher SBR.

Overall, spray chamber design seemed to have only a small effect upon the optimum operating conditions of the plasma for each element. However, response was different for each spray chamber. The BESC had the highest SBR for copper and the RVSC for manganese. It is important to remember, that SBRs are highly dependent upon the background. For example, although the BESC had the highest SBR for copper, the SPSC

had the highest net counts. Similarly for manganese, the RVSC had the best SBR, but the lowest net signal. In this case, the BESC had the highest net signal, over 10,000 c/s better than the other chambers, but the background was elevated, thus reducing the SBR.

With regards to noise, the RVSC was noisy compared with the other spray chambers. This was probably a combination of two effects:- particle size reaching the plasma and pump noise. The work in Chapter 3 showed that the particle size transported through the sample introduction system was greater for the RVSC than for any of the other chambers. The SDPSC and the BESC transported particles less than 8μm and consequently were less noisy than the RVSC.

The second effect was due to pump noise. The RVSC and SPSC did not dampen the noise from the peristaltic pump and cycling of the signal was observed. The SDPSC and BESC, because of their greater volume, were able to dampen this noise.

## 4.3 EFFECT OF SPRAY CHAMBER DESIGN UPON FI CHARACTERISTICS

Having optimised each spray chamber, it was possible to evaluate and compare their use for FI applications. The main considerations were sensitivity, washout time, peak shape and reproducibility.

### 4.3.1 Experimental

The ICP used in this study was a Plasmakon S-35, (Kontron Spektralanalytik, Eching, West Germany). The plasma operating conditions depended upon spray chamber design and were those selected by the simplex optimisation. The outer gas and intermediate gas were fixed at 18 and 0.5Lmin$^{-1}$ respectively. The basis of the flow injection manifold has been described in Section 3.2. A 100µl PTFE loop was used throughout. The sample was supplied to the nebuliser via a peristaltic pump at 0.7mlmin$^{-1}$. This rate was chosen so that it was easier to evaluate peak shape.

### 4.3.2 Reagents

A standard solution containing 5µgml$^{-1}$ manganese was used for the FI work.

### 4.3.3 Results and discussion

Figures 4.7-4.10 show typical FI peaks for 100µl of 5µgml$^{-1}$ manganese. The RVSC is the most sensitive, as it was for continuous flow, followed by the BESC, SDPSC and SPSC. The SPSC was noticeably noisier than the other chambers, especially when the carrier stream flow rate was increased.

The SPSC chamber gave the best peak shape, with regard to rise and fall time. The washout time (at 0.7mlmin$^{-1}$ carrier stream flow rate) was

**FIGURE 4.7**
**TYPICAL FI PEAKS OBTAINED FROM A SPSC (100µl INJECTION VOLUME) USING OPTIMISED CONDITIONS**

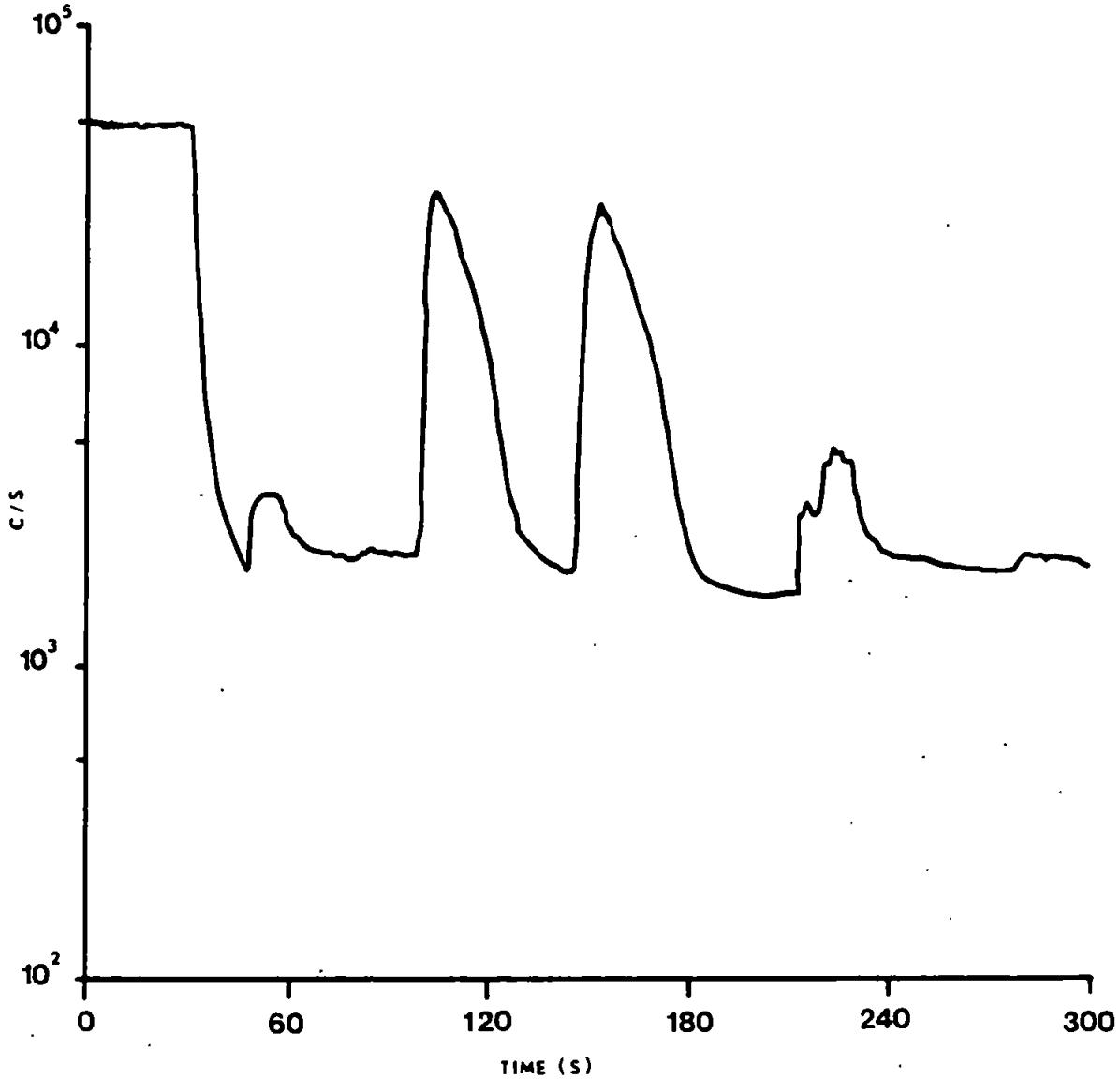

**FIGURE 4.8**
**TYPICAL FI PEAKS OBTAINED FROM A RVSC (100µl INJECTION VOLUME) USING OPTIMISED CONDITIONS**

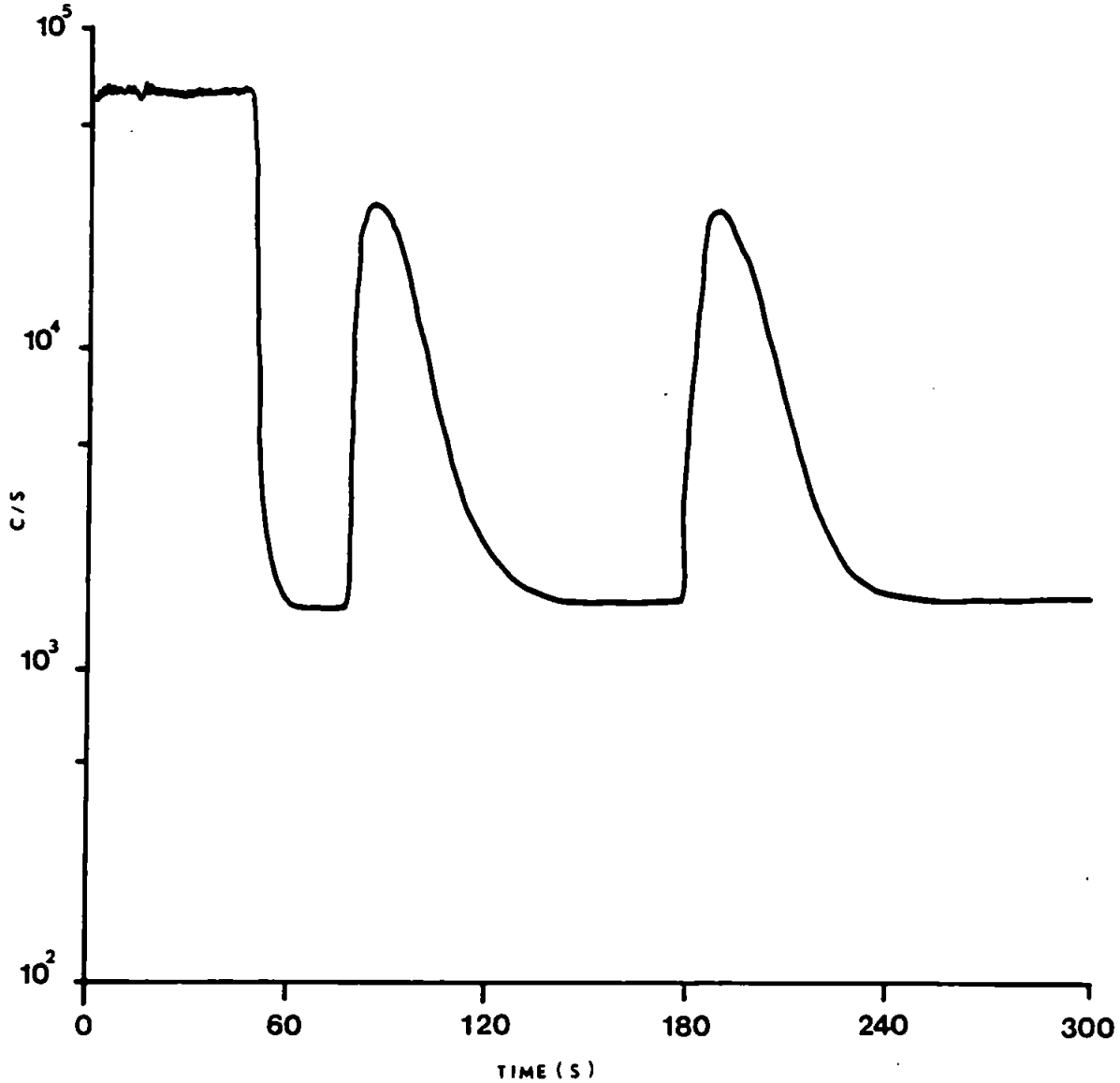

**FIGURE 4.9**
**TYPICAL FI PEAKS OBTAINED FROM A BESC (100µl INJECTION VOLUME) USING OPTIMISED CONDITIONS**

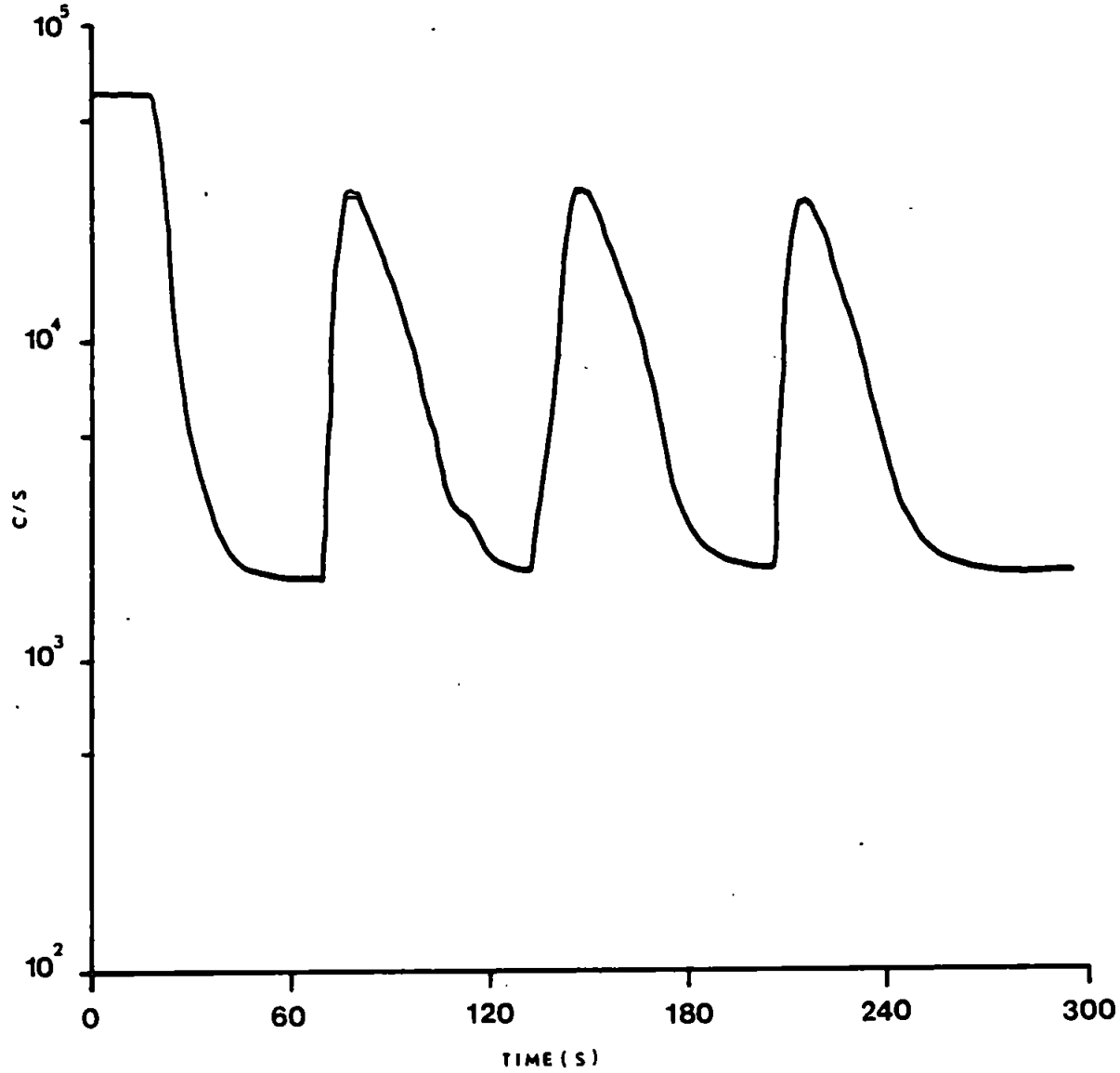

**FIGURE 4.10**
**TYPICAL FI PEAKS OBTAINED FROM A SDPSC (100µl INJECTION VOLUME) USING OPTIMISED CONDITIONS**

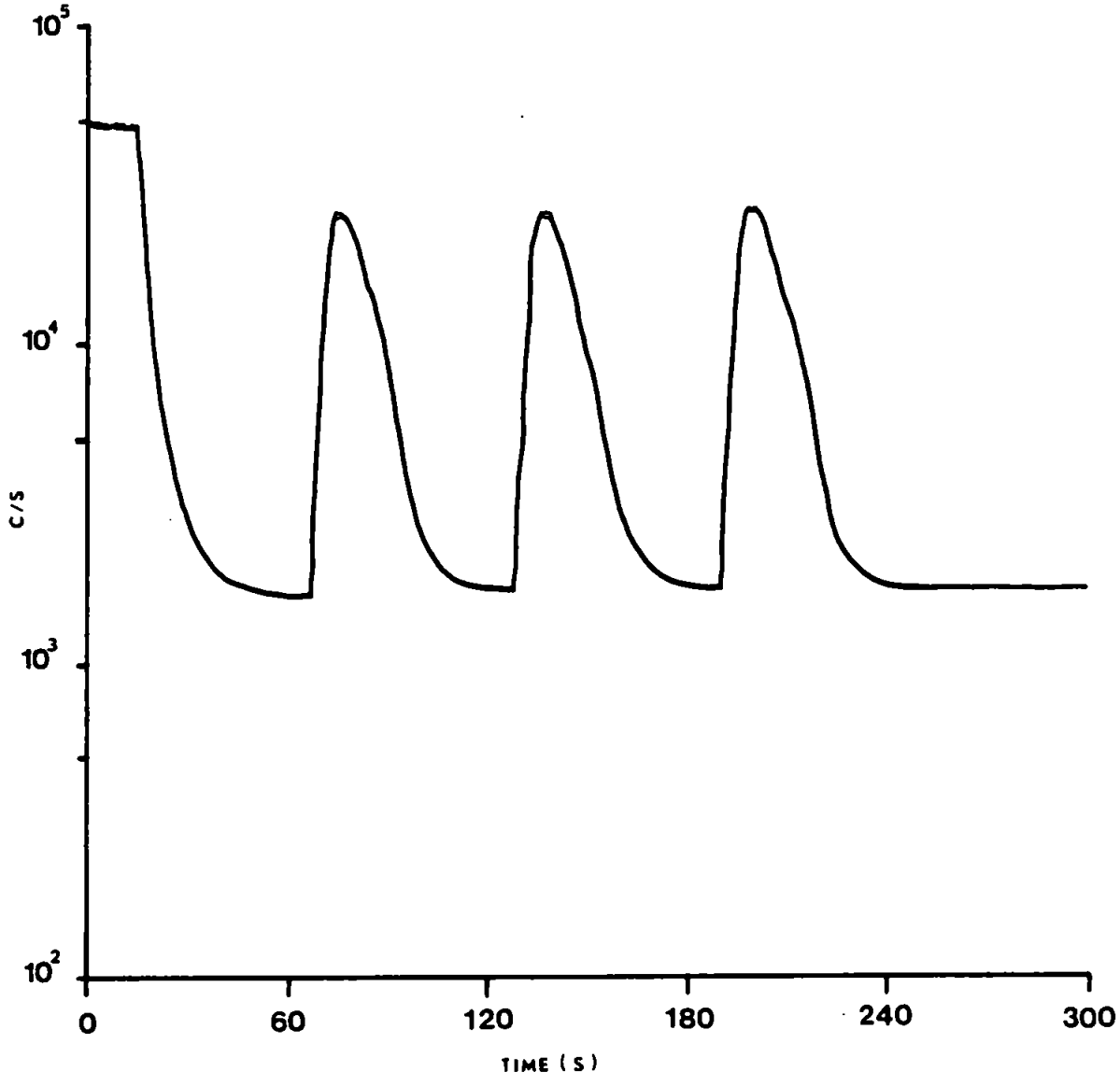

51s. The SDPSC also gave good peak shape and a corresponding washout time of 57s. The RVSC and BESC had washout times of 64 and 75s respectively. These results were a little surprising as it was expected that the BESC and RVSC would have quicker washout times owing to their lower volumes. However, it was noted visually that the aerosol underwent recirculation in these two spray chambers, probably because of the bulbous end which had the combined effect of dropping the pressure in the chamber, and diverting the spray into a cyclone. These two factors evidently increased the residence time in the spray chambers, hence the longer washout times.

In an analysis, the carrier stream flow rate was set to be higher in order to 'sharpen' peak shape as well as increasing sample throughput. RSDs (30) were calculated for each spray chamber with a carrier stream flow of 4.5ml$min^{-1}$ and a sample injection volume of 100µl. The results showed that the BESC gave the best RSD of 3.1%, followed by the SDPSC, 4.1%, RVSC, 5.2% and the SPSC at 13.2%. The high RSD for the SPSC chamber was caused by droplet formation at the upturn part of the chamber. In a continuous mode, cycling of the signal, caused by the inability of the chamber to dampen the pump noise, was observed.

## 4.4 CONCLUSIONS

This work has shown that the design of the four spray chambers under examination, effected the optimum plasma running conditions for a given element. Despite the different transport efficiencies observed in Chapter 3, only slight variations were seen between the chambers, although SBRs

were affected.

Using the optimised conditions, a series of flow injections were performed. The best peak shape (defined by washout time) was given by the SPSC chamber. However, at higher carrier stream flow rates the chamber produced results which were much noisier. The BESC was the most reproducible system and along with RVSC was more favourable with regard to FI applications.

# CHAPTER 5

# DETERMINATION OF TRACE METAL IMPURITIES IN FINE CHEMICALS BY PRECONCENTRATION SLURRY ATOMISATION-ICP-AES

## 5.1 INTRODUCTION

The determination of trace or ultratrace levels of metal ions in fine chemicals is often preceded by a preconcentration step so that analyte concentrations are increased to levels that are easily and reliably measured. This work used the technique of sorption whereby trace metal impurities were adsorbed onto activated carbon as metal chelates of Chrome Azurol S (CAS).

### 5.1.2 Purification of sorbent

In sorption preconcentration, the purity of the sorbent is undoubtedly the most important criterion for trace analysis. Commercial activated carbon originates from plant or animal matter and therefore always contains a percentage of minerals and hence metals. Activated carbon low in metal content can be obtained from carbonising polyvinylidene chloride (127) or cellulose (23). Unfortunately, these carbons are not commercially available. An alternative is to treat commercial activated carbon with hydrofluoric and hydrochloric acids which can reduce the metal content five-fold (128).

### 5.1.3 Modes of analysis

The technique used in this work involved analysing the enriched carbon by slurry atomisation-ICP-AES. The analysis may be performed in either a discrete or continuous mode, depending upon (i) volume of sample available (ii) number of elements to be analysed and (iii) type of spectrometer used. i.e., sequential or simultaneous reader. If only a small volume of sample is available, a number of elements need to be determined and the ICP is sequential, flow injection may be used (discussed in Chapter 3). However, if the ICP spectrometer is a simultaneous instrument it may be possible to analyse the slurry by continuous aspiration without excessive sample consumption.

When concentrated slurries are used it is often necessary to compensate for transport effects which result from variations in sample uptake rate or nebulisation efficiency, caused by the viscosity of the slurry, or solvent-loading. Ebdon and Collier (59) suggested the use of an internal standard to correct for viscosity variations arising from differing slurry concentrations (above 10% m/v).

### 5.1.4 Internal standardisation

Internal standards have been used widely in quantitative analytical emission spectroscopy and it was the introduction of internal standardisation by Gerlach (129) that elevated classical AES to a method for quantitative rather than qualitative analysis. The procedure involves adding identical concentrations of one or more elements to the samples and

standards in order to correct for variations in the analyte response arising from the adverse effects associated with the constituents in the sample matrix, or from instrumental factors. A ratio is calculated between the intensity of the analyte emission line and that of a line of the internal standard element added to the sample. Guidelines have been proposed for matching the physical properties of the analyte and reference elements so that this ratio is not sensitive to variations of the experimental parameters (130, 131). The analyte/internal standard element pair is based upon ionisation energy, excitation energy and partition function of the elements. Myers and Tracy (132) showed that by careful choice of operating conditions, all emission signals can be highly correlated with each other, independent of differences in physical properties and therefore a single internal standard element may be used to improve analytical performance. They found that carrier gas flow rate and viewing height are the two most important factors affecting the correlation between analyte emission signals. However, Ramsey and Thompson (133, 134) have shown, using principle components analysis, that accounting for all the variance encountered in ICP analysis is not possible using only one internal standard. By selecting two internal standard element lines, one an atom line of low excitation potential, the other an ion line of high combined excitation and ionisation potential and using them to correct the responses of all the analytes to forward power and sample uptake rate, then the total variance of routine ICP-AES was reduced by 70%.

Several criteria must be met before an internal standard may successfully compensate for non-random instrumental variability and these have been discussed by Wallace (135). In brief, the internal standard must not

spectrally overlap any desired analyte emission lines; it should not contain the elements being analysed and it must covary with the elements being analysed. The element scandium has regularly been employed as an internal standard (132, 136, 137). It is relatively rare and thus unlikely to occur in most samples and has a comparatively simple ICP spectrum.

## 5.2 EXPERIMENTAL

Two plasma spectrometers were used in this work - a sequential (Plasmakon S-35, Kontron, described in Chapters 3 and 4) and a simultaneous instrument (Spectroflame-ICP, Spectro Analytical Instruments GmbH, Kleve, FRG). The RF generator is crystal stabilised, has a maximum power output of 2.5kW and operates at a frequency of 27.12MHz. The complete sample introduction system, consisting of torch (Fassel type), spray chamber, nebuliser, argon humidifier and safety trap is mounted on a removable plate. Sample introduction is accomplished with an integrated peristaltic pump. Through the use of fibre optics to transmit the light from the plasma to the optic, the instrument can be equipped with up to five individual optical systems, including a monochromator. An internal computer is used to operate and monitor the entire system. For both plasmas, a mini-Ebdon nebuliser (P.S. Analytical) was used with the reduced volume spray chamber (see Chapter 3). Operating conditions for the sequential plasma are as reported in Chapter 4 (optimised conditions). The simultaneous plasma operating conditions are shown in Table 5.1.

For the determination of surface areas of activated carbon, the nitrogen

**TABLE 5.1**

**SIMULTANEOUS PLASMA RUNNING CONDITIONS**

| | |
|---|---|
| Outer gas flow/Lmin$^{-1}$ | 15.0 |
| Intermediate gas flow/Lmin$^{-1}$ | 1.5 |
| Carrier gas flow/Lmin$^{-1}$ | 1.6 |
| Power/kW | 1.0 |

Sample uptake rate 1.6mlmin$^{-1}$

sorption balance was used. The balance can determine surface areas within the range 0.2 - 1000 $m^2g^{-1}$ using samples of 0.25g. The weighing part is contained within the balance head and is connected by a multi-way cable to the electrical control cabinet (C.I. Microforce Balance Mark 2, C.I. Electronics, Salisbury, Wiltshire) and has a 1g capacity. The head unit contains an electronic bridge circuit maintained in continuous balance by a servo system. The balance arm carries a shutter interposed between a lamp and a pair of silicon photocells. When the arm is central the cells have equal resistance and therefore, no bridge current flows. If the arm is displaced slightly, there is a change in the relative illumination of the photocells, thus causing a bridge current. The current passes through a movement coil and equilibrium is rapidly restored. Thus, the head unit electromagnetically balances the torque produced by the sample weight. The vacuum head has B24 glass fittings and is designed to work at pressures down to $1.33 \times 10^{-1}$Pa. The generated weight-proportional current is monitored by the CI mark 2 analogue control unit with fine electrical weight ranges, selected by direct switching. Stabilised power supply and zero adjustment are provided.

## 5.3 PREPARATION OF HIGH PURITY ACTIVATED CARBON FROM CELLULOSE

### 5.3.1 Procedure

The activated carbon was prepared by carbonising cellulose ("Mikrokristallin", E. Merck, Darmstadt, FRG) (23). Approximately 8.5g of cellulose was placed in a 25ml quartz beaker covered with a platinum top

and carbonised in an oven at 800°C for 20 minutes. After cooling, the carbonised cellulose (approximately 1g) was ground to a fine powder and stored in a clean polyethylene bottle.

The purity of the carbon was checked by preparing a 1% slurry (w/v) dispersed in 1% Triton X-100 (BDH Ltd., Poole, Dorset, UK) and analysis by ICP-AES (Plasmakon 5.35)

Adsorption experiments were monitored using a flame atomic absorption spectrometer (IL 151, Thermo-Electron, Warrington, UK) and an air-acetylene flame.

### 5.3.1 Procedure for measuring surface area

The sample was placed in an aluminium foil bucket suspended from the balance with a fine pyrex fibre (27cm long). This enabled the sample to be at least 15cm below the level of the liquid nitrogen, contained in a Dewar flask. This kept the temperature to within ± 0.1°C.

The balance head was coupled by the taps and glass tubing to a two-stage pump, which allowed the pressure to be reduced to $1.33 \times 10^{-2}$Pa, and to a nitrogen reservoir and gauges. The nitrogen pressure was measured by mercury manometers.

The cold trap was immersed in a Dewar flask of liquid nitrogen. This aided outgassing of the sample and reduced the effects of thermal transpiration.

The system was evacuated and the sample degassed at room temperature. True sample weight (i.e. less adsorbed moisture and volatiles) was noted, the balance zero set and the balance unit containing the sample, immersed in liquid nitrogen. A pressure of 4000-6670Pa (30-50mmHg) of nitrogen was introduced and the system allowed to attain equilibrium (approximately 30 minutes), when the nitrogen pressure and uptake were recorded. Six or seven readings were taken in the BET (138) range of 0.05 to 0.30 relative pressure). Thereafter, pressures of 9330-10,660Pa (70-80mmHg) of nitrogen were introduced, giving readings up to the maximum relative pressure available (0.96 - arbitrary units). Measurement of surface area by gas sorption rests on the determination of the monolayer capacity ($X_m$). This work estimated surface areas from the BET equation using $N_2$ sorption of 77k. Discussion and derivation of the BET is given by Lowell (139) and Allen (140). The equation was used in the form

$$\frac{p}{X\,(p_o - p)} = \frac{1}{X_m c} + \frac{(c-1)}{X_m c}\,\frac{p}{p_o} \quad \ldots\ldots 5.1$$

Where X is the amount (g) sorbed per gram adsorbent at equilibrium pressure p, $p_o$ the saturated vapour pressure of the adsorbate and c is a constant. Thus the plot of $\frac{p}{X(p_o - p)}$ versus $\frac{p}{p_o}$ should give a straight line of slope $\frac{(c-1)}{X_m c}$ and intercept $\frac{1}{X_m c}$

### 5.3.2 Results and discussion

The activated carbon produced from the cellulose by air activation was tested for copper and iron and were below that of the water blank for a 1% slurry. The adsorptive property of the carbon was tested and Figure 5.1 shows the adsorption profile of $1\mu g ml^{-1}$ Fe solution containing 10mg CAS at pH3. Very little adsorption was observed, 91% being unadsorbed. It was thought that this was a function of surface area. Using the BET equation, the surface areas of the cellulosic carbon and a commercial activated carbon were calculated. The cellulosic carbon had a surface area of $420 m^2 g^{-1}$, whereas the commercial carbon was nearly double that at $834 m^2 g^{-1}$. The air activation process used in this work was evidently inadequate to produce a carbon with high surface area. Equipment necessary for making high surface area activated carbon was unavailable and therefore the clean-up of commercial activated carbon was investigated.

## 5.4 GRINDING AND CLEAN-UP OF COMMERCIAL ACTIVATED CARBON

### 5.4.1 Procedure

A batch of activated carbon (Darco G-60, Aldrich Chemical Co., Gillingham, Dorset, UK) was ground prior to the clean-up procedure. Activated carbon was placed in a 125ml polyethylene screw-top bottle and zirconia beads (Glen Creston, Middlesex, UK) were added in the ratio of 1:10. A 1% Triton-X100 solution was added until the beads were just covered.

FIGURE 5.1
ADSORPTION OF 1ug $ml^{-1}$ IRON (III) ON ACTIVATED CARBON MADE FROM CELLULOSE, USING CAS CHELATING DYE

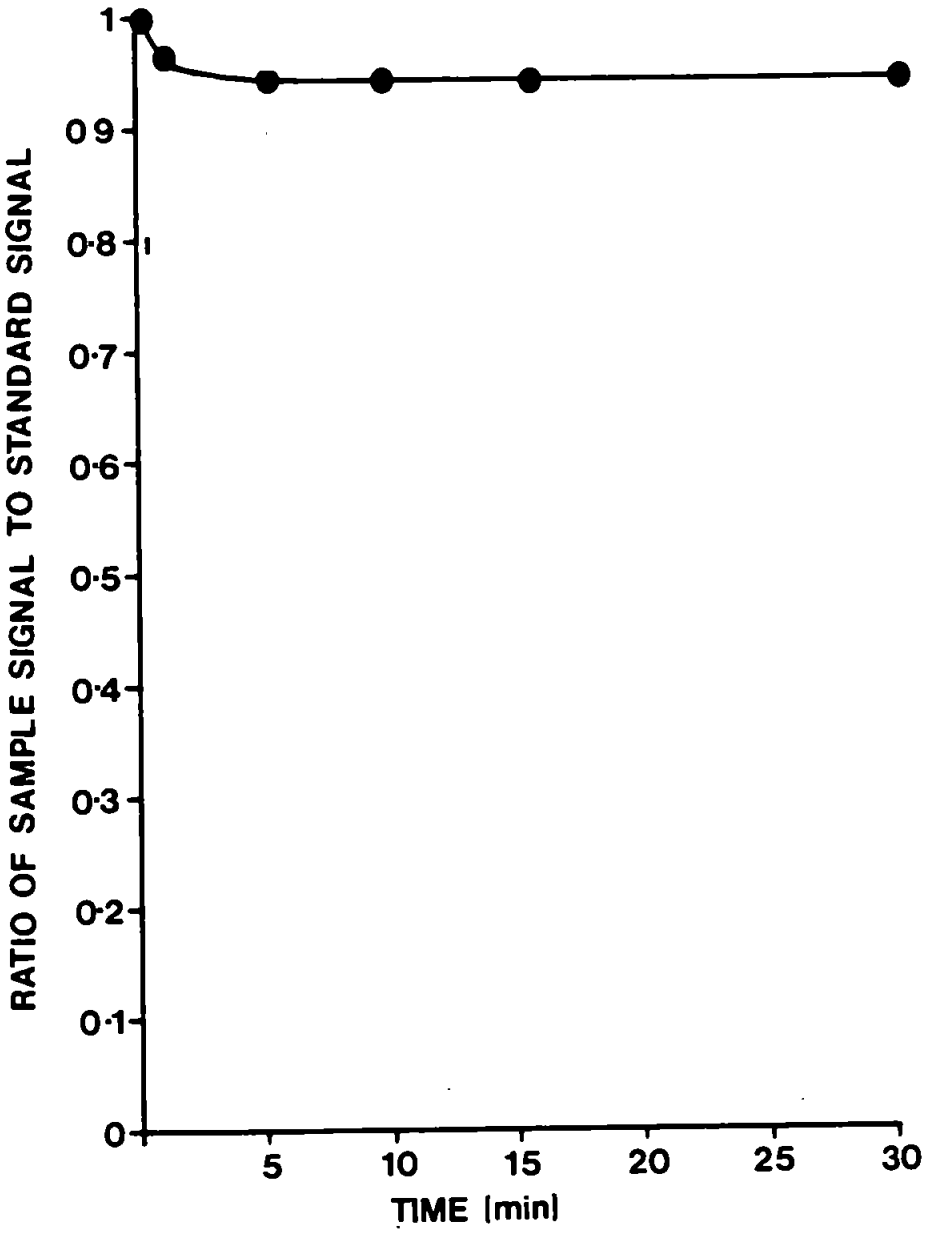

(The bottle had to be shaken until all the carbon had been wetted). The bottle was then sealed tightly and inserted into a micronizer mill (McCrone Research Associates Ltd., London, UK) and ground for 4 hours. The beads were separated from the carbon slurry using a Buchner funnel and the carbon dried in the oven at 105°C. This material was stored in a clean polythene bottle.

For the clean-up procedure, about 15-20g of the ground carbon was placed in a polyethylene beaker. Hydrofluoric acid (40%) (AnalaR, BDH Ltd., Poole, Dorset, UK). was added and stirred with a plastic rod until the carbon was completely covered. This was then left for about 1 hour with occasional stirring. The HF was discarded and more HF was added as before. This procedure was repeated 4 times. The carbon was washed with doubly distilled, deionised water until the pH of the solution rose to between pH4 and pH5. The carbon was transferred to a vacuum filter where HCl (1M) was passed through the filter "cake" to remove any metals that may be insoluble in the fluoride form, for example, Ca and Mg, but soluble as the chloride. This was washed with some water, the carbon dried at 105°C in an oven and stored in a clean, acid-washed polyethylene bottle.

### 5.4.2 **Results and discussion**

To test for metal content, a 1% slurry was prepared in 1% Triton-X100 and analysed by simultaneous ICP-AES. The results are shown in Table 5.2. High levels of calcium, aluminium, magnesium, iron and potassium still remained even after the intensive HF/HCl treatment. Previous analysis

TABLE 5.2
DETERMINATION OF METALS IN HYDROFLUORIC ACID/HYDROCHLORIC ACID–WASHED CAS–COATED ACTIVATED CARBON

| ELEMENT | WAVELENGTH (nm) | CONCENTRATION(in the solid) µg/g |
|---|---|---|
| Sc | 361.36 | 0.13 |
| Ca | 393.37 | 170 |
| Zr | 339.2 | 2.15 |
| Al | 309.27 | 88.4 |
| Mg | 279.55 | 229.8 |
| Mn | 257.61 | 0.67 |
| Co | 238.89 | 0.48 |
| Zn | 213.86 | 0.33 |
| Cu | 324.75 | 0.51 |
| Cr | 267.72 | 0.39 |
| Fe | 259.94 | 54.8 |
| Ni | 231.6 | 0.78 |
| Cd | 226.5 | 0.23 |
| Pb | 220.35 | 2.89 |
| K | 766.49 | 318 |
| Li | 670.78 | 1.82 |
| Na | 589.59 | 430 |
| Ba | 455.4 | 2.41 |
| Sr | 407.77 | 2.93 |

of the untreated carbon showed the iron to be present at over 400$\mu g g^{-1}$ in the solid so there had been some decrease. However, other elements of interest were not present at unacceptably high levels. Although not entirely satisfactory, owing to the unavailability of a pure activated carbon commercially, it was necessary to use this carbon prepared as above for the preconcentration of trace metal impurities from fine chemicals. Before any analyses were performed on the cleaned carbon, (by simultaneous ICP) the possible use of an internal standard was investigated.

## 5.5 EFFECT OF ACTIVATED CARBON SLURRY UPON THE RECOVERY OF ELEMENTS WITH AND WITHOUT SCANDIUM INTERNAL STANDARD

### 5.5.1 Procedure

Two sets of 1 and 5% activated carbon slurries were prepared. The carbon used was that described in section 5.4. To each slurry (4 in total), Ba, Cd, Cu, Co, Cr, Mn, Ni, Pb, Sr and Zn (from a mixed standard) were added so that the overall concentration in the final slurry was 10$\mu g ml^{-1}$ of each element. To all the slurries, 20mg of CAS was added. To one set of slurries, scandium was added to an overall concentration of 10$\mu g ml^{-1}$. The slurries were made up to volume (100ml) in 1% Triton X-100 solution. Prior to analysis, the slurries were placed in an ultrasonic bath for 20 minutes to break up any aggregates and during analysis by simultaneous ICP-AES, the slurries were constantly stirred with a magnetic stirrer.

### 5.5.2 Results and discussion

Table 5.3 shows the effect of slurry concentration upon the recovery of 10 elements (at 10$\mu g ml^{-1}$) with and without Sc internal standard.

The results show that as the concentration of slurry was increased from 1% to 5% there was a degradation in recoveries for the slurries not containing the internal standard. This was presumably caused by transport effects arising from the viscosity of the 5% slurry. The slurries containing the internal standard showed a marked improvement in recoveries over those containing no Sc. For some elements there was a reduction in recovery for the 5% slurry, compared with 1% slurry, for example, Zn, Ba and Sr. For Co, Cr, Ni and Pb, the internal standard over-compensated and gave recoveries over 100%.

The 1% slurries with and without Sc have similar precision. However, the precision for the 5% slurry containing the internal standard was better than the slurry without internal standard. It is important to note that the precision at the 1% level is good with or without internal standard, although there is an improvement with the Sc. For the 5% slurry only the use of an internal standard yields conventional ($\leq$ 2%) precision for ICP-AES.

From Table 5.3, it does not appear necessary to use an internal standard for a 1% slurry, except for Mn, Sr and Zn. The precision between the two sets of data are comparable. However, advantages can be seen from using an internal standard with the 5% slurry, where recoveries are closer

## TABLE 5.3

## EFFECT OF ACTIVATED CARBON SLURRY CONCENTRATION (WITH AND WITHOUT SC INTERNAL STANDARD) UPON RECOVERY

| ELEMENT | 1% | | 5% | |
|---|---|---|---|---|
| | A | B | A | B |
| Mn | 94.1 ± 0.9 | 98.3 ± 0.7 | 86.5 ± 3.1 | 96.3 ± 0.5 |
| Co | 98.9 ± 1.2 | 99.8 ± 1.1 | 92.0 ± 3.0 | 102.6 ± 0.8 |
| Zn | 94.1 ± 0.8 | 98.1 ± 1.5 | 82.8 ± 3.1 | 93.5 ± 1.0 |
| Cu | 98.3 ± 1.2 | 99.6 ± 0.2 | 89.7 ± 4.1 | 98.7 ± 0.2 |
| Cr | 99.4 ± 1.6 | 99.9 ± 0.5 | 94.6 ± 3.0 | 103.6 ± 0.9 |
| Ni | 98.4 ± 1.2 | 99.6 ± 0.8 | 92.1 ± 3.8 | 102.0 ± 0.7 |
| Cd | 94.5 ± 0.9 | 98.4 ± 0.7 | 85.8 ± 3.3 | 98.2 ± 0.3 |
| Pb | 97.7 ± 0.8 | 98.3 ± 1.9 | 87.1 ± 2.5 | 101.0 ± 2.3 |
| Ba | 98.2 ± 1.2 | 100.1 ± 1.2 | 89.6 ± 4.8 | 96.0 ± 0.8 |
| Sr | 93.4 ± 1.2 | 99.1 ± 1.4 | 83.8 ± 4.4 | 90.3 ± 0.9 |

A = No Sc internal standard

B = With Sc internal standard ($10 \mu g ml^{-1}$)

to 100% than those without the Sc.

There is however a difference in the degree of internal standard compensation. Thompson and Houk (141) and Marshall et al (137) were able to explain differences in compensation from examination of ionisation and excitation potentials, which allowed the categorisation of hard and soft lines (142), (atomic lines of elements with low to medium first ionisation potential are termed "soft" and atomic and ionic lines of elements with high first ionisation potential, as well as lines of doubly ionised atoms, are termed "hard"). Table 5.4 shows excitation and ionisation potentials for the elements studied. From Table 5.3 it can be seen that Pb was best compensated by the Sc, followed by Cu, Cd, Ni, Co, Cr, Mn, Ba and Sr. This appears to follow a general trend of decreasing 'difficulty of excitation' (Ip + Ep or Ep) with the exception of copper. Scandium has a summed potential of 10.1eV. It was expected that elements with an energy sum nearer to that of Sc would be compensated for best. Marshall et al, (137) found that using an Sc internal standard, compensation was better for Cu I, a soft line, than for Mn II, a hard line. They claimed that this corresponded to the summed potentials of Cu I and Sc II being marginally closer than Mn II and Sc II. However, the data used was misleading in that they reported that the sum of excitation and ionisation potential for Mn II was 20.45eV, Cu I, 11.53eV and Sc, 15.71eV. This was incorrect as the ionisation potentials quoted for Mn and Sc were second and not first ionisation potentials. They also summed the ionisation and excitation potential for Cu, which is an atomic line.

# TABLE 5.4
# EXCITATION AND IONISATION POTENTIALS

| ELEMENT | WAVELENGTH (nm) | IONISATION POTENTIAL (eV) | EXCITATION POTENTIAL (eV) | ENERGY SUM (eV) |
|---|---|---|---|---|
| Sc(II) | 361.36 | 6.54 | 3.56 | 10.1 |
| Mn(II) | 257.61 | 7.43 | 4.81 | 12.24 |
| Co(II) | 238.89 | 7.86 | 6.24 | 14.1 |
| Zn(I) | 213.86 | — | 5.8 | 5.8 |
| Cu(I) | 324.75 | — | 3.8 | 3.8 |
| Cr(II) | 267.72 | 6.76 | 6.15 | 12.91 |
| NI(II) | 231.6 | 7.63 | 6.39 | 14.02 |
| Cd(II) | 226.5 | 8.99 | 9.27 | 16.26 |
| Pb(II) | 220.35 | 7.41 | 7.37 | 14.71 |
| Ba(II) | 455.4 | 5.21 | 2.72 | 7.93 |
| Sr(II) | 407.77 | 5.69 | 3.04 | 8.73 |

It was difficult to explain some of the effects observed in this work when using the Sc internal standard. For example, it was not known why CuI was compensated for better than, for example, Mn II, whose summed potential was nearer to that of Sc. Also, only one viewing height was used and this may not have been optimal for the elements studied. The results do indicate a general improvement, for the 5% slurry, in recoveries of all the elements compared to those without the internal standard. Also, the variation of the data for the 5% slurry with internal standard, is not that great, with most of the results, with the exception of Zn and Sr, lying within 5% of the full recovery.

## 5.6 EFFECT OF RUNNING TIME UPON RECOVERY, WITH AND WITHOUT INTERNAL STANDARDISATION

### 5.6.1 Procedure

A set of 2% w/v slurries were prepared as in section 5.5.1. One of the slurries was spiked so that the overall slurry contained 10$\mu gml^{-1}$ Sc.

Both slurries were placed in an ultrasonic bath for 20 minutes and during the analysis were stirred constantly with a magnetic stirrer.

### 5.6.2 Results and discussion

Table 5.5 shows the results obtained for the 2% w/v slurries, run continuously over 8 minutes. The recoveries of elements in the slurry containing no Sc show a rapid drop after only 8 minutes running time.

**TABLE 5.5**

**RECOVERIES FOR A 2% M/V SLURRY AFTER 8 MINUTES RUNNING TIME**

| | Recovery % | |
|---|---|---|
| Analyte* | No IS | With IS** |
| Mn | 85.6 ± 2.5 | 97.0 ± 0.6 |
| Co | 85.4 ± 2.8 | 100.7 ± 0.5 |
| Zn | 82.6 ± 3.0 | 95.6 ± 0.90 |
| Cu | 86.6 ± 3.0 | 98.4 ± 0.3 |
| Cr | 86.6 ± 2.1 | 101.2 ± 1.5 |
| Ni | 84.4 ± 2.0 | 100.3 ± 0.8 |
| Cd | 85.0 ± 2.1 | 96.8 ± 0.5 |
| Pb | 79.4 ± 4.2 | 99.9 ± 2.7 |
| Ba | 87.2 ± 5.2 | 97.0 ± 1.3 |
| Sr | 86.6 ± 5.4 | 92.5 ± 1.4 |

* = All analyte elements were added so as to give $10\mu gml^{-1}$ final concentration

** = Internal standard, $10\mu gml^{-1}$Sc

One of the problems of using activated carbon is that it tends to block or semi-block the pump tubing quite easily and this explains why the recoveries are poor for the slurry without Sc addition. However, using the internal standard, the variation in sample delivery was compensated.

## 5.7 DETERMINATION OF METALS IN UREA, SUCROSE AND POTASSIUM CHLORIDE

Having established the usefulness of Sc as an internal standard for the spiked activated carbon slurry work, this procedure was used to determine trace metal impurities in three fine chemicals, using the technique of adsorption of CAS-metal chelates onto activated carbon, followed by slurry atomisation ICP-AES. As Ba and Sr are not easily complexed by the CAS chelating dye, these elements were not determined in this experiment.

### 5.7.1 Procedure

#### 5.7.1.1 Urea

AnalaR Urea (BDH Ltd., Poole, Dorset, UK) (200g) was dissolved in doubly distilled, deionised water to make a 40% solution. CAS (10mg) and activated carbon (0.25g) was added and the pH adjusted to 3 using dilute $HNO_3$. The pH was gradually increased up to pH10 using dilute $NH_3$, the solution being stirred constantly. The carbon was separated from the solution by filtration under reduced pressure and the loaded filter dried in an oven at 105°C. The dried carbon was then made into a 1.25% m/v

slurry (0.25g into 20mls) in 1% Triton X-100 solution and spiked with 0.2$\mu gml^{-1}$ Sc.

5.7.1.2 **Sucrose**

AnalaR sucrose (100g) was dissolved to make a 20% solution and was treated in the same way as the urea, except it was spiked with 0.25$\mu gml^{-1}$ Sc.

5.7.1.3 **Potassium Chloride**

A 20% AnalaR potassium chloride solution was prepared as in 5.7.1.1, but spiked with 5$\mu gml^{-1}$ Sc.

An experimental blank was prepared in the same way as the other solutions and spiked with 0.5$\mu gml^{-1}$ Sc. An effort was made to match the Sc and analyte element concentrations in the ratio of 1:1. Expected values of elements were ascertained from analyses performed on the samples using liquid-liquid extraction with determination by ICP-AES.

5.7.2 **Results and discussion**

Tables 5.6 to 5.8 show the results for urea, sucrose and potassium chloride. There is a striking difference between the results obtained using internal standard and those without, the latter, generally being much lower in value. This was not unexpected due to problems in the sample

**TABLE 5.6**

**ANALYSIS OF UREA**

| ELEMENT | CONCENTRATION FOUND/$\mu gml^{-1}$ | | |
|---|---|---|---|
| | WITH IS* | WITHOUT IS | EXTRACTION** |
| Cu | 0.012 ± 0.0003 | 0.006 ± 0.0002 | <0.1 |
| Fe | 0.102 ± 0.001 | 0.081 ± 0.005 | <0.2 |
| Pb | 0.050 ± 0.002 | 0.009 ± 0.0008 | <0.1 |

* = Internal Standard, Sc at 0.2 $\mu gml^{-1}$

** = Liquid-liquid extraction

**TABLE 5.7**

**ANALYSIS OF SUCROSE**

| ELEMENT | CONCENTRATION FOUND/$\mu gml^{-1}$ | | |
|---|---|---|---|
| | WITH IS* | WITHOUT IS | EXTRACTION** |
| Cu | 0.045 ± 0.002 | 0.016 ± 0.001 | 0.03 |
| Fe | 0.350 ± 0.01 | 0.260 ± 0.038 | 0.02 |
| Pb | 0.193 ± 0.041 | 0.014 ± 0.008 | 0.002 |
| Cd | 0.016 ± 0.004 | 0.00046 ± 0.00041 | 0.014 |
| Ni | 0.052 ± 0.012 | 0.006 ± 0.001 | 0.031 |

* = Internal Standard, Sc at 0.25 $\mu gml^{-1}$

** = Liquid-liquid extraction

**TABLE 5.8**

**ANALYSIS OF POTASSIUM CHLORIDE**

| ELEMENT | CONCENTRATION FOUND/$\mu gml^{-1}$ | | |
|---|---|---|---|
| | WITH IS* | WITHOUT IS | EXTRACTION** |
| Cu | 0.046 ± 0.001 | 0.024 ± 0.0007 | 0.1 |
| Fe | 0.400 ± 0.01 | 0.330 ± 0.02 | 0.4 |
| Pb | 0.317 ± 0.04 | 0.087 ± 0.012 | 1.0 |

* = Internal Standard, Sc at 5 $\mu gml^{-1}$

** = Liquid-liquid extraction

**TABLE 5.9**

**DETERMINATION OF COPPER AND IRON ($\mu g ml^{-1}$) IN UREA, SUCROSE AND POTASSIUM CHLORIDE**

| SAMPLE | ELEMENT | FI-SLURRY ATOMISATION-ICP-AES | IS |
|---|---|---|---|
| Urea | Cu | 0.016 ± 0.003 | 0.012 ± 0.0003 |
| | Fe | 0.17 ± 0.04 | 0.102 ± 0.001 |
| Sucrose | Cu | 0.05 ± 0.01 | 0.045 ± 0.002 |
| | Fe | 0.53 ± 0.12 | 0.35 ± 0.01 |
| KCI | Cu | 0.044 ± 0.006 | 0.046 ± 0.001 |
| | Fe | 0.39 ± 0.06 | 0.40 ± 0.01 |

involving the sorption of trace metal impurities as chelates of CAS, onto activated carbon, and analysis of the carbon by slurry atomisation-ICP-AES. Activated carbon, cleaned by an HF/HCl procedure was used, although this was not entirely satisfactory owing to high levels of Ca, Al, Mg and Fe even after treatment. The usefulness of an internal standard in compensating for sample delivery problems and viscosity effects was shown.

The results obtained by FI-slurry atomisation-ICP-AES showed good agreement with those obtained by continuous nebulisation with an internal standard, although the precision of FI peak height measurement was a problem. However, it is envisaged that refinement of the data capture system could alleviate such problems.

# CHAPTER 6

# CONCLUSIONS AND SUGGESTIONS FOR FUTURE WORK

## 6.1 CONCLUSIONS

The aim of this work was to develop a preconcentration technique for the determination of trace metal impurities in fine chemicals. The method chosen was based upon adsorbing metal ions onto the surface of a solid, followed by direct analysis by slurry atomisation-ICP-AES. A number of parameters were important in the development of the methodology. First and foremost was the selection of a suitable sorbent. Conventional ion-exchange resins were investigated, but failed to preconcentrate metals from strong electrolytic solutions such as 10% potassium nitrate. The chelating resin Chelex-100 looked most promising owing to its ability to preconcentrate metals from 10% potassium nitrate solution, including magnesium, a weakly chelated metal. However, in the final determination technique, problems were encountered in introducing the ground resin into the ICP, due to the Chelex resin causing blockage of the flow injection (FI) valve. The most promising sorbent phase investigated was activated carbon. Metal chelates of Chrome Azurol S (CAS), were formed in the test solutions and powdered activated carbon added. Owing to its extraordinary adsorbability, the carbon adsorbed the metal chelates. The major attraction of using activated carbon as a sorbent was rapidity of adsorption, with equilibration times of less than five minutes. The activated carbon was able to adsorb the CAS-metal complexes from 10% potassium nitrate solution, although it was unable to adsorb magnesium

from such media.

A major disadvantage in the use of activated carbon was the level of impurities. Purity of the solid phase in the sorption process is probably the most important factor. Commercial activated carbon originates from plants or animals, which, by their very nature, contain a percentage of mineral matter and therefore, the metal content is very high. Activated carbon, which had low metal content, was obtained by air-activation of cellulose, which produced a carbon with low metal content. Despite its purity, however, the adsorptive properties of the carbon were very much reduced. This was attributed to a lower surface area than the commercial carbons. The surface areas of the cellulosic carbon and a commercial activated carbon were calculated using the BET equation, from nitrogen adsorption data. It was found that the cellulosic carbon had a surface area of $420 m^{2} g^{-1}$, whereas the commercial carbon was nearly double that at $838 m^{2} g^{-1}$.

Purification of commercial activated carbon was investigated using successive washings of HF, followed by treatment with HCl. This reduced the metal content considerably, although high levels of some elements remained. The procedure developed for the preconcentration technique involved adding CAS to the sample solution, to form the metal chelates, adding activated carbon and adjusting the pH from 3 to 10 with dilute ammonia solution. The solutions were constantly agitated to accelerate the adsorption process. The adsorption step generally took less than ten minutes. The enriched carbon was separated from the bulk solution by filtration under reduced pressure. The 'cake' was dried in an oven at

105°C and made up to whatever volume was required in 1% Triton-X100 solution.

Flow injection (FI) was used as a method of introducing the enriched carbon slurry into the ICP. Sample volumes of 100µl were injected into a carrier stream of water. This work was the first to perform FI of slurries. The technique was validated by the analysis of two Certified Reference Material soils, S01 and S02. Excellent agreement was achieved with the certified values. No blocking of the FI valve was observed and indeed it appeared that the dispersion characteristics of the slurry in the carrier stream were better than with FI of aqueous samples. This was thought to be because the slurry is a two-phase system, thereby reducing dispersion.

In order to reduce dispersion further within the spray chamber, the investigation of smaller volume spray chambers for FI was performed. It was hoped that reducing the volume of the spray chamber would also lead to more favourable transport efficiency, resulting in better sensitivity for small sample volumes. Four spray chamber designs were investigated:- A Scott double pass spray chamber (SDPSC); a single pass spray chamber (SPSC); a bulbous-ended spray chamber (BESC) and a reduced volume spray chamber (RVSC). Using a cascade impactor to collect particles of a 1% slurry, emerging from a 1.8mm injector, transport efficiencies were calculated. The most efficient chamber was the RVSC with a transport efficiency of 0.91%. The SDPSC had the lowest efficiency of 0.42%, additionally it failed to remove larger particles which can cause instability of the plasma. However, the BESC looked promising with a transport

efficiency of 0.66%. It also allowed only particles below 8μm into the plasma.

So that each spray chamber could be directly compared with regards to sensitivity, reproducibility and FI characteristics, it was necessary to optimise plasma running conditions for each spray chamber. This was achieved using the Simplex optimisation routine. Each spray chamber was optimised for copper and manganese. Results showed that for each element, there was little difference in operating conditions. For copper, the best sensitivity was obtained with the BESC and for manganese with the RVSC. The BESC, at high carrier stream flow rates, yielded the best RSD of 3.1%. At low carrier stream flow rates, the SPSC gave the best peak shape, i.e. shortest rise and fall time. However, at higher flow rates the SPSC was noisy with regards to signal. Good peak shape was achieved from both the BESC and the RVSC. Under the optimised conditions, only very small differences were seen in dispersion characteristics which was surprising owing to the differences in spray chamber volumes. The spray chamber chosen for further analyses was the smallest chamber - the RVSC. Owing to the size of the spray chamber, a smaller version of the Ebdon nebuliser was constructed, so that it could fit into the spray chamber.

Continuous nebulisation of slurries was also performed. Owing to sample delivery problems, for example, blocking or semi-blocking of sample delivery tubing, viscosity effects and variations in nebulisation efficiency, an internal standard was used to compensate for these effects. The use of scandium was investigated. There was a definite degradation in

recoveries for all the elements studied, with increasing slurry concentration without internal standardisation. With internal standardisation, however, this was corrected for, and greater recoveries were obtained. The internal standard also corrected for short-term variations in sample delivery with correspondingly better RSDs.

The use of Sc as an internal standard was applied in the determination of trace metal impurities in urea, sucrose and potassium chloride by the preconcentration on activated carbon-slurry atomisation-ICP-AES method described. Flow injection was also performed on the same slurries for comparison. For copper and iron there was general agreement for FI and continuous nebulisation using the internal standard. The RSDs however for the FI were poor but would probably improve with modern integration routines.

This work has shown that a viable technique for the determination of trace metal impurities in fine chemicals, has been successfully developed.

## 6.2 FUTURE WORK

If the technique of adsorption of metal chelates onto activated carbon is to become more than a research project, it is necessary to find an activated carbon with low metal content. This is all the more important when the sorbent material is analysed itself. Although clean-up of commercial activated carbon with HF/HCl reduces the metal content, the presence of Ca, Mg, Al and Fe still remaining, excludes it from determining these elements. Until such a time when analytical grade

activated carbon is manufactured, more work is required in the clean-up process. An alternative would be to make activated carbon from ion-exchange resin beads or some other material, low in metal content. This would require extensive work on optimising the activation process, to obtain a highly activated material with surface areas in excess of $800m^{2}g^{-1}$.

In Chapter 2, it was seen that activated carbon adsorbed complexed metals to differing degrees, depending upon complexing agent used. At present the mechanisms of adsorption are still not certain and more work in elucidating these mechanisms is required, as this will give insight as to why some complexes are adsorbed and others not. With this information it would be possible to use a variety of complexing agents in one solution, in order to obtain maximum adsorption of a wider range of elements. For example, it would be useful to be able to adsorb barium or strontium onto activated carbon as these metals are present in fine chemicals. Chrome Azurol S is not a strong enough chelating agent to chelate them and an alternative agent is required, for example EDTA.

Sample introduction still remains the "Achilles Heel" (69) of plasma spectrometry with typical transport efficiencies of 0.5 - 2%, more work needs to be carried out on the nebulisation system (this includes the nebuliser, spray chamber and injector tube). The ideal nebulisation system would, with higher efficiency, produce a stable aerosol stream of small droplets with narrow particle size distribution and a high transport rate. A number of systems, for example the frit nebuliser, ultrasonic nebuliser and thermospray, have been investigated as possible solutions

to this problem. These however, are solution-based systems and are therefore not readily applicable for slurry work. Frit nebulisation could be adapted to slurry work, although segregation of particle size due to gravity, may be a problem.

Often only small volumes of sample are available for analysis, as was the case in this work. Flow injection was used as a method of sample introduction with success. However, there were problems related to sensitivity. Sensitivity in FI can be increased by reducing the dispersion of the sample with the carrier stream. The major area that dispersion takes place, is in the spray chamber. It is envisaged that reducing the residence time in the spray chamber will reduce dispersion and hence increase sensitivity. Work is required to produce a chamber with a short residence time but still meeting the criteria of an ideal nebulisation system. The chamber also needs to be able to dampen pressure pulses from the peristaltic pump supplying the carrier stream.

A better data handling system is required for FI so that peak heights and areas are automatically calculated.

## REFERENCES


1) Devyatykh, G.G., and Karpov, Y.A., Talanta, 1987, 34, 123

2) Mizuike, A., "Enrichment techniques for inorganic trace analysis", Springer-Verlag, Berlin, 1983

3) Minczewski, J., Chwastawska, J., and Dybczynski, "Separation and preconcentration methods", Ellis Horwood Ltd., Chichester, 1982

4) Leydon, D.E., and Wegscheider, W., Anal.Chem., 1981, 53, 1059

5) Tolg, G., Mizuike, A., Zolotov, Y.A., Hiraide, M., and Kuz'min, N.M., Pure and Appl. Chem., 1988, 60, 1417

6) Riley, J.P., and Skirrow, "Chemical Oceanography", Vol. 3, Academic Press, New York, 1975

7) Cheng, C.J., Akagi, T., and Haraguchi, H., Anal. Chim. Acta, 1987, 198, 173

8) Van Berkel, W.W., Overbosch, A.W., Feenstra, G., and Maessen, F.J.M.J., J. Anal. At. Spectrom, 1988, 3, 249

9) Leyden, D.E., and Luttrell, G.H., Anal. Chem., 1975, 47, 1612

10) Leyden, D.E., Luttrell, G.H., Sloan, A.E., and DeAngelis, N.J., Anal. Lett., 1975, 8, 51

11) Murthy, R.S.S., Holzbecher, J., and Ryan, D.E., Rev. Anal. Chem., 1983, 6, 113

12) Marina, M.L., Gonzalez, V, and Rodriguez, A., Microchem. J., 1986, 33, 275

13) Jackwerth, E., Lohmar, J., and Wittler, G., Fresenius Z. Anal. Chem., 1973, 1, 266

14) Ponec, V., Knor, Z., and Cerny, S., "Adsorption on solids"., Butterworth and Co. Ltd., Czechoslovakia, 1974

15) Piperaki, E., Berndt, H., and Jackwerth, E., Anal. Chim. Acta, 1978, 100, 589

16) Vanderborght, B.M., and Van Grieken, R.E., Anal. Chem., 1977, 49, 311

17) Jackwerth, E., Fresenius Z. Anal. Chem., 1974, 271, 120

18) Ryan, E.E., and Murthy, R.S.S., unpublished results cited from reference 7

19) Sigworth, E.A., and Smith, S.B., J. Am. Water Works Assoc., 1972, 64, 386

20) Heuss, E., and Lieser, K.H., J. Radioanal. Chem., 1979, 50, 289

21) Beinrohr, E., Rojcek, J., and Garaj, J., Analyst, 1988, 113, 1831

22) Jackwerth, E., and Berndt, H., Anal. Chim. Acta, 1975, 74, 299

23) Beinrohr, E., and Berndt, H., Mikrochim. Acta, 1985, 1, 199

24) Berndt, H., and Messerschmidt, J., Fresenius Z. Anal. Chem., 1981, 308, 104

25) Berndt, H., Messerschmidt, J., and Reiter, E., Fresenius Z. Anal. Chem., 1982, 310, 230

26) Kerfoot, W.B., and Vaccaro, R.F., Limnol. Oceanogr., 1973, 18, 689

27) Berndt, H., Jackwerth, E., and Kimura, M., Anal. Chim. Acta, 1977, 93, 45

28) Jones, P., and Schwedt, G., In press

29) Ambrose, A.J., Ebdon, L., Jones, P., submitted to Anal Proc.

30) Van der Sloot, H.A., Wals, G.D., and Das, H.A., Anal. Chim. Acta, 1977, 90, 193

31) Gilbert, P.T., Anal. Chem., 1962, 34, 1025

32) Langmyhr, F.J., Analyst, 1979, 104, 993

33) Van Loon, J.C., Anal. Chem., 1980, 52, 955A

34) Willis, J.B., Anal. Chem., 1975, 47, 1752

35) Fry, R.C., and Denton, M.B., Anal. Chem., 1977, 49, 1413

36) O'Reilly, J.E., and Hale, M.A., Anal. Lett., 1977, 10, 1095

37) Fuller, C.W., Hutton, R.C., and Preston, B., Analyst, 1981, 106, 913

38) Stupar, J., and Ajlec, R., Analyst, 1982, 107, 144

39) Fagioli, F., Landi, S., Locatelli, C., and Bighi, C., Anal. Lett., 1983, 16 275

40) Fagioli, F., and Landi, S., Anal. Lett. 1983, 16, 1435

41) Carrion, N., de Benzo, Z.A., Eljuri, E.J., Ippoliti, F., and Flores, D., J. Anal. At. Spectrom., 1987, 2, 813

42) Ebdon, L., and Pearce, W.C., Analyst, 1982, 107, 942

43) Ebdon, L., and Lechotycki, A., Microchem. J., 1986, 34, 340

44) Ebdon, L., and Lechotycki, A., Microchem. J., 1987, 36, 207

45) Ebdon, L., and Parry, H.G.M., J. Anal. At. Spectrom., 1987, 2, 131

46) Ebdon, L., and Evans, E.H., J. Anal. At. Spectrom., 1987, 2, 317

47) Ebdon, L., and Parry, H.G.M., J. Anal. At. Spectrom., 1988, 3, 131

48) Ebdon, L., and Parry, H.G.M., In press

49) Miller-Ihli, N.J., J. Anal. At. Spectrom., 1988, 3, 109

50) Lynch, S., and Littlejohn, D., J. Anal. At. Spectrom., 1989, 4, 157

51) Mohamed, N., Brown, R.M., and Fry, R.C., Appl. Spectrosc., 1981, 35, 153

52) McCurdy, D.L., Wichman, M.D., and Fry, R.C., Appl. Spectrosc., 1985, 39, 984

53) Sparkes, S.T., and Ebdon, L., Anal. Proc., 1986, 23, 410

54) Watson, A.E., and Moore, G.L., S. Afr. J. Chem., 1984, 37, 81

55) Watson, A.E., S. Afr. J. Chem., 1986, 39, 147

56) Halicz, L., and Brenner, I.B., Spectrochim. Acta, 1987, 42B, 207

57) Ebdon, L., and Wilkinson, J.R., J. Anal. At. Spectrom., 1987, 2, 39

58) Ebdon, L., and Wilkinson, J.R., J. Anal. At. Spectrom., 1987, 2, 325

59) Ebdon, L., and Collier, A.R., J. Anal. At. Spectrom, 1988, 3, 557

60) Foulkes, M.E., Ebdon, L., and Hill, S.J., Anal. Proc., 1988, 25, 92

61) Ebdon, L., Foulkes, M.E., and Hill, S.J., In press

62) Ebdon, L., and Foulkes, M.E., In press

63) Verbeek, A.A., and Brenner, I.B., J. Anal. At. Spectrom., 1989, 4, 23

64) Ambrose, A.J., Ebdon, L., Foulkes, M.E., and Jones, P., J. Anal. At. Spectrom., 1989, 4, 219

65) Williams, J.G., Gray, A.L., Norman, P., and Ebdon, L., J. Anal. At. Spectrom., 1987, 2, 469

66) Ebdon, L., Foulkes, M.E., Parry, H.G.M., and Tye, C.T., J. Anal. At. Spectrom., 1988, 3, 753

67) Greenfield, S., Jones, I.L., and Berry, C.T., Analyst, 1964, 89, 713

68) Ebdon, L., and Collier, A.R., Spectrochim. Acta, 1988, 43B, 355

69) Browner, R.F., and Boorn, A.W., Anal. Chem., 1984, 56, 786A

70) Dale, L.S., and Buchanan, S.J., J. Anal. At. Spectrom., 1986, 1, 59

71) Sharpe, B.L., J. Anal. At. Spectrom., 1988, 3, 613

72) Sharpe B.L., J. Anal. At. Spectrom., 1988, 3, 939

73) Spendley, W., Hext, G.R., and Himsworth, F.R., Technometrics, 1962, 4, 441

74) Ebdon, L., Mowthorpe, D.J., and Cave, M.R., Anal. Chim. Acta, 1980, 115, 171

75) Montaser, A., Huse, G.R., Wax, R.A., Chan, S.K., Golightly, D.K., Kane, J.S., and Dorrzapf, A.F., Anal. Chem., 1984, 56, 283

76) Ebdon, L., and Cave, M.R., Analyst, 1982, 107, 172

77) Ebdon, L., Cave, M.R., and Mowthorpe, D.J., Anal. Chim. Acta, 1980, 115, 179

78) Ohls, K., and Sommer, D., Fresenius Z. Anal. Chem., 1979, 296, 241

79) Salin, E.D., and Horlick, G., Anal. Chem., 1979, 51, 2284

80) Kirkbright, G.F., and Walton, S.J., Analyst, 1982, 107, 276

81) Abdullah, M., Fuwa, K. and Haraguchi, H., Spectrochim. Acta, 1984, 39B, 1129

82) Salin, E.D., and Sing, R.L.A., Anal. Chem., 1984, 56, 2596

83) Cope, M.J., Kirkbright, G.F., and Burr, P.M., Analyst, 1982, 107, 611

84) Thompson, M., Goulter, J.E., and Siepur, F., Analyst, 1981, 106, 32

85) Carr, J.W., and Horlick, G., Spectrochim. Acta, 1982, 37B, 1

86) Christian, G.D., and Ruzicka, J., Spectrochim. Acta, 1987, 42B, 157

87) Ruzicka, J., and Hansen, E.H., Anal. Chim Acta, 1975, 78, 145

88) Tyson, J.F., Analyst, 1985, 110, 419

89) Greenfield, S., Spectrochim. Acta, 1983, 38B, 93

90) McLeod, C.W., J. Anal. At. Spectrom., 1987, 2, 549

91) Garbarino, G.R., Taylor, H.E., Spectrochim. Acta, 1983, 38B, 323

92) Ito, T., Kawaguchi, H., and Mizuike, A., Bunseki Kagaku, 1980, 29, 332

93) Willard, H.H., and Horton, C.A., Anal. Chem., 1950, 22, 1190

94) Theis, M., Z. Anal. Chem., 1955, 144, 106, 192, 275

95) Musil, A., and Theis, M., Z. Anal. Chem., 1955, 144, 427

96) Srivastava, S.C., Sinha, S.N., and Dey, A.K., Bull Chem. Soc. Jap., 1963, 36, 268

97) Seth, R.L., and Dey, A.K., Jnl. Ind. Chem. Soc., 1962, 39, 773

98) Langmyhr, F.J., and Klausen, K.S., Anal. Chim. Acta, 1963, 29, 149

99) Sanyal, P., and Mushran, S.P., Chim. Anal., 1967, 49, 231

100) Jones, P., Pers. Comm., 1988

101) "Stability Constants" Chemical Society special publication. No.17, 1964

102) Greenfield, S., Jones, I.Ll., and Berry, C.T., "Plasma Light Source for Spectroscopic Investigation", US Patent 3,467,471, 1969

103) Hoare, H.C., and Mostyn, R.A., Anal. Chem., 1967, 39, 1153

104) Dagnall, R.M., Smith, D.J., West, T.S., and Greenfield, S., Anal. Chim. Acta, 1976, 54, 397

105) Boumans, P.W.J.M., "Inductively Coupled Plasma Emission Spectroscopy, Part II", John Wiley & Sons, Inc., New York, 1987

106) Montaser, A., and Golightly, D.W., "Inductively Coupled Plasmas in Analytical Atomic Spectrometry", UCH Publishers, Inc., USA, 1987

107) La Freniere, K.E., Rice, G.W., and Fassel, V.A., Spectrochim. Acta, 1985, 40B, 1495

108) Norman, P., Ph.D Thesis (Plymouth Polytechnic), CNAA, 1987

109) Irving, H.M.N.H., Freiser, H., and West. T.S., Eds., "Compendium of Analytical Nomenclature", Pergamon Press, Oxford, 1978

110) Stupar, J., and Dawson, J.B., Appl. Opt., 1968, 7, 1351

111) Koirtyohann, S.R., and Pickett, E.E., Anal. Chem. 1966, 38, 1087

112) Olson, K.W., Haas, J., and Fassel, V.A., Anal. Chem., 1977, 49, 632

113) Smith, D.D., and Browner, R.F., Anal. Chem., 1982, 54, 533

114) Maessen, J.M.J., Coevert, P., and Balke, J., Anal. Chem., 1984, 56, 899

115) Ripson, P.A.M., and de Galan, L., Spectrochim. Acta, 1981, 36B, 71

116) Novak, J.W., and Browner, R.F., Anal. Chem., 1980, 52, 792

117) Cresser, M.S., and Browner, R.F., Spectrochim. Acta, 1980, 35B, 73

118) Brereton, R.G., Analyst, 1987, 112, 1635

119) Nelder, J.A., and Mead, R., Comput. J., 1965, 7, 308

120) Yarbro, L.A., and Deming, J.N., Anal. Chim. Acta, 1974, 73, 391

121) Greenfield, S., and Burns, D.T., Anal. Chim. Acta, 1980, 113, 205

122) Moore, G.L., Humphries-Cuff, P.J., and Watson, A.E., Spectrochim. Acta, 1984, 39B, 915

123) Carpenter, R., and Ebdon, L., J. Anal. At. Spectrom., 1986, 1, 265

124) Ebdon, L., and Carpenter, R.C., Anal. Chim. Acta, 1987, 200, 551

125) Norman, P., Unpublished work, 1986

126) Barnes, R.M., "Applications of Inductively Coupled Plasmas to Emission Spectroscopy, Conf. Proc.", Franklin Institute Press, Philadelphia, 1977

127) Van der Sloot, H.A., Hoe de, D., Zonderhuis, J., and Meijer, C., Netherlands Energy Research Foundation Report, ECN-80, 1980

128) Vanderborght, B.M., and Van Grieken, R.E., Anal. Chim Acta, 1977, 89, 399

129) Gerlach, W., Z. Anorg. Allgem. Chem., 1925, 142, 383

130) Barnett, W.B., Fassel, V.A., and Kniesley, R.N., Spectrochim Acta, 1968, 23B, 643

131) Barnett, W.B., Fassel, V.A., and Kniesley, R.N., Spectrochim Acta, 1970, 25B, 139

132) Myers, S.A., and Tracy, D.H., Spectrochim. Acta, 1983, 38B, 1227

133) Ramsey, M.H., and Thompson, M., Analyst, 1984, 109, 1625

134) Ramsey, M.H., and Thompson, M., Analyst, 1985, 110, 519

135) Wallace, G.F., At. Spectrosc., 1984, 5, 5

136) Schmidt, G.J., and Slavin, W., Anal. Chem., 1982, 54, 2491

137) Marshall, J., Rodgers, G., and Campbell, W.C., J. Anal. At. Spectrom., 1988, 3, 241

138) Brunauer, S., Emmett, P.H., and Teller, E., J. Amer. Chem. Soc., 1938, 60, 309

139) Lowell, S., "Introduction to Powder Surface Area", John Wiley and Sons, Inc., New York, 1979

140) Allen, T., "Particle Size Measurement", Chapman and Hall, London, 1981

141) Thompson, J.J., and Houk, R.S., Appl. Spectrosc., 1987, 41, 801

142) Boumans, P.W.J.M., and Lux-Steiner, M.Ch., Spectrochim. Acta, 1982, 37B, 97

## MEETINGS

(i) Analytical Division of the RSC, meeting on 'Research and Development Topics in Analytical Chemistry', 8th and 9th July 1987, Glasgow.

(ii) Atomic Spectroscopy Group and Western Region jointly with the Peninsula Section of the RSC, meeting on 'New Perspectives in Atomic Spectroscopy', 3rd and 4th September 1987, Plymouth.

(iii) North East Region, Atomic Spectroscopy and Molecular Spectroscopy Groups jointly with the UV Spectrometry Group and Atomic Spectrometry Updates of the RSC, meeting on 'Recent Advances in Atomic and Molecular Spectroscopy', 19th and 20th March 1988, Hull.

(iv) Atomic Spectroscopy Group of the RSC jointly with the Spectroscopy Group of the Institute of Physics, 'Fourth Biennial National Atomic Spectroscopy Symposium', 29th June - 1st July 1988, York.

(v) Analytical Division of the RSC, meeting on '25th Anniversary of Research and Development Topics in Analytical Chemistry', 18th - 19th July 1988, Plymouth.

(vi) Austrian Society for Microchemistry and Analytical Chemistry jointly with the German Working Group for Applied Spectroscopy, '1989 European Winter Conference on Plasma Spectrochemistry', 8th - 14th January 1989, Reutte.

(vii) Analytical Division of the RSC, meeting on 'Research and Development Topics in Analytical Chemistry', 21st and 22nd March 1989, Dublin.

## LECTURES AND ASSOCIATED STUDIES

(i) RSC Lecture, 30th October 1986, Plymouth Polytechnic.
Dr. J.D.R. Thomas, 'Liquid and Enzyme Membrane Electrodes'.

(ii) RSC Lecture, 23rd January 1987, Exeter University,
Professor J. Miller, 'Illuminations in Analytical Chemistry'.

(iii) RSC Lecture, 20th February 1987, Plymouth Polytechnic.
Dr. A. Ure, 'Atomic and Ion Spectra'.

(iv) SERC Vacation School 13th - 18th September 1987.
UMIST, 'Instrumentation and Analytical Science'.

(v) RSC Lecture, 13th November 1987, Plymouth Polytechnic.
Dr. A. Howard, 'Speciation'.

(vi) RSC Lecture, 29th January 1988, Plymouth Polytechnic.
Professor A. Townsend, 'Flow Injection Analysis - The First Decade'.

(vii) RSC Lecture, 7th October 1988, Plymouth Polytechnic.
Professor C.A. McAuliffe, 'The Binding and Activation of Sulphur Dioxide by Manganese Complexes'.

(viii) Research Visit, 18th October 1988, ICI, Brixham.

(ix) RSC Lecture, 20th January 1989, Plymouth Polytechnic.
Dr. P.J. Worsfold, 'Flow Injection - Hands-off Analysis'.

(x) RSC Lecture, 17th February 1989, Plymouth Polytechnic.
Professor M. Barber, 'Modern Mass Spectrometry'.

(xi) Research Colloquia, weekly meetings, October 1986 to September 1989, Plymouth Polytechnic.

## PRESENTATIONS AND PUBLICATIONS

Resulting from the work reported in this thesis the following papers have been presented and published.

(a) **Presentations**

1. "Some preliminary studies on flow injection - inductively coupled plasma - atomic emission spectrometry - slurry atomisation". Poster presented at Atomic Spectroscopy Group and Western Region conference on "New perspectives in atomic spectroscopy", Plymouth Polytechnic, September, 1987

2. "Some studies on flow injection - inductively coupled plasma - atomic emission spectrometry - slurry atomisation". Poster presented at Fourth Biennial National Atomic Spectroscopy Symposium, University of York. June, 1988

3. "Analysis of fine chemicals by ion-exchange resin - flow injection - slurry atomisation - inductively coupled plasma - atomic emission spectrometry". Poster presented at Research and Development Topics in Analytical Chemistry meeting, Plymouth Polytechnic, July, 1988

4. "Sample introduction approaches for the analysis of pure chemicals by ion-exchange resin preconcentration slurry atomisation". Poster presented at 1989 European Winter Conference on Plasma Spectrochemistry, Reutte, January, 1989

5. "A novel preconcentration technique for the determination of trace elements in fine chemicals". Paper presented at Research and Development Topics in Analytical Chemistry, Dublin, March, 1989

(b) **Publications**

1. Ambrose, A.J., Ebdon, L., Foulkes, M.E., and Jones, P., "Direct Atomic Spectrometric Analysis by Slurry Atomisation. Part 8. Flow injection Inductively Coupled Plasma Atomic Emission Spectrometry" J. Anal. At. Spectrom., 1989, 4, 219

2. Ambrose, A.J., Ebdon, L., and Jones. P., "A novel preconcentration technique for the determination of trace elements in fine chemicals". Anal. Proc., 1989. In the Press

# Direct Atomic Spectrometric Analysis by Slurry Atomisation

# Part 8.* Flow Injection Inductively Coupled Plasma Atomic Emission Spectrometry†

**Andrea J. Ambrose, Les Ebdon,‡ Michael E. Foulkes and Philip Jones**
*Department of Environmental Sciences, Plymouth Polytechnic, Drake Circus, Plymouth, Devon PL4 8AA, UK*

The analysis of slurries by flow injection inductively coupled plasma atomic emission spectrometry (FI-ICP-AES) was investigated and the optimum spray chamber design, sample injection volume, carrier stream flow-rate and injector diameter were determined. Particular advantages were obtained by using a novel low-volume spray chamber. A 500-µl injection gave a sensitivity equivalent to that of continuous nebulisation. A torch injector tube of 3 mm internal diameter was the optimum. The analytical potential of the optimum arrangement was demonstrated by the analysis of Certified Reference Material soils SO1 and SO2 (CANMET) for Ca, Fe, Mg, Mn, Cu and V. Excellent agreement with certified values and acceptable precision (2% relative) were obtained.

**Keywords:** *Slurry atomisation; flow injection; inductively coupled plasma; atomic emission spectrometry; soil analysis*

Conventionally, sample introduction into the inductively coupled plasma (ICP) is based on the continuous nebulisation of a flowing carrier stream which produces a steady-state signal. When there is an adequate amount of sample this does not pose a problem; however, often only a small volume of sample is available for analysis. Hence there is a need for methods of sample introduction that do not depend on large volumes of sample. A number of potentially suitable discrete sampling techniques are available, *e.g.*, the direct sample insertion device (DSID), whereby a graphite rod, loaded with a microlitre volume of sample, is inserted into the tip of a conventional sample introduction tube in the centre of an ICP torch.[1–4] Electrothermal vaporisation ICP atomic emission spectrometry (AES)[5] is another microsampling approach that has been used. Laser ablation has become more frequently applied recently and has been used to volatilise micro-samples for subsequent analysis by ICP-AES.[6,7] Unfortunately, the technique is difficult to calibrate and sample inhomogeneity may lead to poor precision.

One of the most promising methods for discrete sample introduction is flow injection (FI). Nearly 1000 papers have been published on FI[8] since its inception in 1975 by Růžička and Hansen.[9] Flow injection includes a range of techniques whereby a discrete sample volume is injected into a continuously flowing carrier stream. The sample is dispersed in the carrier stream to some extent. Dispersion is a function of volume injected, tube dimensions and flow-rate. Applications to atomic spectrometry represent a significant fraction of FI papers and this field has recently been reviewed by Tyson.[10] Surprisingly few of these publications refer to plasma spectrometry, although such application has been demonstrated.[11] Many discrete sampling techniques used in ICP-AES cause air entrainment, which results in instability of the plasma. Flow injection is particularly useful as entrainment does not occur when using this technique.

Previous papers in this series have shown the advantages of slurry atomisation plasma spectrometry,[12–16] principally as regards enhanced speed and accuracy of analysis by eliminating tedious sample preparation stages. Just as sample volumes may be limited in aqueous solution analysis, so also may the solid samples used to prepare the suspensions or slurries employed in this method. Hence FI may be as useful in slurry atomisation as in solution atomisation. This study was designed to illustrate the applicability of FI to slurry atomisation ICP-AES.

## Experimental

The plasma emission spectrometer used was a sequential computer-controlled, fully integrated ICP (Plasmakon S-35, Kontron Spektralanalytik, Eching, FRG). The plasma operating conditions were as follows: power (net forward), 1.5 kW; carrier gas flow-rate, 1.5 l min$^{-1}$; outer gas flow-rate, 15 l min$^{-1}$; and intermediate gas flow-rate, 0.4 l min$^{-1}$. This instrument incorporates a data acquisition system which does not have a direct analogue to digital converter (ADC) between the photomultiplier tube (PMT) and the computer. Instead, a system of voltage to frequency conversion is used whereby the PMT is gated (time base regulated) by the computer. Such a system offers clear advantages for FI as this more rapid data reading facility, compared with a normal ADC, means that sampling rate problems associated with ADCs used in FI work were not encountered. A Minipuls, peristaltic pump (Gilson, Luton, Bedfordshire, UK) together with a six-port switching valve (P.S. Analytical, Orpington, Kent, UK) and 0.8 mm i.d. PTFE tubing formed the basis of the FI manifold.

A variety of PTFE injection loop volumes (100–500 µl) and connecting tube lengths were used. The sample was supplied to the nebuliser via the peristaltic pump. The sample was introduced into the plasma in the form of an aerosol which was produced by a high-solids PTFE nebuliser (Ebdon nebuliser; P.S. Analytical). The aerosol was carried into an in-house designed spray chamber (Fig. 1). Initial studies performed with a conventional Scott double-pass spray chamber were disappointing. Presumably the large volume of this chamber caused excessive dilution of microlitre-sized samples with the carrier stream. Hence the spray chamber shown was designed in an attempt to combine minimal spray chamber volume with convenience of use and to avoid designs which introduced excessive noise.

Particle size measurements were performed using the electrical sensing zone technique (Coulter Counter TAII; Coulter Electronics, Luton, Bedfordshire, UK).

### Reagents

For the preliminary experiments, Dowex 50W-X8 (100–200 mesh) ion-exchange resin (BDH, Poole, Dorset, UK) was

* For Part 7, see reference 16.

† Presented at the Fourth Biennial National Atomic Spectroscopy Symposium (BNASS), York, UK, 29th June–1st July, 1988.

‡ To whom correspondence should be addressed.

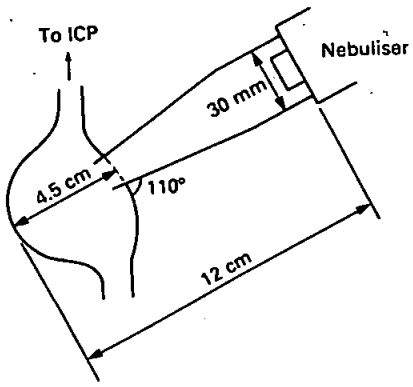


Fig. 1. Reduced-volume spray chamber

used. Validation experiments were carried out using two Certified Reference Material (CRM) soils, SO1 and SO2 (CANMET, Ottawa, Ontario, Canada).

All reagents were of analytical-reagent grade (BDH) and all solutions were prepared with doubly distilled, de-ionised water.

### Sample Preparation

*Ion-exchange resin slurry preparation*

Ion-exchange resin (1 g) was weighed into a 50-ml polypropylene screw-topped bottle and 10 g of polyacrylic spheres (Glen Creston, Stanmore, Middlesex, UK) were added. This was then shaken for a period until the particle size of the slurry was below 8 μm, typically 2–4 h. The slurry and grinding medium were separated and washed through a Büchner funnel into a calibrated flask. Copper was then added to a total concentration of 20 μg $ml^{-1}$.

An aqueous 20 μg $ml^{-1}$ copper solution was also prepared.

*Certified Reference Material preparation*

The comminution method chosen involved shaking a known amount of reference soil with tetrasodium pyrophosphate dispersant solution (over-all concentration of dispersant 1% *m/V*) and zirconia grinding medium (10 g) in a sealed polypropylene bottle for 3 h.[17] The spheres were washed and removed from the solution and made up to the required volume. Particle size distributions of the soils are shown in Figs. 2 and 3.

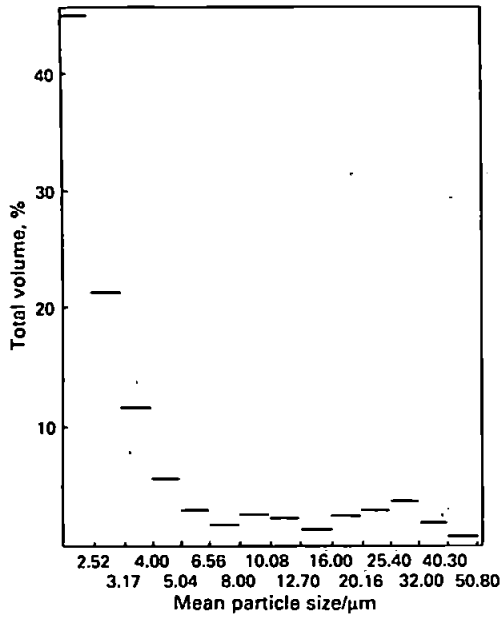


Fig. 2. Particle size distribution of SO1 after grinding

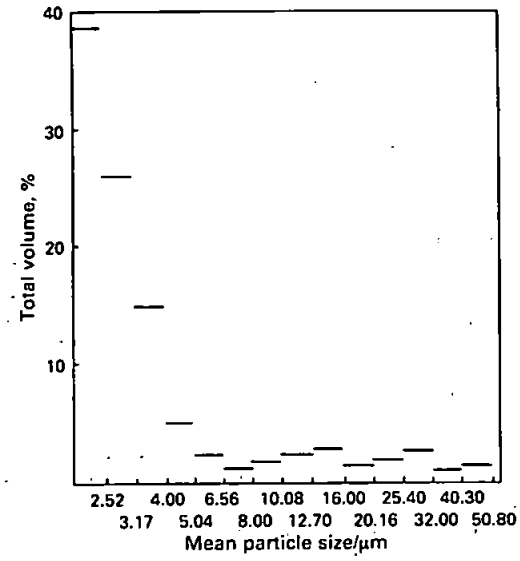


Fig. 3. Particle size distribution of SO2 after grinding

## Results and Discussion

Before any analyses were performed, the controlling parameters were investigated. Variables studied included spray chamber design, sample injection volume, carrier stream flow-rate and injector tube size.

### Spray Chamber Design

Preliminary experiments were performed using a conventional Scott double-pass spray chamber. However, as mentioned earlier, this caused excessive dispersion. The spray chamber was replaced with a single-pass design. Problems were encountered with the formation of condensation at the base of the injector tube, causing instability of the plasma. This was attributed to the spray not being conditioned, *i.e.*, larger droplets were reaching the injector tube.

The spray chamber chosen (Fig. 1) was longer than the straight-through variety with a bulbous end. As the slurry emerged from the nebuliser some of the larger particles impacted on the adjacent glass surfaces. The larger particles should be eliminated by the bends in the chamber and go to drain. In the Scott double-pass spray chamber, particles that have negotiated the reverse direction between the inner and outer tubes travel back along the spray chamber, where gravitational forces and impaction may cause more particles to drop out. With the spray chamber shown in Fig. 1, the particles do not have to travel along a second chamber but enter directly into the injector tube. The spray chamber was found to have a 50% better sensitivity than the Scott double-pass design.

### Sample Injection Volume

An ion-exchange resin slurry (10% *m/V*) containing 20 μg $ml^{-1}$ of copper was used in this experiment. Fig. 4 compares the response for the copper-spiked ground resin and an aqueous sample with the same concentration, with an increasing injection volume. The slurry response tended to be slightly higher than the aqueous response and it is thought that this was due to the slurry being a two-phase system, thereby reducing dispersion. As can be seen from the graph, the signal increased with increasing injection volume. This was not

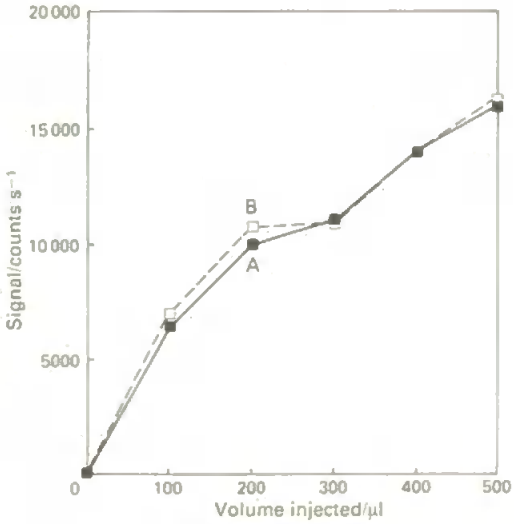


**Fig. 4.** Graph showing the effect of varying injection volume on signal for (A) a 10 µg ml$^{-1}$ copper solution and (B) a resin slurry spiked with the same concentration of copper

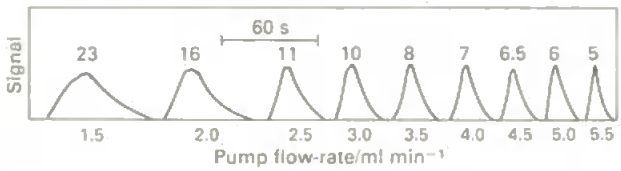


**Fig. 5.** Effect of carrier stream flow-rate on peak height and shape. Copper, 10 µg ml$^{-1}$, 300-µl injection. Numbers on peaks are peak widths at half-height (mm)

unexpected because dispersion at smaller volumes is increased and so the sample is more "dilute" when it reaches the plasma.

Previous work showed that with a typical Scott double-pass spray chamber a 500-µl injection gave a response 75% of that obtained by continuous nebulisation. The spray chamber shown in Fig. 1 alleviated this problem, so that the signals from continuous and discrete nebulisation were comparable to sample volumes of 500 µl and above. This was particularly advantageous as it meant that standards could be either nebulised continuously or introduced by FI.

### Carrier Stream Flow-rate

The carrier stream used in this experiment was doubly distilled, de-ionised water. The flow-rate was controlled by a peristaltic pump with variable speed settings. Fig. 5 shows the effect of increasing the pump flow-rate on the signal. As the carrier stream flow-rate was increased the peak height signal increased slightly. At low carrier stream flow-rates the nebuliser is starved and therefore operates more efficiently than at higher flow-rates when the nebuliser is flooded. A flow-rate of 5.5 ml min$^{-1}$ was chosen as this gave a peak with good sensitivity and symmetry (Fig. 5).

### Effect of Torch Injector Size

Two torch injector tubes with internal diameters of 1.5 and 3 mm were investigated. The difference in response obtained using these two injectors is shown in Fig. 6. As can be seen, the 3 mm injector tube gives a much higher response than the 1.5 mm tube for a 1% soil slurry containing 10 µg ml$^{-1}$ of Ca. Previous work[18] has shown that injector tube diameter has a major influence on the particle size of the slurry reaching the plasma; smaller diameter injection tubes exclude larger slurry particles and thereby lower the signal obtained. Unfortunately, with the 3 mm i.d. injector tube, the noise increases.

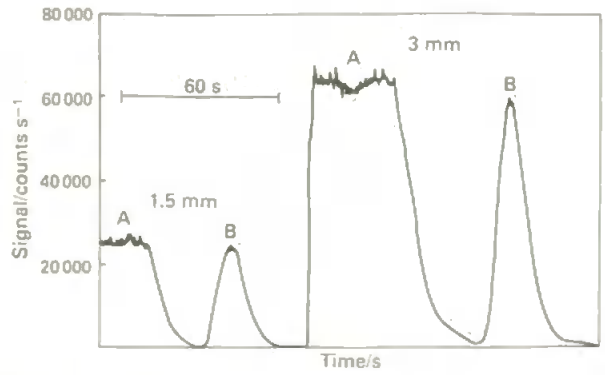


**Fig. 6.** Effect of torch injector tube diameter on signal for (A) continuous and (B) discrete sampling for a 1% soil slurry (10 µg ml$^{-1}$ Ca)

**Table 1.** Determination of elements in CRM soils SO1 and SO2 using FI slurry atomisation ICP-AES

| Soil | Element | Experimental result* | Certified value |
|---|---|---|---|
| SO1 . . . . | Ca, % | 1.75 ± 0.02 | 1.8 ± 0.07 |
| | Fe, % | 5.9 ± 0.13 | 6.0 ± 0.13 |
| | Mg, % | 2.25 ± 0.17 | 2.31 ± 0.003 |
| | Mn, % | 0.089 ± 0.001 | 0.089 ± 0.003 |
| | Cu/µg g$^{-1}$ | 59 ± 0.084 | 61 ± 3 |
| | V/µg g$^{-1}$ | 132 ± 5 | 139 ± 8 |
| SO2 . . . . | Ca, % | 1.95 ± 0.11 | 1.96 ± 0.1 |
| | Fe, % | 5.3 ± 0.16 | 5.56 ± 0.16 |
| | Mg, % | 0.54 ± 0.02 | 0.54 ± 0.03 |
| | Mn, % | 0.068 ± 0.012 | 0.072 ± 0.002 |
| | Cu/µg g$^{-1}$ | 8.0 ± 0.08 | 7 ± 1 |
| | V/µg g$^{-1}$ | 60 ± 5 | 64 ± 10 |

* Means of six replicate determinations ± 2 standard deviations.

### Analysis of Slurries of Certified Reference Materials

To validate the FI slurry atomisation ICP-AES technique two slurries of CRM soils SO1 and SO2 were prepared, 0.1% *m/V* for minor element determinations and 5% *m/V* for trace elements. Results obtained by FI slurry atomisation using conventional aqueous standards for calibration are shown in Table 1. It can be seen that the technique offers excellent agreement with certified values for all six elements studied. Typically the precision was around the 2% (relative) level, which is similar to that obtained with this instrumentation for aqueous solutions.

## Conclusions

Flow injection slurry atomisation ICP-AES has been shown to be a viable analytical technique. A new design of spray chamber offering excellent characteristics for FI-ICP-AES has been developed. Overall the technique combines many of the advantages of FI with the greater sample throughput and other advantages of slurry atomisation. The application of FI to slurries is as convenient as to solutions and no major instrumental modifications are required. Indeed, the more favourable dispersion characteristics of slurries may be advantageous compared with FI of solutions.

We acknowledge the provision of support under the SERC CASE scheme to two of us, A. J. A. (in collaboration with BDH) and M. E. F. (in collaboration with the BP Research Centre).

## References

1. Salin, E. D., and Horlick, G., *Anal. Chem.*, 1979, **51**, 2284.
2. Kirkbright, G. F., and Walton, S. J., *Analyst*, 1982, **107**, 276.

3. Abdullah, M., Fuwa, K., and Haraguchi, H., *Spectrochim. Acta, Part B*, 1984, **39**, 1129.
4. Salin, E. D., and Sing, R. L. A., *Anal. Chem.*, 1984, **56**, 2598.
5. Cope, M. J., Kirkbright, G. F., and Burr, P. M., *Analyst*, 1981, **106**, 32.
6. Thompson, M., Goulter, J. E., and Siepur, F., *Analyst*, 1981, **106**, 32.
7. Carr, J. W., and Horlick, G., *Spectrochim. Acta, Part B*, 1982, **37**, 1.
8. Christian, G. D., and Růžička, J., *Spectrochim. Acta, Part B*, 1987, **42**, 157.
9. Růžička, J., and Hansen, E. H., *Anal. Chim. Acta*, 1975, **78**, 145.
10. Tyson, J. F., *Analyst*, 1985, **110**, 419.
11. Greenfield, S., *Spectrochim. Acta, Part B*, 1983, **38**, 93.
12. Ebdon, L., and Wilkinson, J. R., *J. Anal. At. Spectrom.*, 1987, **2**, 39.
13. Ebdon, L., and Wilkinson, J. R., *J. Anal. At. Spectrom.*, 1987, **2**, 325.
14. Ebdon, L., and Collier, A. R., *J. Anal. At. Spectrom.*, 1988, **3**, 557.
15. Sparkes, S. T., and Ebdon, L., *J. Anal. At. Spectrom.*, 1988, **3**, 563.
16. Ebdon, L., Foulkes, M. E., Parry, H. G. M., and Tye, C. T., *J. Anal. At. Spectrom.*, 1988, **3**, 753.
17. Sparkes, S. T., and Ebdon, L., *Anal. Proc.*, 1986, **23**, 410.
18. Ebdon, L., and Collier, A. R., *Spectrochim. Acta, Part B*, 1988, **43**, 355.

NOTE—References 12–16 are to Parts 1, 3, 5, 6 and 7 of this series, respectively.

*Paper 8/03272F*
*Received August 10th, 1988*
*Accepted October 3rd, 1988*